UNIVERSITÀ DEGLI STUDI DI VERONA

DIPARTIMENTO DI MEDICINA
SEZIONE DI PATOLOGIA GENERALE

Scuola di Dottorato di Scienze della Vita e della Salute
Dottorato di Ricerca in Infiammazione, Immunità e Cancro

Ciclo XXXV

TESI DI DOTTORATO DI RICERCA

Unbalances of the brain tissue resident memory CD8+ T cell compartment amplify Alzheimer's disease like pathology

S.S.D. MED/04 PATOLOGIA GENERALE

Coordinator: Prof. Vincenzo Corbo

Supervisor: Prof.ssa Gabriela Constantin

Dottoranda: **Dott.ssa Eleonora Terrabuio**

Unbalances of the brain tissue resident memory CD8+ T cell compartment amplify Alzheimer's disease like pathology
Eleonora Terrabuio
Tesi di Dottorato
Verona,
ISBN

CONTENTS

SUMMARY

Alzheimer's disease (AD) is a neurodegenerative disorder affecting several millions of people worldwide. Classical neuropathological hallmarks of AD are the presence of amyloid beta (Aβ) deposits and hyperphosphorylated tau protein, leading to the formation of neurofibrillary tangles (NFTs). Neuroinflammation has been also shown to be a key contributor to AD pathology and chronic activation of microglial cells, which are brain resident immune cells, have a key role during the inflammatory responses in the central nervous system (CNS). Moreover, growing evidence demonstrated that peripheral innate and adaptive immune cells also contribute to AD development. However, the contribution of CD3+ T cells, and in particular of CD8 lymphocytes, in AD pathogenesis is still unclear. Recent studies demonstrated a detrimental role for CD8+ T cells in the AD course, reporting a clonal expansion of effector memory CD45RA+ (T_{EMRA}) CD8+ T cells in the cerebrospinal fluid (CSF) of AD specimens and suggested a contribution of CD8+ T lymphocytes to neuronal dysfunction in mice with AD-like disease. However, no study investigated phenotypical and functional alterations of CD8+ T cells taking place in the AD brains during the early stages of disease. To understand the phenotype of brain CD8 T cells in AD, we obtained single-cell RNA sequencing data showing a profound dysregulation of CD8 T cell compartment in the CNS of 3xTg-AD mice during early disease. Notably, we found a significant increase of pro-inflammatory CD103- Trm (tissue resident memory) cells paralleled by a significant decrease of CD103+ Trm lymphocytes in the brain of 3xTg-AD mice compared to sex- and age-matched WT control animals. This suggests a loss of the immune protection exerted by memory-like CD103+ Trm CD8+ T cells and an increase of pro-inflammatory CD103- Trm CD8+ T lymphocytes, potentially promoting disease development. Moreover, we observed a significant decrease in the percentage of detrimental CD103- Trm CD8+ T lymphocytes, paralleled by an increase of CD103+ Trm CD8+ T cells in the brain of 3xTg-AD/*Itgal*$^{-/-}$ animals lacking LFA-1 integrin compared to conventional control 3xTg-AD animals, clearly indicating a role for LFA-1 integrin in the accumulation of CD103- Trm CD8+ T cells into the CNS during AD-like disease. These data were supported by single-cell RNAseq studies and flow cytometry experiments performed on peripheral blood lymphocytes, showing a drastic increase of LFA-1 expression on circulating activated T cells, further pointing to a role for LFA-1 integrin in the accumulation of pro-inflammatory CD8 T cells in the brain of AD mice. Notably, peripheral CD8+ T cells depletion ablated brain CD103- population and improved cognition and reduced neuropathology in 3xTg-AD mice, suggesting a peripheral origin and a detrimental role for CD8+ CD103- T cells in AD. CD103- Trm population upregulated *Gzmk* gene as well as granzyme K (GrK) protein in the brains of 3xTg-AD mice compared to controls, suggesting a potential key role for this molecule in AD. Imaging experiments using time-lapse wide-field microscopy revealed that neurons

in contact with pro-inflammatory CD103- Trm CD8+ T cells showed significantly higher cytoplasmic Ca^{2+} levels compared to neurons co-cultured with CD103+ Trm CD8+ T cells, clearly indicating that CD103- Trm CD8+ T cells invading the brain of 3xTg-AD mice induce intracellular Ca^{2+} dysregulation, an event previously associated with neuronal functional alterations. Importantly, GrK directly induced a significant increase of intracellular Ca^{2+} release in neurons from 3xTg-AD mice, suggesting that this molecule is responsible for neuronal dysfunction induced by CD103- cells. Moreover, we observed that GrK triggered neuronal dysfunctions in a dose-dependent manner, by binding to PAR-1 receptor expressed by neurons, uncovering a new neurotoxic mechanism mediated by CD8 T cells in AD-like disease.

In conclusion, we found a novel CD8+ T cell-mediated GrK-dependent cytotoxic mechanism underlying AD, highlighting the role of CD8+CD103- T lymphocytes in neuronal dysfunction, accumulation of abnormal Aβ and tau, and cognitive impairment and suggesting that targeting the neurotoxic mechanisms exerted by CD8+ T cells could interfere with early pathogenesis of AD.

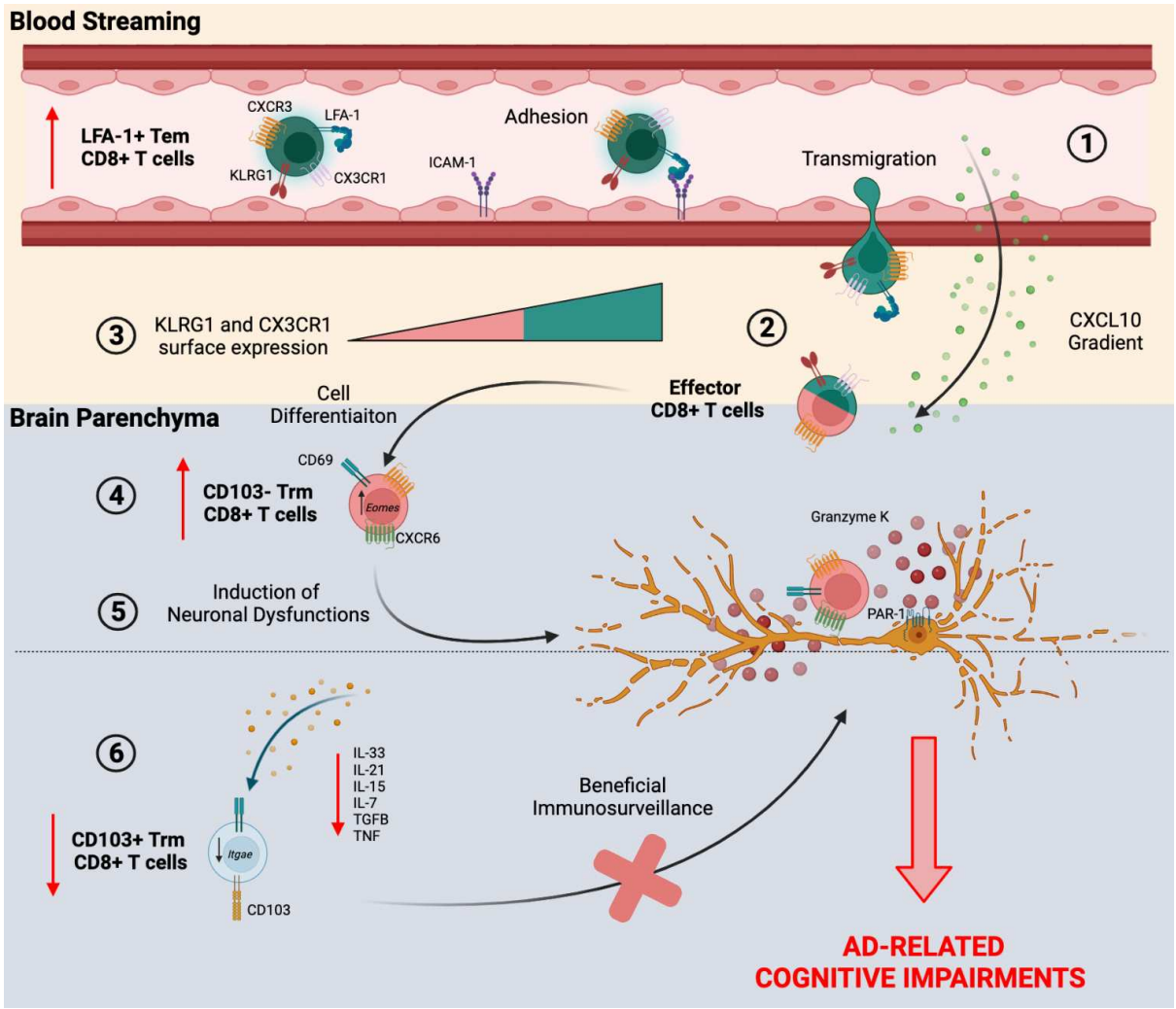

Graphical abstract showing the results mentioned above in the Summary section.

ABBREVIATIONS

3xTg-AD	Triple transgenic Alzheimer's disease mouse
AD	Alzheimer's disease
ALS	Amyotrophic Lateral Sclerosis
APC	Antigen-presenting cell
APOE	Alipoprotein
APP	Amyloid precursor protein
Aβ	Amyloid beta
BACE1	β-Site APP cleaving enzyme 1
BACE2	Beta-site amyloid precursor protein-cleaving enzyme 2
BBB	Blood brain barrier
CFC	Contextual fear conditioning
CH	Chron's disease
CHK1	Checkpoint Kinase 1
CNS	Central Nervous System
CSF	Cerebrospinal fluid
CTL	Cytotoxic T lymphocytes
CTLA-4	Cytotoxic T-lymphocyte-associated protein-4
EBV	Epstein Barr Virus
EOFAD	Early onset familial Alzheimer's disease
ES	Enrichment score
FC	Flow cytometry
GO	Gene Ontology
GPCR	GTP-binding protein-coupled receptor
Gr	Granzyme
GSA	Gene Set Analysis
GSEA	Gene Set Enrichment Analysis
HD	Huntington disease
IBA1	Ionized calcium-binding adapter molecule 1
IF	Immunofluorescence
IHC	Immunohistochemistry
I.P.	Intraperitoneal
ICAM-1	Intercellular adhesion molecule-1
IL	Interleukin

IFN	Interferon
KEGG	Kyoto Encyclopedia for Genes and Genomes
KIR	Killer immunoglobulin-like receptor
KLF2	Kruppel-like factor 2
KLRG1	Killer cell lectin-like receptor subfamily G, member 1
LAG-3	Lymphocyte-activation gene 3
LFA-1	Lymphocyte function-associated antigen-1
LOAD	Late onset Alzheimer's disease
LTP	Long-term potentiation
MAPK	Mitogen-activated protein kinase
MAPs	Microtubule-associated proteins family
MCI	Mild cognitive impairment
MFI	Mean Fluorescent Intensity
MHC	Major histocompatibility complex
MS	Multiple sclerosis
MWM	Morris water maze
NES	Normalized Enrichment Score
NFTs	Neurofibrillary Tangles
NK	Natural Killer
NKR	Natural Killer-associated Receptors
OF	Open Field
PAR-1	Protease activated receptor family 1
PBS	Phosphate buffered saline
PD	Parkinson disease
PD-L1	Phospholipase D1
PFA	Paraformaldehyde
PSEN-1	Presenilin-1
ROS	Reactive oxigen species
SASP	Senescent-associated secretory phenotype
S1PR1	Sphingosine-1-phosphate receptor 1
S1PR5	Sphingosine 1-phosphate receptor 5
Tcm	T central memory
TCR	T cell receptor
Teff	T effector

Tem	T effector memory
T_{EMRA}	T lymphocytes re-expressing CD45RA molecule
Tex	Exhausted T cells
TGF	Tumor growth factor
TIM-3	T-cell immunoglobulin and mucin domain-3
Tmem	Memory T cells
Tmpe	T memory precursor effector cells
Trm	Tissue resident memory
TNF	Tumor necrotic factor
UC	Ulcerative colitis
UMAP	Uniform Manifold Approximation and Projection
VCAM-1	Vascular cell adhesion molecule-1
VLA-4	Very-late antigen-4
WT	Wild type
ZEB-2	Zinc finger E-box binding homeobox 2

INTRODUCTION

ALZHEIMER'S DISEASE: SIGNS AND SYMPTOMS

Alzheimer's disease (AD) is the most diffuse neurodegenerative disorder in the world affecting around 50 million people worldwide, and this number is expected to increase due to an increase of the life expectancy[1]. AD is characterized by a progressive decline of cognitive functions and of the ability to carry out activities of daily living [2]. Based on these changes it is possible to divide AD in three stages:

- **Preclinical phase:** The patient shows no cognitive impairments. However, measurable changes in the levels of some biomarkers, such as amyloid-beta (Aβ) fragments and hyperphosphorylated tau protein, are recorded. Moreover, a shrinking of hippocampus is present [1].
- **Mild cognitive impairment (MCI):** Characterized by mild changes in memory and thinking abilities, but the ability to carry out everyday activities is still maintained[1,3].
- **Dementia:** The ability to carry out everyday activities is completely lost, and several behavioral symptoms appear[1].

In the early stages of the pathology, it is difficult to differentiate between age-related cognitive changes and the AD onset. Indeed, the most common initial symptom of AD is a gradual decrease in learning and in the ability to remember novel information. This is due to the loss of neurons in brain regions usually involved in forming new memories, such as cortex and hippocampus. Neuronal death and memory loss are consequences of the accumulation of Aβ fragments, which form Aβ plaques outside neurons, together with the accumulation of abnormal forms of tau protein, which aggregate leading to the formation of intraneuronal neurofibrillary tangles (NFTs)[3,4]. Extracellular amyloid plaques cause neuronal death interfering with neuron-to-neuron communication at synapses level. Differently, NFTs induce cellular alterations blocking the transport of nutrients and other essential molecules inside neurons. The presence of amyloid plaques and NFTs in the cerebral tissue of AD patients is usually evaluated *post-mortem* through histopathological analysis. Indeed, these features, together with the dramatic brain shrinkage caused by neuronal loss, the presence of widespread debris from dead and dying neurons, and neuroinflammation could be considered as classical hallmarks of advanced forms of AD[4].

DIAGNOSIS OF ALZHEIMER'S DISEASE

In the past, AD-related neuropathological changes were not measured *in vivo*, and the disease was definitively diagnosed only *post-mortem* through histopathological studies. Differently, nowadays,

specific criteria for AD diagnosis exist, based on different approaches and tools. Among them, the study of cerebrospinal fluid (CSF) biomarkers and brain imaging techniques, such as magnetic resonance imaging (MRI) and positron emission tomography (PET), are the most used[1,5]. Thanks to these novel and advanced approaches, the international working group (IWG) integrated biological based approaches and clinical manifestations establishing new criteria to diagnose AD. This now permits to recognize the disorder *in vivo* before the onset of the dementia stage[3,6].

CSF is considered the ideal source of biomarkers in AD being in direct contact with the cerebral tissue[5]. Accordingly, the concentration of CSF several proteins reflects with good diagnostic accuracy the pathophysiological features of the disease. For example, AD patients characteristically display low CSF concentrations of Aβ-42 peptides, combined with high concentrations of total-tau (T-Tau) and phosphorylated-tau (P-Tau) proteins. This pattern of CSF biomarkers is commonly considered the "AD signature" in the CSF[3,7].

Other approaches used to put in evidence changes in brain structure and functions in the early stages of the disease are structural MRI and functional PET neuroimaging, which represent non-invasive methods able to ascertain the pathological changes that evolve in the brain during the AD course[5,8]. MRI is a technique that takes advantage from a pulse of radiofrequency able to modify the energy state of protons and to emit a radiofrequency signal when the pulse is turned off. Structural MRI can assess brain atrophy, caused by neuronal loss, showing changes in tissue characteristics through alterations in the emitted radiofrequency signal (Fig.1)[9]. These studies showed that the earliest site of brain atrophy in AD is at the level of enthorinal cortex, followed by alterations in the hippocampus, amygdala, and parahippocampus[10]. Differently, PET is a technique used for the assessment of Aβ fragments deposition in the AD brains. Aβ-plaques are detected using the radiolabelled Pittsburg compound-B (PiB) (Fig.1)[9]. PET is a useful method for the diagnosis of AD, but the main limitation is that amyloid plaques by themselves are insufficient for a positive identification of AD. Thus, the advent of a PET tau-pathology tracer has been a very important discovery to further confirm of the diagnosis of AD. Indeed, combining Aβ-PET and tau-PET is now possible to discriminate between different neurodegenerative disorders, also monitoring disease progression in alive patients[3].

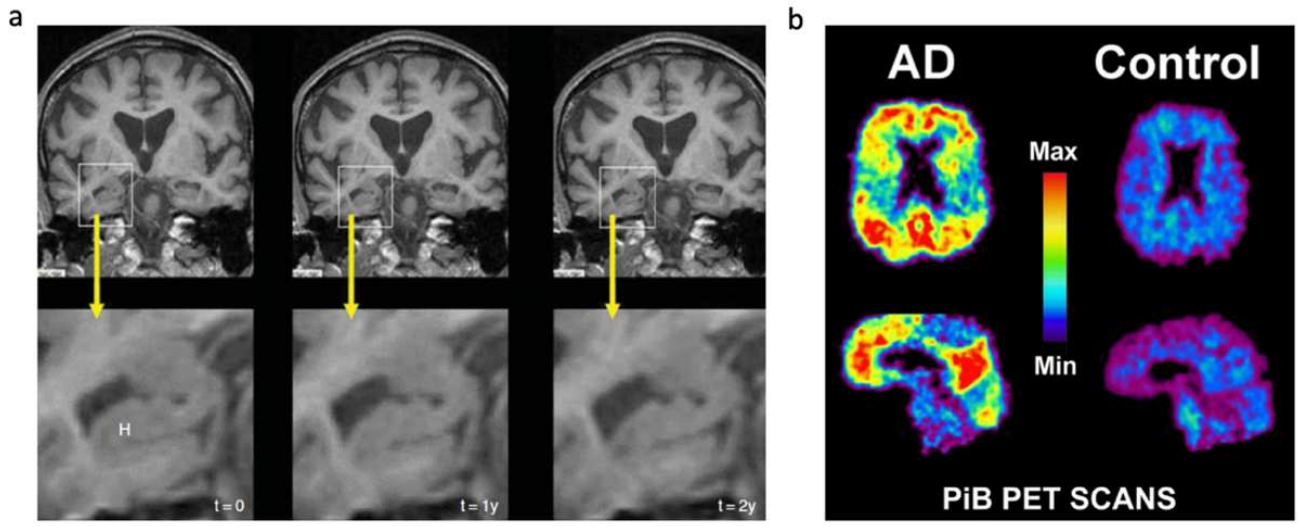

Figure 1. MRI and PET images from AD brains. a. MRI from an individual with autopsy-proven AD. Progressive hippocampal atrophy as the individual progressed from memory complaints (lefts column, t = 0) to fulfil criteria for AD. **b**. PET images from an AD patient VS a normal control. Red and yellow areas indicate high concentration of PiB, marking amyloid deposition (Adapted from Johnson et al., Cold Spring Harbor Laboratory Press, 2012).

RISK FACTORS FOR ALZHEIMER'S DISEASE

AD is a multifactorial disorder which causes remain largely unknown. Indeed, most AD cases belong to the sporadic form of the disease and are not linked to genetic risk factors[11]. Aging is strictly related to the development of sporadic AD. Indeed, an exponential growth in the incidence rates of the disease is shown between 65 and 85 years[1,3,12]. In addition to this, a correlation between age and vascular-metabolic disorders exists, as revealed by epidemiological and clinical studies. In fact, raised blood pressure and high levels of serum cholesterol may precede and increase the AD risk[13]. It seems that atherosclerotic lesions, formed by high levels of cholesterol in the blood, could mediate AD pathology inducing vascular changes, and facilitating the deposition of Aβ plaques in the brain, leading to cognitive decline or inducing neuroinflammatory immune responses[14]. Ageing is also associated to an increased risk to develop diabetes, which, in turn, contributes to the etiology of AD. Accordingly, insulin insensitivity has been yet strictly connected with memory deficits and cognitive decline, which are both classical AD symptoms[15]. In addition to this, it seems that the association between environment or lifestyle and polygenic factors plays a crucial role in AD development. For example, current evidence suggests that environmental agents, such as an unhealthy diet, are fundamental in the determination of the AD outcome[16,17]. Indeed, a high caloric intake represents an important risk factor for the development of the disorder, while fish consumption was found to reduce the risk of getting AD[17]. One of the possible explanations is that a diet rich in fatty acids and proteins could contribute to alter the metal ion balance in AD patients, leading to inflammation and oxidative stress, promoting neurodegenration[16,17].

To date, the only accepted genetic risk factor for sporadic AD is apolipoprotein 4 (APOE4) protein[3,13]. There are evidences that between 40%-65% of people affected by AD retain one or two copies of the *APOE4* allelic variant, facilitating the pathophysiology of AD by promoting NFTs formation and Aβ-plaques deposition[3,11,13]. Moreover, APOE4 induces neurotoxicity and oxidative stress, as well as the increase of blood-brain-barrier (BBB) permeability, which is a highly specialized endothelial cell membrane surrounding cerebral micro-vessels[13,18]. It represents a linkage between circulating cells and neuronal cells, and it is extensively and dramatically damaged in AD, as well reported in literature, leading to a not-controlled brain invasion by peripherally activated innate and adaptive immune cells[19,20]. Triggering receptor expressed on myeloid cells-2 (TREM2) variants are now also considered genetic risk factor for AD. Indeed, recent studies revealed that rare coding variants of TREM2 correlated with an elevated risk to develop AD[21].

FORMS OF ALZHEIMER'S DISEASE

AD can be divided in two forms: (i) early-onset familiar AD (EOFAD), and (ii) sporadic late-onset AD (LOAD). EOFAD is an uncommon AD form related to less than 5% of the total cases. It is characterized by an early onset (<60 years), and by an autosomal dominant gene pattern of inheritance. This means that only one copy of the altered gene is sufficient to cause the disorder. The genes normally found mutated in EOFAD are: (i) amyloid protein precursor (*APP*), (ii) presenilin 1 (*PSEN-1*), and (iii) presenilin 2 (*PSEN-2*)[3,22]. All of them are involved in Aβ toxic fragments formation, which accumulate in the brain leading to the formation of amyloid plaques.

Contrarily, LOAD is the most common form of the disease (95% of total cases), and it is defined by an onset age above 65 years. It is characterized by a genetically complex pattern of inheritance, in which genetic risk factors work together with environmental factors and life exposure events (toxic metals, antimicrobials, pesticides and insecticides, air pollutants, and industrial and commercial chemicals) to determine lifetime risk for AD. For this reason, it is more difficult to identify LOAD-associated genetic loci[23,24].

NEUROPATHOLOGICAL ALTERATIONS OF ALZHEIMER'S DISEASE

The main neuropathological hallmarks of AD include (i) extracellular amyloid plaques formation, (ii) intracellular NFTs deposition, (iii) neuronal and (iv) synaptic loss, and (v) neuroinflammation. Altogether these changes lead to brain atrophy and to the following AD-associated cognitive impairments[1,2].

Amyloid plaques

Amyloid plaques are defined as fibril deposits with a compact core[2,4]. They originate from the aggregation of amyloidogenic Aβ-fragments, which are produced by the altered proteolysis of APP. Indeed, the processing of this type 1 transmembrane protein (605-770 amino acids) can be formally divided into two separated pathways (Fig.2)[3,25]:

- **Non-amyloidogenic pathway:** cleavages mediated by α- and γ-secretases
- **Amyloidogenic pathway:** cleavages mediated by β- and γ-secretases

The common step shared between these two pathways is the last cleavage performed by γ-secretase (Fig. 2), an enzymatic complex composed by presenilin 1 (PS1) or presenilin 2 (PS2), nicastrin, anterior pharynx-defective 1 and presenilin enhancer 2. However, in the non-amyloidogenic pathway APP is firstly cleaved at position 83 by α-secretase, a membrane bound endoprotease, thus producing a large amino-terminal ectodomain (sAPPα), which is secreted into the extracellular environment. Differently, the carboxy-terminal fragment (CTF83) is retained into the cell membrane, and it undergoes to a subsequent proteolysis mediated by γ-secretase. Interestingly, sAPPα, in contrast to Aβ-fragments, has a key role in the positive maintenance of neuronal plasticity[3,25].

The alternative cleavage pathway of APP is the amyloidogenic one, which drives the formation of soluble toxic Aβ-fragments. In this case the first proteolysis is mediated by β-secretase (Fig. 2) at position 99 of APP. The isoform of β-secretase involved in APP processing is B-site APP-cleaving enzyme 1 (BACE1) protein[26]. After the cleavage, a soluble peptide called sAPPβ and the 99-amino-acids carboxy-terminal fragment (CTF99) are formed. The first is released in the extracellular space, while the second one remains within the cell membrane, and it is then cleaved by γ-secretase, generating different forms of damaging Aβ-peptides (Fig.2)[25]. Among them, Aβ40 is the most abundant fragment, whereas Aβ42 peptide is produced only in the 10% of the cases. Many other isoforms of Aβ-peptides exist, such as Aβ34, Aβ38, Aβ39 and Aβ43, however Aβ40 and Aβ42 are the most important in AD[27]. Indeed, Aβ40 is normally found in the CSF of AD subjects, while Aβ42 is the predominant component of senile plaques in the parenchyma[28]. These two isoforms differ in their sequence for the presence, in Aβ42 peptide, of two more amino-acids (isoleucine and alanine) at the N-terminal[28]. Due to these two added non-polar hydrophobic amino acids, Aβ42 can self-associate inducing the formation of oligomers as first, and then of insoluble fibers and amyloid plaques. Hence, Aβ42 could be considered the most neurotoxic form of Aβ-peptides, and the formed oligomers showed synaptic effects, disturbing the functioning of postsynaptic N-Methyl-D-Aspartate

(NMDA) receptors, affecting calcium influx and altering several downstream cascades and postsynaptic α-amino-3-hydroxy-5-methyl-4-isoxazolepropionic acid (AMPA) receptors[29,30].

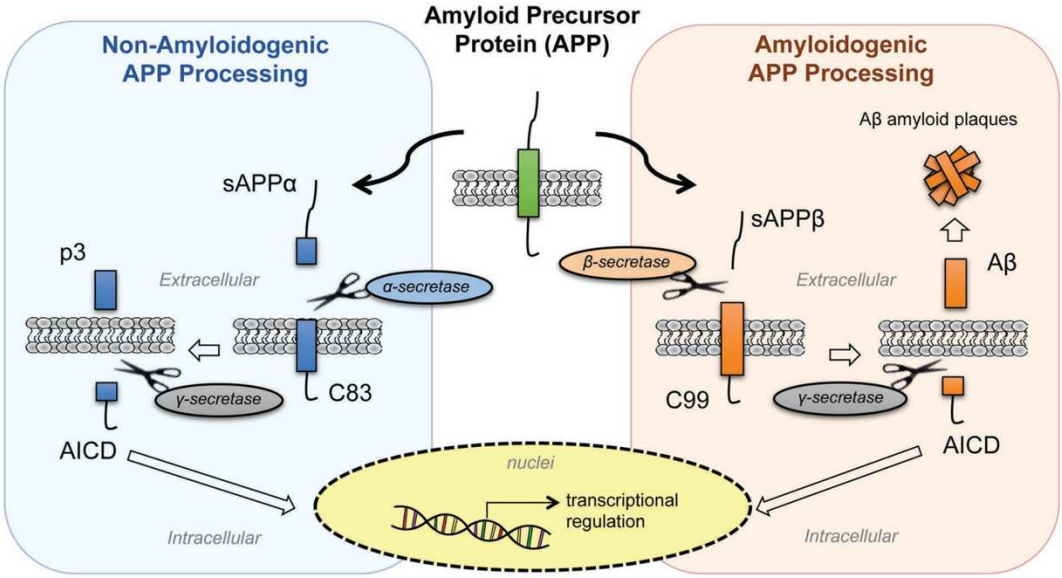

Figure 2. Non amyloidogenic *versus* amyloidogenic pathways. The two pathways involve different types of secretases. Depending on this, steaky amyloidogenic peptides could be formed or not. In the non-amyloidogenic pathways (left), the first cleavage is mediate by α-secretase, forming the sAPPα fragment, released in the extracellular space, and the membrane bound C83 peptide, which undergoes a second cleavage mediated by γ-secretase. In the amyloidogenic APP processing (right), the first cleavage is differently mediated by β-secretase, originating an extracellular sAPPβ peptide and a C99 membrane bound peptide, which is next cleaved by γ-secretase (From Ristoi et al., Frontiers in Physiology, 2020).

Neurofibrillary tangles (NFTs)

NFTs have been firstly described as intraneuronal filamentous inclusions within the perikaryal region of pyramidal neurons[31]. NFTs are considered fundamental microscopic lesions associated with AD development, and their presence in the brain is required for disease diagnosis[4]. The most abundant component of tangles is an abnormally hyperphosphorylated and aggregated form of tau protein. Indeed, in AD, this abnormal tau protein becomes insoluble, lacking affinity for microtubules and generating paired helical filament structures, leading in the end to NFTs formation (Fig. 3)[32]. From the structural point of view, tau is a microtubule associated protein (MAP) discovered in 1986 by Marc Kirschner and colleagues, encoded by chromosome 17q21-22 in humans[33,34]. It is formed by a C-terminal half, that interacts with microtubules, a proline rich region in the middle, and a N-terminal half, called projection domain, which establish interactions with other cell components[35]. The classical epitopes bound by AT8 and AT180 antibodies, both used in immunohistochemical studies to stain P-Tau protein, are found in the middle of tau proline-rich region [36].

The normal function of tau protein is to interact with tubulin, promoting microtubules formation and stabilization. These activities are regulated by phosphorylation events. Indeed, tau protein binds to microtubules in its de-phosphorylated form. However, when enzymes such as mitogen-activated protein kinases (MAPKs), glycogen synthase kinase 3β (GSK3β), and cyclin-dependent kinase 5 (Cdk5) mediate tau phosphorylation, the protein detaches from microtubules (Fig. 3)[32,35]. This mechanism is well controlled during homeostasis, but it is jammed in AD, where tau protein undergoes hyperphosphorylation. Despite the molecular mechanisms triggering hyperphosphorylation events in AD are still not completely understood, it is quite clear that this abnormal P-Tau is unable to bind tubulin, leading to an inhibition of microtubules assembly. This globally results in microtubule disruption and cellular alterations (Fig. 3). In addition, the hyperphosphorylated state of tau protein removes charge differences at its carboxy- and amino-terminals, sustaining oligomer aggregation and NFTs formation (Fig. 3)[32].

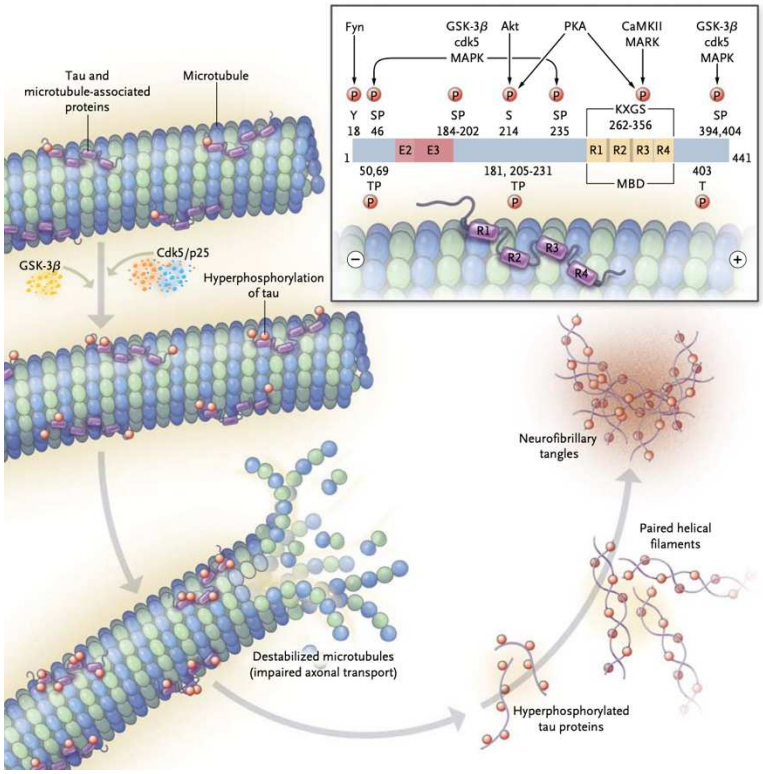

Figure 3. Neurofibrillary tangles (NFTs) formation. Herein it is shown the pathway leading to the formation of NFTs in AD. GSK-3β and Cdk5/p25 mediate tau protein hyperphosphorylation. Hyperphosphorylated tau protein detaches from microtubules inducing subsequent events: (i) microtubules destabilization and impaired axonal transport in neurons, and (ii) paired helical filaments formation, which aggregate forming NFTs (From Querfurth et al., The new England Journal of Medicine, 2010).

Synaptic loss

Synaptic loss is the first indicator of AD progression[4]. Accordingly, synaptic injuries are also present in the early phases of the disease before amyloid plaques formation. Indeed, alteration of synaptic

plasticity seem to be specifically driven by dimers and trimers of amyloid peptides, which are produced during early disease[37]. Synaptic loss in AD is usually revealed through immunohistochemical approaches using antibodies against pre- or post-synaptic proteins, or through transmission electron microscopy (TEM) studies[38]. An example of a pre-synaptic protein classically analyzed to study synaptic loss in AD is synaptophysin. It is an integral membrane protein present on small synaptic vesicles in the brain[39]. The immunohistochemical approaches for the study of synaptophysin allowed to understand that the number of synapses decreases along with disease progression and with the occurrence of cognitive alterations[38,40,41]. However, nowadays, it is still not clear if synaptic loss precedes, follows, or is coincident with neuronal loss.

Neuronal loss

The progressive development of AD is associated to a dramatic and gradual neuronal loss, which determines brain atrophy and shrinkage[2,4]. Neuronal loss starts in the pre-clinical phase of the disease before the formation of amyloid plaques and NFTs. It firstly involves specific brain areas, such as the hippocampal CA1 field, the dentate fascia, the subiculum, and the layer 2 of the entorhinal cortex. Then neuronal loss spreads also in the temporal, frontal and parietal lobes of the brain cortex. In the end, during the final stages of the disorder, neurons of the olfactory bulbs, amygdala, basal nucleus of Meynert, substantia nigra, locus coeruleus, and the dorsal raphe nucleus are also lost [42]. This extended neuronal death is determined by Aβ-fragments accumulation in the AD brain. Indeed, several studies demonstrated that Aβ-peptides in their aggregated oligomeric form can determine AD-like neuronal changes both *in vitro* and *in vivo*[43]. Despite it is still not clear how Aβ fragments can specifically mediate neuronal dysfunctions and death in AD, one suggestion is that they can bind RAGE receptor, determining an increase of intracellular oxidative stress[44]. Moreover, it was demonstrated that amyloid peptides could induce free radicals and reactive oxygen species (ROS), damaging cellular membranes. In turn, increasing levels of oxidative stress could enhance the accumulation of Aβ-fragments in neurons, creating a vicious cycle[45]. Another interesting factor involved in AD-linked neurodegenerative process is the activation of the complement system. Indeed, Aβ40 and Aβ42 fragments, the two most important toxic forms of peptides produced following the amyloidogenic APP cleavage, directly activate both the alternative and the classical pathways of the complement system. This induces the production of C3a, C5a, and the membrane attack complex (MAC) molecules. The function of MAC is to form pores in the cell membrane leading to cell lysis. Importantly, astrocytes and microglia normally produce complement regulatory proteins (CReg) and membrane bound CReg, which allow these cells to be protected from MAC action. Conversely,

neurons are unable to produce these specific protecting molecules. Thus, the activity of MAC on neurons can alter their functions, triggering neuronal death and brain atrophy[46].

NEUROINFLAMMATION IN ALZHEIMER'S DISEASE

Neuroinflammation, represented by an inflammation of the nervous tissue, has been emerged in the last decade as a core phenomenon of AD pathology[12,47–55]. During homeostasis, the main function of neuroinflammation is to protect the CNS against infections, injuries, stress, or other pathological conditions. Under all these disease processes, microglia is the first population undergoing cellular activation. Indeed, it belongs to the resident innate immune system of the CNS, and it could be considered the first line of defense in the nervous tissue[56]. Astrocytes, another type of resident glial cells, are fundamental for the maintenance of the BBB structure and may also play a key role during neuroinflammatory responses[57]. Both microglia and astrocytes, once activated, release a wide variety of pro-inflammatory chemokines and cytokines and may recall a huge number of peripheral leukocytes to the site of inflammation [47,48].

The presence of neuroinflammation in the AD brains was evident since Dr. Alois Alzheimer's studies[47]. However, for many years, the molecular mechanisms behind this phenomenon, and its implications, were not clear. Nowadays, much evidence underlines that chronic neuroinflammation contributes to AD development[12,49–54]. Indeed, both Aβ-fragments and tau-oligomers enhance brain inflammation, supporting microglia activation and the subsequent secretion of pro-inflammatory cytokines, such as interleukin-1β (IL-1β), IL-6, and tumor necrosis factor α (TNFα)[58,59]. This establishes a detrimental vicious cycle, in which Aβ-fragments and tau-peptides continuously promote microglial cells and astrocytes activation, and the subsequent recruiting of peripheral immune cells into the brain, leading to an uncontrolled and chronic neuroinflammatory state[60] (Fig. 4).

In conclusion, neuroinflammatory responses may have a double role in the CNS: promote the repair of brain damage and lead to the return to a homeostatic condition, whereas, under chronic inflammation, leads to abnormal structural and functional brain changes and consequent cognitive alterations.

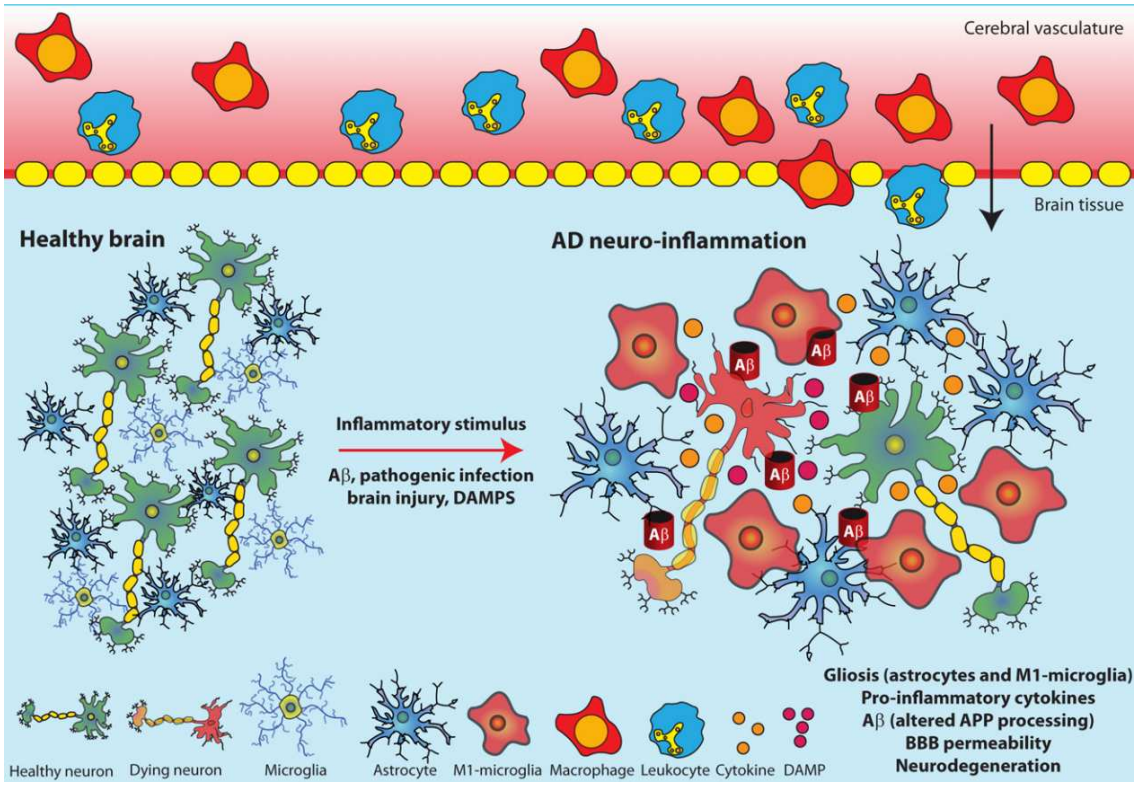

Figure 4. Neuroinflammation in AD. AD is characterized by the presence of a strongly neuroinflammatory environment, which enhances AD pathogenesis leading to the formation of a vicious cycle. Indeed, astrocytes and microglial cells activated by Aβ peptides and tau oligomers release pro-inflammatory cytokine and chemokines, altering BBB permeability and recalling peripherally activated immune cells. BBB damage sustains, in turn, brain invasion by peripheral leukocytes, boosting neuroinflammation and neurodegeneration (From Minter et al., Journal of Neurochemistry, 2016).

Microglia

Microglial cells are the resident macrophages of the CNS and become activated during pathological conditions. They respond to inflammation stimuli removing cellular debris or damaged cells through phagocytosis. Thus, microglial activation is fundamental in morbid conditions to maintain homeostasis. However, its chronic activation leads to detrimental effects[61]. In fact, in a chronically inflamed environment, microglial cells continually release proinflammatory cytokines, ROS intermediates, proteinases, and complement proteins, globally favoring neuronal damages[59,61]. Moreover, if, on one hand, microglia activation is induced by the presence of Aβ-oligomers, on the other hand, activated microglial cells themselves enhance Aβ-peptides formation[60,62] (Fig. 5). In this vicious cycle, Aβ-oligomers could be considered as both the cause and the consequence of neuroinflammation in the AD brains. Furthermore, in this prolonged low-grade chronic inflammation, microglial cells shorten their cellular processes, enlarging their soma instead, acquiring an ameboid, unfunctional, phenotype, and sustaining the disease course[62,63].

Astrocytes

Astrocytes are glial cells present all along the CNS. Differently from microglia, astrocytes are morphologically heterogeneous. In fact, it is possible to distinguish (i) filamentous astrocytes, present in the white matter, and (ii) protoplasmic astrocytes, found in the grey matter[64]. Importantly, astrocytes have been identified as crucial players in AD pathology, where Aβ-oligomers stimulate them inducing their reactive phenotype[65]. As a consequence, several transcriptional factors and detrimental molecules, such as nuclear factor-kappa B (NF-κB), TNFα, IL-1β, and cyclooxygenase-2 (COX-2), are produced, promoting inflammation63 (Fig. 5). Besides, these pro-inflammatory molecules secreted by activated astrocytes enhance the expression of the secretases involved in the conversion of APP into neurotoxic and insoluble Aβ-oligomers. This establishes another detrimental vicious cycle in AD, which strengthens with disease progression. These data are supported by the fact that reactive astrocytes have an increased expression of BACE1 and PS-1 proteins, which are fundamental for the generation of toxic Aβ-fragments. Hence, astrocytes are involved in both stimulation of neuroinflammation and Aβ-oligomers generation and this was previously confirmed by the co-localization of amyloid plaques and activated astrocytes in the AD brains[59,66,67].

Brain infiltration by peripheral leukocytes

Nowadays, it is unanimously accepted by the scientific community that peripheral leukocytes invading the AD brains play a crucial detrimental role in inducing disease pathogenesis and progression. Indeed, despite circulating immune cells patrol the CNS during homeostasis, under inflammatory states several studies, including our owns observed an uncontrolled brain invasion of activated leukocytes from the blood stream[12,49–54,68]. This phenomenon is amplified by the extended BBB damage characterizing the AD condition19,66 (Fig. 5). Indeed, BBB in the healthy brain strictly controls the entrance of circulating immune cells into the cerebral tissue, whereas leaky CNS barriers in AD lose this capability, functioning instead as broken gates[20,69].

To date, both innate and adaptive immune cells were detected in the CNS of AD-like mouse models and human patients[12,49–51,54,68]. Interestingly, neutrophils are the most abundant cell population belonging to the innate immunity detected in AD brains, while CD8+ T-lymphocytes seem to be the most important subset of the adaptive immune system able to migrate into the cerebral tissue in AD[12,49–51]. Whereas the role of neutrophils in AD has been previously demonstrated by our group, the impact of CD8+ T cells in AD pathogenesis and progression is still unclear[49]. However, innate and adaptive immune responses are tightly interconnected, we cannot exclude a possible crosstalk between neutrophils and CD8+ T cells also in AD, as recently reported for other disorders [70].

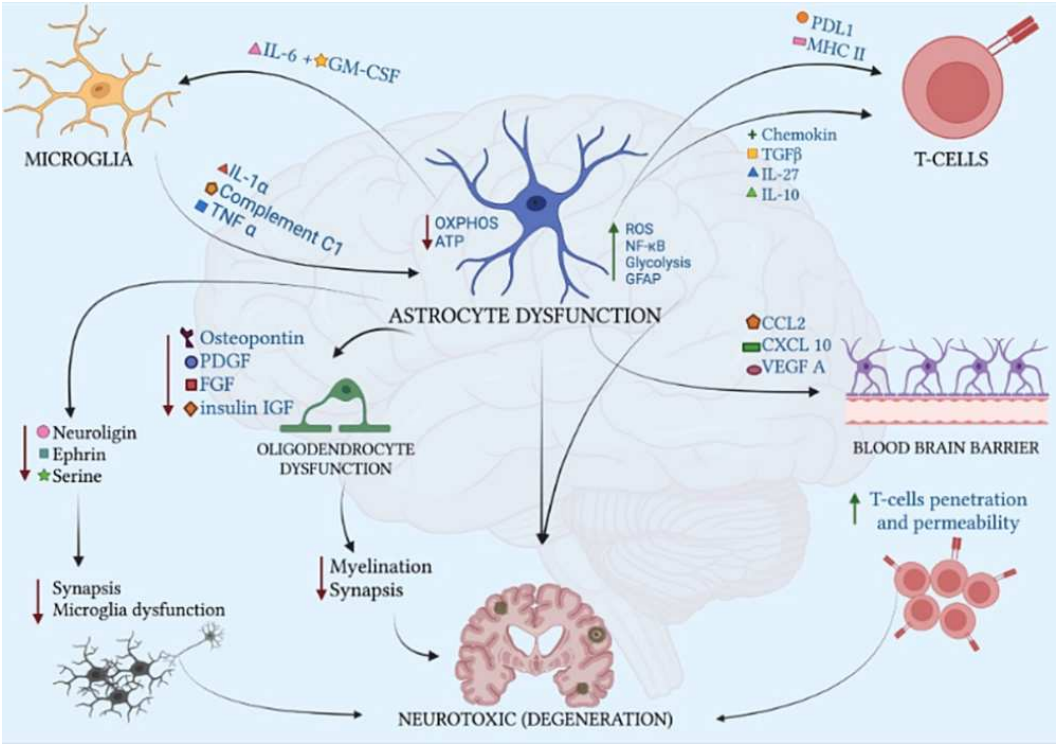

Figure 5. Astrocytes, microglia, and peripheral leukocytes in the AD brain. Reactive astrocytes, active microglia, and peripheral leukocytes invading the AD brains work together in sustaining disease progression. All these cell populations release huge amount of pro-inflammatory molecules in the extracellular environment, boosting, in turn, neuroinflammation and the related neurodegeneration, leading to cognitive impairments classically associated to the AD course (From Hussain et al., Cureus, 2022)

Mechanisms for leukocyte recruitment into the AD brain

Peripherally activated immune cells invade the AD brain throughout a multistep process regulated by adhesion molecules and chemoattracts. It is a cascade of adhesion and activation events in the site of inflammation that ends with leukocytes extravasation. The simplified classical four steps model involves: (i) tethering and rolling on vascular endothelium mediated by selectins, (ii) chemokine-mediate activation, (iii) arrest, and (v) transmigration mediated by integrins[71]. Thus, expression patterns of adhesion molecules and chemokine receptors, upregulated in inflammatory states, regulate the specificity of leukocyte migration.

In AD, intracellular adhesion molecule-1 (ICAM-1) and vascular adhesion molecule 1 (VCAM-1) adhesion molecules were upregulated on brain vessels, suggesting that their counter ligands lymphocyte function-associated antigen-1 (LFA-1), also referred as CD11a/CD18, and very late antigen-4 (VLA-4), also referred as CD49d/CD29, could play a key role in mediating leukocyte trafficking in AD[71–73]. Our previous works demonstrated this hypothesis, showing that LFA-1 integrin mainly directs neutrophils trafficking into the AD brains, while VLA-4 integrin is mostly used by CD4+ T lymphocytes to invade the CNS of AD-like animal models[49,74].

LFA-1 integrin is composed by two subunits/chains: (i) α- (CD11a), and (ii) β- (CD18). This heterodimer is exposed on the cell surface in three possible different conformational states: (i) close/bent, when the integrin has low affinity for the ligand, (ii) closed/extended, where the integrin is extended allowing for interactions with the ligand, and (iii) open/extended, where the integrin had high affinity for its ligand[72,73]. Following inflammatory insults, LFA-1 integrin gradually changes its conformation from close/bent to open/extended, binding its ligand ICAM-1, and driving leukocyte trafficking as previously described[71]. However, LFA-1 integrin plays a crucial role also in T cell activation. Indeed, under basal conditions it has been detected organized in small clusters and bound to the cytoskeleton, suggesting this may help to induce initial cell adhesion to the antigen-presenting cell (APC) upon T cell receptor (TCR) engagement[72,73].

CD8+ T CELLS: ORIGIN AND DIFFERENTION

T lymphocytes are adaptive immune cells that, in mammals, originate from the hematopoietic stem cells (HSCs) lineage in the fetal liver during early life, and in the bone marrow later during their evolution. HSCs firstly differentiate in multipotent progenitors, and then in lymphoid progenitors. Next, a small portion of these immature cells migrate into the thymus becoming early thymic progenitors (ETP), which undergo a gradual reprogramming into fully mature and functional T cells. This occurs due to positive and negative selections, that remove auto-reactive immature T cells leading to their apoptosis[75]. During this maturation process, T lymphocytes acquire the TCR expression, which is a multiprotein complex composed of two variable antigen-binding chains: αβ or γδ[76]. TCR has a key role in antigenic recognition. In particular, it can't recognize antigens in their natural form, but it binds to linear peptides that have been processed and presented by major histocompatibility complex (MHC) molecules on the surface of APCs, such as dendritic cells, macrophages and B lymphocytes. Depending on the nature and the concentration of the antigen (Ag), type of APC and cytokines present in the microenvironment, T cells could differentiate in two different classes: (1) helper CD4+ or (2) cytotoxic CD8+ T lymphocytes[77].

CD8+ T lymphocytes are released in the circulation as mature naïve cells, which provide peripheral immune surveillance searching for their cognate Ag in lymphoid organs[77]. After Ag encounter, naïve CD8+ T lymphocytes undergo cellular activation, becoming effector CD8+ T cells, whose main function is to mediate the apoptosis of target cell via direct and indirect immune mechanisms[78,79]. Indeed, on one hand, they establish contacts with the target cell via FasL-CD95 (FasR) binding, inducing the activation of caspase cascade[80]. Similarly, they release huge amounts of granzymes and perforins directed toward the target cell, favoring its apoptosis. On the other hand, effector CD8+ T lymphocytes produce pro-inflammatory cytokines, such as TNF-α and IFN-γ, which stimulate the

expression of MHC-I and FasR molecules on the surface of target cell, indirectly sustaining its death[80]. After Ag clearance, most of effector CD8+ T lymphocytes undergo a controlled apoptosis during the "contraction phase" of the immune response, and only a small fraction of them survives as memory CD8+ T cells[77,81,82]. The role of memory T cells is to provide peripheral immune protection from experienced Ags, in the circulation as well as inside the tissues[77].

Naïve CD8+ T cells

Naïve CD8+ T lymphocytes are mature circulating cells newly emerged from the thymus. They can acquire a wide variety of effector functions depending on the external clues[83]. Indeed, their differentiation program is not totally pre-determined, but it is, instead, modelled by conditions such as inflammatory states and ageing. Thus, naïve CD8+ T cells could be considered as a reservoir of unconditioned lymphocytes, able to specifically adapt themselves to different threats. Phenotypically, they are characterized in mice by the expression of CD62L (L-selectin) and CD197 (CCR7) surface markers, whereas in humans also by the exposure of CD45RA epitope[79,84,85]. CD62L (L-selectin) and CD197 (CCR7) molecules confer to naïve CD8+ T cells a re-circulating behavior[84]. Indeed, they are both considered "homing receptors" for lymphocytes, allowing them to enter secondary lymphoid organs[86]. There, naïve CD8+ T cells have the chance to encounter their cognate Ag exposed by APCs[87]. When this happens, activated naïve CD8+ T cells undergo drastic phenotypical changes, losing the expression of "homing receptors", and starting a proliferation and differentiation program resulting in an "army" of effector CD8+ T lymphocytes[77,85,88,89].

Effector CD8+ T cells

Differently from naïve CD8+ T cells, the fate of effector T lymphocytes is better defined. Indeed, these cells are specifically activated and directed toward pathogen-derived or tumor-derived peptides, previously presented by MHC-I molecules exposed on APCs in lymphoid organs[77]. Effector CD8+ T lymphocytes express on their surface CD44 and CD69 markers instead of "homing receptors", thus losing the capability to enter secondary lymphoid organs, but invading peripheral tissues instead[90]. Moreover, effector CD8+ T cells can be distinguished by the surface expression of: (i) CD95 (FasR) molecule, which supports the direct CD8-mediated killing mechanisms, and of (ii) Ki-67 proliferation marker[90–92]. This occurs because, in the "effector phase" of the immune response, CD8+ T cells undergo a massive clonal expansion, during which a small number of Ag-specific effector T lymphocytes proliferate into expanded clones[77,82]. This "army" of effector CD8+ T lymphocytes is able to fight against the pathogens due to their high cytotoxic potential. Indeed, they secrete a wide variety of effector and cytotoxic molecules, including granzymes, perforins, IFN- γ, TNF and IL-2[93].

Upon Ag clearance, short-lived effector KLRG1+ CD127- CD8+ T cells undergo a selective apoptosis, while effector KLRG1+ CD127+ CD8+ T lymphocytes persist and survive as exKLRG1 long-lived memory T cells[77,82]. This is called the "contraction phase" of the immune reaction, during which immunological memory is shaped. Importantly, KLRG1, the killer cell lectin-like receptor subfamily G, member 1, is induced in highly proliferative and effector CD8+ T cells under inflammatory signals, and it is classically exposed by murine as well as human effector CD8+ T lymphocytes[84]. However, it has been recently reported that a small fraction of effector CD8+ T cells never express this lectin-like receptor. These cells have been referred as memory precursors effector (Tmpe) cells with an increased survival during the "contraction phase" of the immune response, and a high developmental plasticity[82]. Accordingly, Tmpe cells retain the capability to differentiate in all subsets of memory cells, playing a critical role in long-term protective immunity[94–97].

Memory CD8+ T cells

The immunological memory provided by CD8+ T cells consists in the capability to respond more rapidly and effectively to pathogens that have been previously encountered, preventing the disease state. Thus, during the "memory phase" of the immune response, memory CD8+ T cells that have already experienced the Ag patrol the body, protecting it from already known threats[77].

The memory compartment of CD8+ T lymphocytes comprises three different cell subsets: (i) T central memory (Tcm), (ii) T effector memory (Tem), and (iii) tissue resident memory (Trm)[98]. Generally, all these memory populations originate from effector CD8+ T lymphocytes during the "contraction phase" of the immune response, as described above. However, it has been recently reported that effector T cells expressing the CX3CR1 chemokine receptor on their surface preferentially differentiate in Tem lymphocytes[99]. Contrarily, Tcm cells seem to arise from CX3CR1- precursors[81]. The different origin of Tcm and Tem reflects their phenotypical and functional dissimilarities. Indeed, Tcm CD8+ T lymphocytes, similarly to naïve CD8+ T cells, expose CD62L (L-selectin) and CD197 (CCR7) "homing receptors" on their surface, in line with the re-circulating behavior that they share[97]. However, differently from naïve CD8+ T lymphocytes, Tcm cells express CD44 molecule in mice, and both CD44 and CD45RO epitopes in humans, denoting their memory nature and phenotype82. When Tcm CD8+ T cells encounter their cognate Ag, they differentiate into Tem CD8+ T lymphocytes. Similarly to effector CD8+ T cells, these lymphocytes lose the expression of "homing receptors" during the so-called "second expansion phase", acquiring instead the capability to invade peripheral tissues and release cytotoxic molecules after clonal expansion. Then, when Ag is successfully cleared, the population of Ag-specific Tcm CD8+ T lymphocytes is re-established. Overall, the main function of Tcm and Tem CD8+ T lymphocytes is to provide a systemic immune

protection[84]. Differently, local protective immune responses are orchestrated by Trm CD8+ T lymphocytes, whose profile is quite different from all the other subsets of CD8+ T cells[99]. This cell population didn't receive much attention in the past. However, in the last years, several studies were performed on this subset of memory CD8+ T lymphocytes during homeostasis as well as under different diseased conditions[12,70,94,95,100–107]. Particularly, Trm CD8+ T cells are not recirculating lymphocytes that reside in both lymphoid and non-lymphoid organs for long periods of time. They are organized in lymphoid niches placed near anatomical and physiological barriers, acting as tissue sentinels ready to trigger Ag-specific protection against reinfections[84,108]. Despite further studies are still required to elucidate the precise microenvironment clues needed to establish and maintain the population of Trm CD8+ T cells into different peripheral tissues, it is quite clear that IL-15, IL-7, TGF-β, IL-21, TNF and IL-33 soluble factors play a crucial role in the existence of this CD8+ T cell subset92,107,108. For example, alterations in the TGF-β signaling induce impairments in the differentiation of Trm T lymphocytes in salivary glands and in the intraepithelial layer of the intestine[110]. In addition to this, retention of Trm CD8+ T cells into peripheral tissues is mediated by CD69 and CD103 molecules, both classically exposed on the surface of human and murine Trm CD8+ T lymphocytes[84,98,111]. Indeed, on one hand, CD69 inhibits the expression of sphingosine-1-phosphate receptor 1 (S1PR1) molecule, promoting T cell residency, whereas, on the other hand, CD103 integrin, the adhesion receptor for E-cadherin, contribute to CD8+ T cell retainment into tissues[112]. Particularly, all Trm CD8+ T lymphocytes express CD103 integrin in lymphoid tissues, whereas its expression could be lost by Trm CD8+ T cells in non-lymphoid tissues[108]. Accordingly, different studies reported the presence of both CD103+ CD69+ and CD103- CD69+ Trm CD8+ T lymphocytes in several non-lymphoid tissues, such as liver, brain, gut, skin, and lungs[12,94,95,102,105,106,113,114].

Recent studies demonstrated that CD103+ and CD103- Trm CD8+ T cells originate from two distinct differentiation paths and are characterized by slightly different effector functions[82,95,105]. Indeed, CD103- Trm lymphocytes arise from exKLRG1 effector CD8+ T cells, and they could be distinguished from the CD103+ counterpart due to their cytotoxic potential[102]. Instead, the precursors of CD103+ Trm cells, which are characterized by a lower expression of granzymes and other effector molecules, seem to be KLRG1- Tmpe CD8+ effector T lymphocytes[82,94,95,102]. In addition to this, KLRG1- Trm CD8+ T lymphocytes express *Id3* transcriptional factor (TF), contrarily to the exKLRG1 counterpart, suggesting a memory-like beneficial role for CD103+ Trm cells, while supporting an effector-like phenotype for CD103- Trm CD8+ T lymphocytes[115]. Altogether, these data show the existence of heterogenicity within the Trm CD8+ T cell population[99].

Importantly, Trm CD8+ T lymphocytes are now easier to study than in the past due to the identification of a core gene signature characterizing both human and murine Trm lymphocytes. Indeed, it is now well established in literature that the Trm compartment of CD8+ T lymphocytes upregulates *CXCR6* "homing receptor" gene, and *ITGA1* gene, encoding for CD49a collagen-binding integrin, downregulating instead *SELL* and *CX3CR1* genes, encoding for CD62L and CX3CR1 molecules, respectively[84,98]. Moreover, *Runx3*, *Notch*, *Bhlhe40*, *Blimp1* and its homolog *Hobit*, and the AP-1 TF family members, including *Jun*, *Junb*, *Jund*, *Fos*, *Fosb*, and *Batf* were identified as crucial TFs in the regulation of Trm cells formation[99]. TFs induced by interferon signaling, such as *Stat1*, *Irf1*, *Irf7*, and *Irf9*, or related to the NF-κB signaling pathway, including *Bcl3*, *Rela*, *Relb*, *Rel*, and *Nfkb2* were also enriched in Trm T lymphocytes[99].

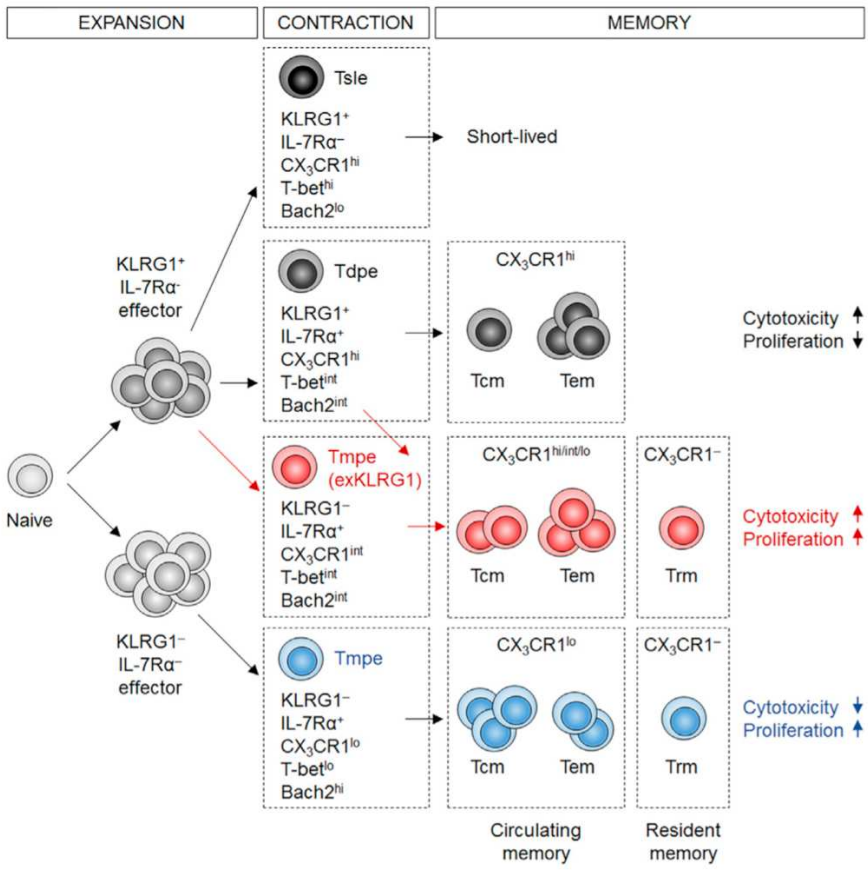

Figure 6. Effector and contraction phases of the immune response Fare clic o toccare qui per immettere il testo..

Following Ag presentation, CD62L+ CD197+ naïve CD8+ T lymphocytes undergo cell activation and clonal expansion during the effector phase of the immune response. KLRG1+ CD127- short lived (Tsle) and KLRG1+ CD127+ long-lived (Tdpe) effector CD8+ T cells are subsequently produced. After Ag clearance, during the contraction phase of immune reaction, Tsle undergo cell death, while Tdpe lose KLRG1 expression, differentiating into exKLRG1 memory CD8+ T cells (Tmpe). Among Tmpe lymphocytes, Tcm, Tem and CD103- Trm CD8+ T cells could be detected. In parallel, KLRG1- effector CD8+ T lymphocytes differentiate into CD103+ Trm CD8+ T cells, characterized by low cytotoxicity and high proliferation capacities (From Herndler-Brandstetter et al., Immunity, 2018).

Exhausted CD8+ T cells

All stages of the immune response and their players are perfectly coordinated and functioning under acute inflammatory states, when Ag is successfully cleared by the immune reaction. However, this perfectly synchronized mechanism is jammed when inflammation become chronic due to persistent Ag stimulation[116]. In this condition, memory T cells gradually become dysfunctional, undergoing an unconventional cell fate, called exhaustion, which is translated in poor effector functions and a decreased proliferative potential[117]. Importantly, T lymphocyte exhaustion is not simply considered an alteration of the cell phenotype and functions, but it represents a distinct differentiation state, considerably different from the memory one[118,119]. Besides, exhausted (Tex) CD8+ T cells retain the same characteristic features under different conditions, thus permitting to define a gene signature for them. Among the marker genes of this population, TCR-signaling related genes, for example *Batf*, *Egr2*, *Ezh2*, *Irf4*, *Nfatc1*, *Nfatc2*, *Nr4a1*, *Nr4a2*, and *Nr4a3*, were detected[118,120–124]. This confirmed that a constant engagement of persistent Ag is a crucial driver of T cell exhaustion[125].

Hyporesponsive Tex cells are also defined by the high surface expression of programmed cell death-1 (PD-1), lymphocyte-activation gene 3 (LAG-3), CD244 (2B4), T-cell immunoglobulin and mucin domain-3 (TIM-3), cytotoxic T-lymphocyte-associated protein-4 (CTLA-4), and CD160 inhibitory receptors, whose simultaneous expression supports Tex cell dysfunction[117,118,124,126–128] (Fig. 7). In accordance with this, the combined blockade of PD-1 and LAG-3, PD-1 and CTLA-4, or PD-1 and TIM-3 pathways induces the recovery of Tex CD8+ T cells functions[124,129–131]. Interestingly, these inhibitory receptors bind a wide variety of ligands, suggesting that microenvironment clues, such as ligands availability, could regulate the functionality of Tex CD8+ T lymphocytes[117,132,133]. Importantly, Tex lymphocytes are not entirely devoid of effector functions, exhibiting instead uncontrolled (i) IL-2 production, (ii) degranulation, and (iii) IFNγ and TNF release, which are all hierarchically lost[117,133] , [Jiang 2021; Jiang 2015] (Fig. 7).

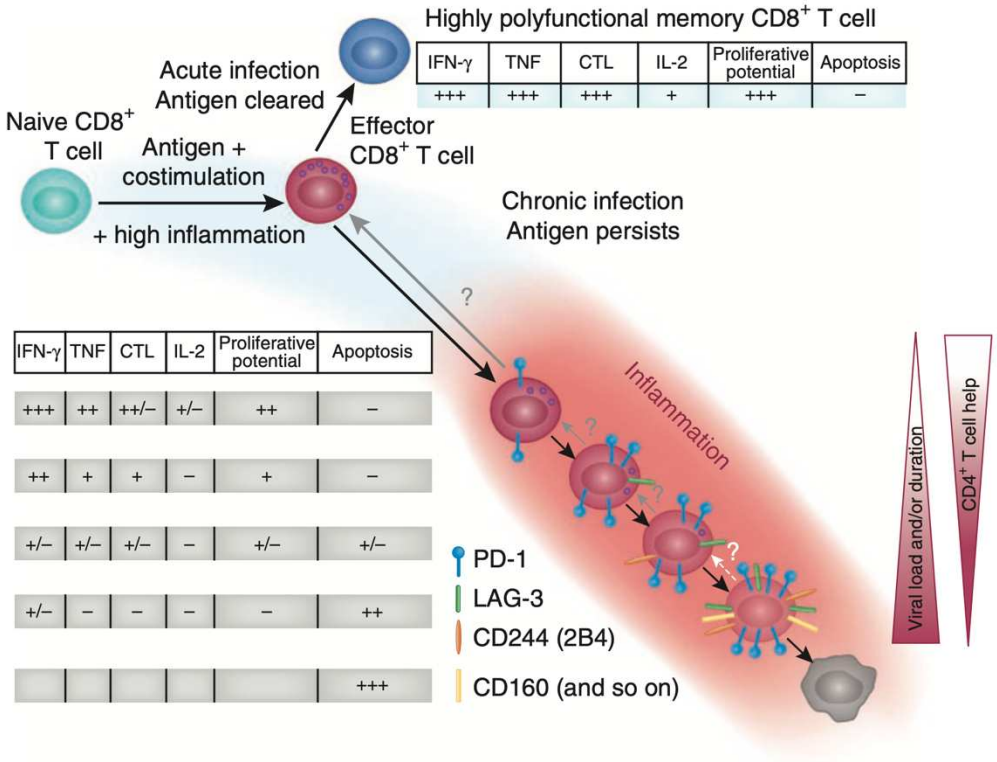

Figure 7. Hierarchical CD8+ T lymphocytes exhaustion during chronic infections. During chronic infections, when Ag is not successfully cleared, the continuously inflamed environment drives a gradual and hierarchical loss of effector functions and proliferative capacities. Together with this, surface expression of inhibitory receptors, including PD-1, LAG-3, CD244 and CD160, is increased (From Wherry et al., Nature Immunology, 2011).

Senescent CD8+ T cells

Senescent CD8+ T cells are characterized by cell cycle arrest and poor proliferation, combined with severe functional abnormalities, similarly to those occurring during T cell exhaustion[117,126,133–135]. Accordingly, immune senescence is also strictly associated to chronic inflammation[126,136]. Despite this, senescent CD8+ T lymphocytes, differently from Tex lymphocytes, continue to release cytokines, such as IL-6 and IL-8, and cytotoxic granules, revealing a pro-inflammatory senescent-associated secretory phenotype (SASP) for them[136,137]. CD8+ T cells in senescence are characterized by the simultaneous expression of PD-1, KLRG-1, and CD57 surface markers[135,138–142]. Besides, human terminally differentiated effector memory CD8+ T cells reexpressing on their surface CD45RA molecule (T_{EMRA} cells) also present senescence characteristics[134,142]. T_{EMRA} lymphocytes arise from effector/Tem CD8+ T cells mainly during chronic inflammation, auto-immune diseases, cancer, and ageing[84,143]. Interestingly, a certain degree of heterogenicity has been revealed also for T_{EMRA} lymphocytes in the tumor microenvironment. Indeed, it was recently shown that effector/Tem CD8+ T cells differentiate into classical CD27- CD28- T_{EMRA} subset in the presence of high antigenicity, while they lead to CD27+ CD28+ T_{EMRA} cells under low antigenicity conditions[143].

Among them, the CD27- CD28- subset of T_{EMRA} cells was characterized by an increased expression of pro-inflammatory molecules, confirming that the strength of TCR engagement is crucial to induce the senescent phenotype[143]. New findings could elucidate the role of CD27+ CD28+ T_{EMRA} CD8+ T lymphocytes during homeostasis or disease conditions. Nevertheless, the most interesting feature of T_{EMRA} and senescent CD8+ T cells as well is the capability to express on their surface natural killer (NK)-associated receptors (NKR), such as NKG2D, NKG2C, NKG2A and killer immunoglobulin-like receptor (KIR) families compared to non-senescent CD8+ T cells[135]. This highlighted that, differently from Tex cells, T_{EMRA} lymphocytes are not just dysfunctional and non-proliferative cells; but they seem to be reprogrammed lymphocytes, which final aim is to recognize and kill the target cells through both TCR and NKR recognition mechanisms[135]. In the light of this, T_{EMRA} cells can still exploit crucial protective functions in disease conditions and ageing, and, thus, their role must not be overlooked. For example, it was shown that T_{EMRA} cells were capable of killing tumor cell lines in an MHC-1-independent manner due to their NKR expression[135]. This suggests that the gain of senescent CD8+ T_{EMRA} cells may be beneficial, especially during ageing, when they enable the retention of a broad spectrum of effector functions important for the killing of malignant and infected cells. However, on the other hand, the acquisition of NK-like functions may also have negative implications, inducing or sustaining chronic and auto-immune disorders[144]. In line with this, it was demonstrated that pro-inflammatory cytokines released by senescent CD8+ T cells can reinforce the external inflammatory milieu[136]. Overall, further efforts are needed to elucidate the role of T_{EMRA} cells under homeostatic conditions and during pathologies, especially those emerging during late life.

CD8+ T CELLS DURING HOMEOSTASIS AND AGEING

CD8+ T cells provide a solid immune protection throughout life, preventing the disease state and maintaining homeostasis over decades. Despite this, the composition of CD8+ T cell compartment considerably changes depending on tissue microenvironment and ageing. For example, naïve CD8+ T cells are preferentially located in blood, spleen, and lymph nodes, where they have the chance to encounter new Ags. Differently, tissues such as lung, gut, and brain, are populated mostly by memory CD8+ T cells, which provide rapid *in situ* protection against reinfections[84,145]. In addition to this, in infancy, when the greatest number of new antigens are encountered and immunological memory is shaping, most of CD8+ T cells are naïve lymphocytes newly emerged from the thymus. Next, Ag exposure drives the differentiation of naïve CD8+ T cells into memory T lymphocytes, which begin to accumulate during childhood till the adulthood, when their levels are maintained over decades. Indeed, in adultness, fewer new Ags are encountered, and the shaped immunological memory works to maintain homeostasis[145]. Differently, aging is characterized by the "immunosenescence"

phenomenon, which determines a decrease in the number of memory CD8+ T cells, counterbalanced by the increase of senescent CD8+ T lymphocytes, especially in blood and blood-rich sites, such as spleen and lungs[139,144–146].

Immunosenescence in elderly is tightly associated with another process, called "inflammageing", defined as a chronic, unresolved, and systemic low-grade inflammation in absence of pathogens[140,147]. Indeed, the decreased adaptive immune response reinforces the innate immunity, which, releasing pro-inflammatory mediators, leads to the increase of the grade of systemic inflammation. This creates a vicious cycle, contributing, in turn, to immunosenescence itself. Furthermore, inflammageing also sustains the accumulation of Tex and senescent PD-1+ TOX+ CD8+ T cell in many anatomical areas, including brain, spleen, lungs, liver, and fat. In these organs, they constitute up to 60% of all CD8+ T cells, suggesting dramatic and systemic immune alterations undergoing ageing[100,140,148]. Overall, this is translated into a global decline of the functionality of the T cell compartment, which, combined with an increased apoptotic rate of T lymphocytes, supports the pathogenesis and progression of a wide variety of age-related disorders, including neurodegeneration[84]. Accordingly, among other evidence, it was recently demonstrated that CD8+ T cells accumulate in the brains of old healthy mice and aged humans, driving myelinated axons degeneration, and the consequent motor decline, by the release of GrB cytotoxic molecule[100]. Similarly, it was shown that clonally expanded INF-γ-producing CD8+ T cells infiltrate old neurogenic niches in the healthy brain, inhibiting the proliferation of neural stem-cells[148].

Despite these evidences clearly demonstrating that CD8+ T lymphocyte alterations characterize aging sustaining neurodegeneration and motor disfunctions, it is still under debate if they are the cause or the consequence of age-related micro-environment perturbations. Indeed, it has been recently shown that the reduced nutritional availability of glucose, amino-acids, and lipids in old tissues can negatively modulate T cells functioning. In support of this, metabolic alterations have been included among the most evident differences between young and old T lymphocytes[149]. Thus, the immune changes considered as characteristics of aging could be viewed instead as the manifestation of elderly-related environmental interferences, which, therefore, can be modulated by lifestyle factors. This leads us to consider age-related T cell dysfunctions as normal, but controllable alterations, which can be alleviated by nutrition and exercise.

CD8+ T CELLS IN ALZHEIMER'S DISEASE

Immunosenescence and inflammageing could be considered as intrinsic, but modulable, consequences of ageing. However, their early emergence has been observed in patients with neurodegenerative and neuroinflammatory disorders, including AD, Parkinson disease (PD), and

multiple sclerosis (MS)[80,147]. In all individuals with these diseases, the well-balanced inflammatory and anti-inflammatory equilibrium is lost, leading to a prolonged and uncontrolled inflammation. Moreover, although the primary causes of these diseases are different, they are all characterized by the accumulation of dysfunctional CD8+ T cells in the CNS, together with a progressive neurodegeneration[12,50,52–55,80,150–152]. Despite this, further studies are still required to completely elucidate the role of CD8+ T lymphocytes, and, especially, of their subsets, in each of these CNS disorders. Indeed, most of studies were conducted considering CD8+ T cells as a *unicum*, and not taking into consideration the extent of the previously described heterogenicity of this cell population[51–54]. For example, most of the studies performed on AD investigated only the changes of the whole CD8+ T cell population in mice developing only amyloid pathology, which do not perfectly mimic the human form of AD[51,53]. However, recently, the heterogenicity of the CD8+ compartment of T lymphocytes has been taken into consideration in AD, leading to the identification of clonally expanded CD8+ T_{EMRA} cells in the CSF of AD individuals[50]. Surprisingly, these T_{EMRA} lymphocytes were clonally expanded not against AD-specific Ags, such as Aβ peptides or tau protein, but against Epstein-Barr virus (EBV) Ags[50]. Despite these data are not evidence of a causal link between EBV infectivity and AD, they suggest that senescence of CD8+ T lymphocytes has a crucial, but still unclear, role in AD development. Accordingly, it has been reported that shorter telomer length in CD8+ T cells is directly connected with AD severity, and this correlated also with higher plasma TNF-α levels, lower CD28 expression, and increase sensitivity to apoptosis[153–155].

Furthermore, the absence of clonal expansion toward disease-specific Ags strongly suggests that, in AD, the trafficking of CD8+ T lymphocytes to the CNS could be more stochastic than controlled[12,50]. Accordingly, the damage of CNS barriers previously described in AD, can favor aspecific CD8+ T cells brain invasion from the circulation[20,69]. Recent studies have shown that, once migrated into the parenchyma, CD8+ T lymphocytes may contribute to neuronal dysfunctions and consequent cognitive impairmens[51]. However, in this work the authors did not investigate the phenotypical features of damaging CD8+ T lymphocytes detected in the brain of mice with AD-like disease, leaving so far unknown the identity of these cells. A very recent published work studying the phenotype and behavior of CD8+ T lymphocytes in AD demonstrated that CD8+ T cells detected in the AD brain have a unique gene signature, corresponding to that of Trm lymphocytes[12]. Overall, existing literature support CD8 T cell heterogeneity in AD and a role for T_{EMRA} and Trm cells subsets in the pathogenesis of this disorder. However, there are still many open questions on CD8 T cell role in AD, including which are the molecular mechanisms throughout which CD8+ T cells shape neuronal function, or how we can defuse the detrimental activity of CD8+ T lymphocytes in AD. Our

data presented in this PhD thesis address some of the current unanswered questions on the role of CD8 T cells in AD.

MATERIAL AND METHODS

All chemicals, kits and antibodies are listed in the following "Table1".

Table 1 | List of reagents.

Reagents	Assay	Source	Identifier
7-AAD Viability Staining Solution	FC	BioLegend	Cat # 420404
Anti-CD16/32 Fc-Block	FC	Campoverde	Cat # 101302
Anti-CD11a/CD18 FITC	FC	Miltenyi Biotech	Cat # 130-114-422
Anti-CD103 BV421	FC	BD Biosciences	Cat # 562771
Anti-CD8 APC-H7	FC	BD Biosciences	Cat # 560182
Anti-CD69 BV650	FC	BD Biosciences	Cat # 740460
Anti-TCRgd PE-CF594	FC	BD Biosciences	Cat # 563532
Anti-CD62L PE	FC	BD Biosciences	Cat # 553151
Anti-CD45 BV605	FC	BD Biosciences	Cat # 563053
Anti-CD27 APC	FC	BD Biosciences	Cat # 560961
Anti-CD11b APC-R700	FC	BD Biosciences	Cat # 564985
Anti-Ly6g BV510	FC	BD Biosciences	Cat # 740157
Anti-CD4 PE-Cy7	FC	BD Biosciences	Cat # 552775
Anti-CD197 (CCR7) BV786	FC	BD Biosciences	Cat # 564355
Anti-CD44 BV711	FC	BD Biosciences	Cat # 563971
Viobility TM Fixable Dye 405/520	FC	Miltenyi Biotech	Cat # 130-109-814
Anti-CD45 APC-Vio770	FC	Miltenyi Biotech	Cat # 130-110-662
Anti-CD8 PE-Cy7	FC	Biolegend	Cat # 100722
Anti-CD3 BV650	FC	BD Biosciences	Cat # 564378
Anti-GrK	FC/IF	ThermoFisher Scientific	Cat # PA550980
Goat anti-rabbit AlexaFluor 488	FC	ThermoFisher Scientific	Cat # A11034
Anti-VLA-4 (CD49d) PE-Cy7	FC	BioLegend	Cat # 103618
Anti-Ly6g BV421	FC	BD Biosciences	Cat # 562737
Anti-CD44 BV510	FC	BD Biosciences	Cat # 563114
Anti-CD45 BV786	FC	BD Biosciences	Cat # 564225
Anti-CD4 APC	FC	BD Biosciences	Cat # 553051
Anti-CD45 BV480	FC	BD Biosciences	Cat # 566095
Anti-KLRG1	FC	BD Biosciences	Cat # 561621
Fixation Buffer	FC	BD Biosciences	Cat # 55655
Staining Perm Wash Buffer	FC	BD Biosciences	Cat # 554723
Collagenase crude type IA	FC	Merck Millipore	Cat # C2674-100MG
Deoxiribonuclease I crude lyophilized	FC	Merck Millipore	Cat # DN25-100MG
Recombinant Mouse IL-2 Protein	*In Vitro* cultures	R&D Systems	Cat # 402-ML
Recombinant Mouse IL-7 Protein	*In Vitro* cultures	R&D Systems	Cat # 407-ML-025
Neurobasal medium	*In Vitro* cultures	ThermoFisher Scientific	Cat # 21103049
Corning® 500 mL RPMI 1640 1X	Cell isolation/ *In Vitro* cultures	Corning	Cat # 15-040-CV
B-27 Plus Supplement (50X)	*In Vitro* cultures	ThermoFisher Scientific	Cat # 17504044
Glutagro supplement	*In Vitro* cultures	Corning	Cat # 25-015-CI
Penicillin-Streptomycin	*In Vitro* cultures	Sigma Merck	Cat # P4333
Poly-D-lysine hydrobromide	*In Vitro* cultures	Sigma Merck	Cat # P6407
Laminin	*In Vitro* cultures	Merck Millipore	Cat # 11243217001
Ionomycin calcium salt from Streptomyces conglobatus	*In Vitro* cultures	Sigma-Aldrich	Cat # I0634
Purified GrK	*In Vitro* cultures	TEMA Ricerca	Cat # CSB-EP010084MO
SCH79797	*In Vitro* cultures	DBA	Cat # Hy-14993
Biotracker 609 Red Ca2+ AM Dye	Live Imaging	Merck Millipore	Cat # SCT021
CellTracker TM Blue CMAC Dye	Live Imaging	ThermoFisher Scientific	Cat # C34552
Anti-Ras isotype antibody	*In Vivo* Treatment	Homemade	Homemade
Anti-mouse CD8α	*In Vivo* Treatment	BioXCell	BE0061
Normal goat serum	IHC/IF	Vector Labs	Cat # S1000
Bovine Serum Albumin	IHC/IF	Sigma Merck	Cat # A4503
Anti-β-Amyloid, 1-16 Antibody (6E10)	IHC	BioLegend	Cat# SIG-39320
Tau Monoclonal Antibody (HT7)	IHC	Thermo Fisher	Cat # MN1000
Phospho-Tau (Thr231) Monoclonal Antibody (AT180)	IHC	Thermo Fisher	Cat # MN1040
Triton™ X-100	IHC	Sigma Merck	Cat # X-100
Hydrogen peroxide solution	IHC	Sigma Merck	Cat # H1009
VECTASTAIN® ABC-HRP Kit, Peroxidase	IHC	Vector Labs	Cat # PK-6100
Vector® NovaRED® Substrate Kit, Peroxidase (HRP)	IHC	Vector Labs	Cat # SK-4800
Eukitt® Quick-hardening mounting medium	IHC	Sigma Merck	Cat # 03989
Anti-ZO1	IF	ThermoFisher Scientific	Cat # 40-2200
DAPI	IF	Sigma-Aldrich	Cat # D9542
Anti-CD8α	IF	Abcam	Cat # Ab4055
Anti-CD103	IF	Abcam	Cat # Ab129202
Goat anti-rabbit AlexaFluor 647	IF	ThermoFisher Scientific	
Dako Fluorescence Mounting Medium	IF	Dako	Cat # S3023
Fetal Bovine Serum	IF	Sigma Merck	Cat #F7524
TWEEN® 20	IF	Sigma Merck	Cat # P1379
PBS 1X	Cell Isolation	Corning	Cat # 20-031-CV
HBSS 10X	Cell Isolation	ThermoFisher Scientific	Cat # 14025092
Adult Brain Dissociation kit	Cell Isolation	Miltenyi Biotech	Cat # 130-107-677
Non-neuronal biotin antibody cocktail	Cell Isolation	Miltenyi Biotech	Cat # 130-115-389
CD8 T cell isolation kit	Cell Isolation	Miltenyi Biotech	Cat # 130-104-075
Percoll®	Cell isolation	Merk Millipore	Cat # GE17-0891-01
Dextran from Leuconostoc spp.	Cell isolation	Sigma Merck	Cat # 31392
Heparin bms	Cell isolation	BRISTOL-MYERS SQUIBB	AIC 13732019
Chromium Single Cell 3′ GEM, Library & Gel Bead Kit v3	Sequencing	10X Genomics	Cat # PN-1000092
Chromium NextGem Single Cell 3' GEM Library & Gel Bead kit v3.1, 4rx	Sequencing	10X Genomics	Cat # PN-1000128

Chromium Next GEM Chip G Single Cell kit, 16 rxn	Sequencing	10X Genomics	Cat # PN-1000127
NextSeq® 500 High Output v2.5 Kit (150 cycles)	Sequencing	Illumina	Cat # 20024907
Sucrose	Brain Storage	Sigma Merck	Cat # 84100
Sodium azide	Brain Storage	Sigma Merck	Cat # S8032
OCT gel (optimum cutting temperature)	Brain Storage	DDK Italia	Cat # 22-118

FC = Flow Cytometry, IHC/IF= Immunohistochemistry/Immunofluorescence staining,

Mice

The mouse strains 3xTg-AD (MMRRC stock no. 34830-JAX), *Itgal*$^{-/-}$ (stock no. 005257) and wild-type strains B6129SF2/J (stock no. 101045) were purchased from the Jackson Laboratory. 3xTg-AD mice harbor human mutations for APP, PSEN1 and TAU proteins, developing both amyloid and tau pathologies. We crossed 3xTg-AD and *Itgal*$^{-/-}$ mice to obtain a transgenic line with all transgenes from the 3xTg-AD and *Itgal*$^{-/-}$ models (APPSwe, tauP301L, PS1M146V knock-in and LFA-1 knockout). Animals were group housed in pathogen-free climate-controlled facilities and were provided with food and water *ad libitum*. Research involving animals was authorized by the Ethical Committee from the University of Verona and by the Italian Ministry of Health, Department of Veterinary Public Health, Nutrition and Food Safety, Directorate General of Animal Health and Veterinary Medicine (authorization no. 164/2016-PR), as required by Italian legislation (D. Lgs 26/2014) as per the application of European Directive (2010/63/UE). All efforts were made to minimize the number of animals used and their suffering during the experimental procedures.

Isolation of leukocytes from mouse tissues

Mice were anesthetized and perfused through the left cardiac ventricle by injecting 40 ml of cold phosphate-buffered saline 1X (PBS 1X) with calcium and magnesium.

Meninges

Individual meninges (dura, arachnoid, and pia mater) were carefully removed from the interior aspect of skulls and surfaces of brains with fine surgical curved scissors and forceps, and enzymatically digested with a collagenase/DNase I solution at 37 °C for 15 min. The cell pellets were washed, resuspended in ice-cold PBS 1X and, after cell blocking with an anti-CD16/32 Fc-Block (1:100, BD Biosciences) for 10 minutes at RT, stained for extracellular markers for 25 minutes in staining buffer (PBS1X with 10% Fetal Bovine Serum - FBS) at 4°C. The primary antibodies used for CD8+ T cells detection and characterization were: CD11a/CD18 FITC (1:50, Miltenyi Biotech), CD103 BV421 (1:50, BD Biosciences), CD8 APC-H7 (1:50, BD Biosciences), CD69 BV650 (1:50, BD Biosciences), TCRγδ PE-CF594 (1:50, BD Biosciences), CD62L PE (1:50, BD Biosciences), CD45 BV605 (1:50, BD Biosciences), CD27 APC (1:50, BD Biosciences), CD11b APC-R700 (1:50, BD Biosciences), Ly6G BV510 (1:50, BD Biosciences), CD4 PE-Cy7 (1:50, BD Biosciences), CD197 BV786 (1:50, BD Biosciences), and CD44 BV711 (1:50, BD Biosciences). Cells were then stained with 7AAD viability dye (BD biosciences) for 5 minutes at RT before flow cytometry analysis.

Alternatively, samples were stained with Viobility™ Fixable Dye (1:100, Miltenyi Biotec) for 15 minutes RT in the dark. After washing, cells were stained with CD45 APC-Vio770 (1:100, Miltenyi Biotec), CD8 PE-Cy7 (1:100, BioLegend), CD103 BV421 (1:100, BD Biosciences), CD3 BV650 (1:100, BD Biosciences) surface markers for 25 minutes at 4°C in the dark. Cells were washed and resuspended firstly in Fixation buffer (BD Biosciences) and next in Intracellular Staining Perm Wash Buffer 1X (BD Biosciences). In the end, sample was stained with the anti-GrK primary antibody (1:100, PA550980, ThermoFisher Scientific) for 25 minutes at 4°C in the dark, and then with the AlexaFluor488 secondary antibody (1:100 ThermoFisher Scientific) for other 25 minutes at 4°C in the dark.

Brain

Brains were collected in ice-cold RPMI culture medium, separated from the choroid plexus and pia mater. They were homogenized using a gentleMACS Dissociator (Miltenyi Biotec), and enzymatically digested with a collagenase/DNase I solution at 37 °C for 45 min. Cells were passed through a 70-µm cell strainer into a new tube for Percoll gradient centrifugation, and cells recovered from the interphase were washed with PBS 1X. After cell blocking by an anti-CD16/32 Fc-Block (1:100, BD Biosciences) for 10 minutes at RT, sample was stained with the appropriate antibodies panel for 25 minutes in staining buffer (PBS1X with 10% FBS) at 4°C. The primary antibodies used for CD8+ T cells detection and characterization were: CD11a/CD18 FITC (1:50, Miltenyi Biotech), CD103 BV421 (1:50, BD Biosciences), CD8 APC-H7 (1:50, BD Biosciences), CD69 BV650 (1:50, BD Biosciences), TCRγδ PE-CF594 (1:50, BD Biosciences), CD62L PE (1:50, BD Biosciences), CD45 BV605 (1:50, BD Biosciences), CD27 APC (1:50, BD Biosciences), CD11b APC-R700 (1:50, BD Biosciences), Ly6G BV510 (1:50, BD Biosciences), CD4 PE-Cy7 (1:50, BD Biosciences), CD197 BV786 (1:50, BD Biosciences), and CD44 BV711 (1:50, BD Biosciences). Cells were then stained with 7AAD viability dye (BD biosciences) for 5 minutes at RT before flow cytometry analysis. Alternatively, samples were stained with Viobility™ Fixable Dye (1:100, Miltenyi Biotec) for 15 minutes RT in the dark. After washing, cells were stained with CD45 APC-Vio770 (1:100, Miltenyi Biotec), CD8 PE-Cy7 (1:100, BioLegend), CD103 BV421 (1:100, BD Biosciences), CD3 BV650 (1:100, BD Biosciences) surface markers for 25 minutes at 4°C in the dark. Cells were washed and resuspended firstly in Fixation buffer (BD Biosciences) and next in Intracellular Staining Perm Wash Buffer 1X (BD Biosciences). In the end, sample was stained with the primary anti-GrK antibody (1:100, PA550980, ThermoFisher Scientific) for 25 minutes at 4°C in the dark, and then with the AlexaFluor488 secondary antibody (1:100 ThermoFisher Scientific) for other 25 minutes at 4°C in the dark.

Blood

Blood samples were collected from the retro-orbital plexus of anesthetized mice using sodium heparinized capillaries and were mixed with an equal volume of 1% dextran plus 10 U/ml sodium heparin. After pelleting the erythrocytes, the overlying supernatant plasma/dextran suspension of leukocytes was washed in PBS, followed by erythrocyte lysis by sodium chloride (NaCl) 0.2% and 1.2%. Then, cells were blocked using an anti-CD16/32 Fc-Block (1:100, BD Biosciences) for 10 minutes at RT and stained with appropriate antibodies for 25 minutes in staining buffer (PBS1X with 10% FBS) at 4°C. The primary antibodies used for CD8+ T cells detection and characterization were: CD11a/CD18 FITC (1:50, Miltenyi Biotech), CD62L PE (1:50, BD Biosciences), TCRγδ PE-CF594 (1:50, BD Biosciences), VLA-4 PeCy7 (1:50, Biolegend), Ly6G BV421 (1:50, BD Biosciences), CD44 BV510 (1:50, BD Biosciences), CD45 BV786 (1:50, BD Biosciences), CD4 APC (1:50, BD Biosciences), CD11b APC-R700 (1:50, BD Biosciences), and CD8 APC-H7 (1:50, BD Biosciences). Cells were then stained with 7AAD viability dye (BD biosciences) for 5 minutes at RT before flow cytometry analysis.

Spleen

Spleens were mechanically disrupted, and single-cell suspensions were obtained by passing the cells through a 70-µm strainer. After erythrocyte lysis by NaCl 0.2% and 1.2%, the cells were blocked using an anti-CD16/32 Fc-Block (1:100, BD Biosciences) for 10 minutes at RT and stained with appropriate antibodies for 25 minutes in staining buffer (PBS1X with 10% FBS) at 4°C. The primary antibodies used for CD8+ T cells detection and characterization were: CD11a/CD18 FITC (1:50, Miltenyi Biotech), CD103 BV421 (1:50, BD Biosciences), CD8 APC-H7 (1:50, BD Biosciences), CD69 BV650 (1:50, BD Biosciences), TCRγδ PE-CF594 (1:50, BD Biosciences), CD62L PE (1:50, BD Biosciences), CD45 BV605 (1:50, BD Biosciences), CD27 APC (1:50, BD Biosciences), CD11b APC-R700 (1:50, BD Biosciences), Ly6G BV510 (1:50, BD Biosciences), CD4 PE-Cy7 (1:50, BD Biosciences), CD197 BV786 (1:50, BD Biosciences), and CD44 BV711 (1:50, BD Biosciences). Cells were then stained with 7AAD viability dye (BD biosciences) for 5 minutes at RT before flow cytometry analysis.

Liver

Livers were collected in ice-cold RPMI culture medium. They were mechanically homogenized firstly using a scalpel and then using a gentleMACS Dissociator (Miltenyi Biotec). Then they were enzymatically digested with a collagenase/DNase I solution at 37 °C for 30 min. Cells were passed through a 70-µm cell strainer into a new tube for Percoll gradient centrifugation, and cells recovered from the interphase were washed with PBS 1X. Thus, we stained samples with Viobility™ Fixable Dye (1:100, Miltenyi Biotec) for 15 minutes RT in the dark. After washing, cells were stained with

CD45 APC-Vio770 (1:100, Miltenyi Biotec), CD8 PE-Cy7 (1:100, BioLegend), CD103 BV421 (1:100, BD Biosciences), CD3 BV650 (1:100, BD Biosciences) surface markers for 25 minutes at 4°C in the dark. Cells were washed and resuspended firstly in Fixation buffer (BD Biosciences) and next in Intracellular Staining Perm Wash Buffer 1X (BD Biosciences). In the end, sample was stained with the primary anti-GrK antibody (1:100, PA550980, ThermoFisher Scientific) for 25 minutes at 4°C in the dark, and then with the AlexaFluor488 secondary antibody (1:100, ThermoFisher Scientific) for other 25 minutes at 4°C in the dark. Alternatively, CD8+ T cells were enriched in the sample by negative selection using a CD8a+ T cell isolation kit following the manufacturer's instructions. After cell blocking by an anti-CD16/32 Fc-Block (1:100, BD Biosciences) for 10 minutes at RT, sample was stained with the appropriate antibodies panel for 25 minutes in staining buffer (PBS1X with 10% FBS) at 4°C. The primary antibodies used for the identification and cell sorting of CD8+ T cells subsets were: CD103 BV421 (1:20, BD Biosciences), and CD8 APC-H7 (1:520, BD Biosciences). Cells were then stained with 7AAD viability dye (BD biosciences) for 5 minutes at RT before cell sorting.

Flow cytometry analysis

Flow cytometry analysis was performed using LSR Fortessa X-20 flow cytometer (BD) with BD FACSDiva software (8.0.1 BD). Data were analyzed with FlowJo Software. As gating strategy, we take cell of interest discriminating doublets. We counted as living cells those negative for 7AAD viability dye. Cells were next gated for CD45 expression, identifying leukocytes. Next, we removed all the other cell subsets (Neutrophils Ly6g+ CD11b+; Myeloid cells CD11b+; γδ T cells TCR γδ +; CD4+ T cells) before detecting CD8+ T cells. Among these cells, we gated CD103+ CD69+ and CD103- CD69+ lymphocytes in brain, meninges, and spleen (Fig. 8 a-c). Differently, in blood samples we gated CD44+ KLRG1+, and CD44+/- KLRG1- CD8+ T cells, also calculating the mean fluorescent intensity (MFI) of CD11a/CD18 expression on these cell subsets and the percentage of cells expressing LFA-1 integrin on the whole population of CD8+ T lymphocytes (Fig. 8 d). Moreover, we evaluate GrK intracellular expression in brain, meningeal, and hepatic CD8+ T lymphocytes. Viable CD45+ CD8+ T cells were tested for the expression of GrK and CD103 molecules, and GrK- CD103-, GrK^{MED} CD103-, and GrK^{HIGH} CD103- populations were analyzed. Of note, we tested the anti-GrK antibody before to proceed with the experiments. A GrK+ population was correctly detected in the stained sample compared to unstained and FITC Fluorescence Minus One (FMO) control (Fig. 8 n-q). All experimental groups consisted of both male and female.

Cell sorting

Livers were collected from 3xTg-AD mice between 6 and 8 months of age, and dissociated and stained as previously described. Hepatic CD103+ CD8+ and CD103- CD8+ T cells were sorted using FACSAria Fusion device (BD) with BD FACSDiva software (8.0.1 BD) from the viable population (Fig. 8 e). Of note, we confirmed that the isolated hepatic CD8+ T cells expressed CD69+ surface molecule, ensuring the Trm phenotype of these cells before proceeding with the cell sorting (Fig. 8 f). Next, freshly sorted CD8+ T cells were washed and seeded in complete RPMI medium supplemented of 2.5% antibiotics, 1% glutamine, 10%FBS, IL-2 (5 ng/ml, R&D systems) and IL-7 (5 ng/ml, R&D systems) overnight before *in vitro* co-cultures. We performed experiments with cells isolated from male and female mice, recording no differences.

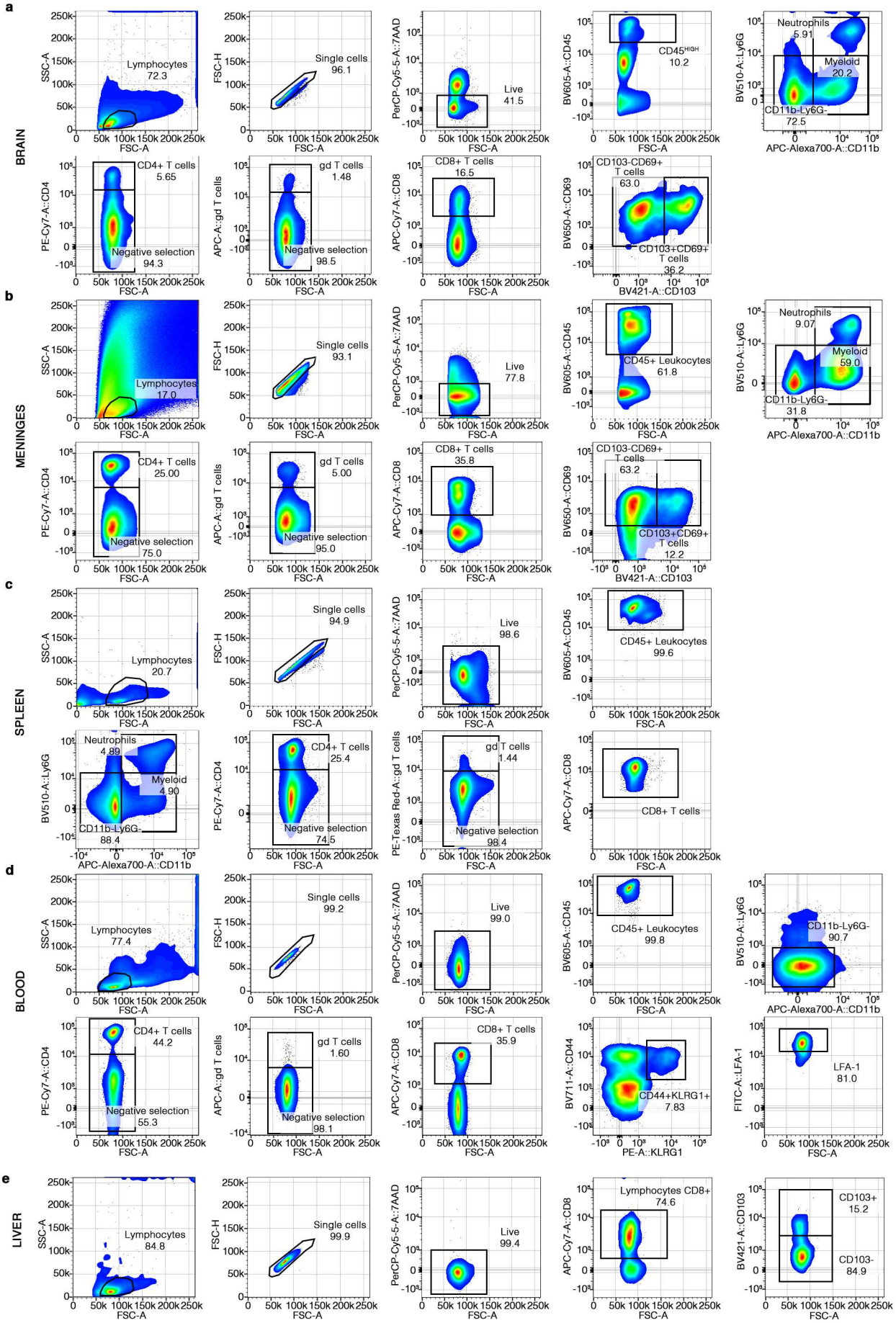
a
BRAIN
Lymphocytes 72.3
Single cells 96.1
Live 41.5
CD45HIGH 10.2
Neutrophils 5.91
Myeloid 20.2
CD11b-Ly6G- 72.5
CD4+ T cells 5.65
Negative selection 94.3
gd T cells 1.48
Negative selection 98.5
CD8+ T cells 16.5
CD103-CD69+ T cells 63.0
CD103+CD69+ T cells 36.2
b
MENINGES
Lymphocytes 17.0
Single cells 93.1
Live 77.8
CD45+ Leukocytes 61.8
Neutrophils 9.07
Myeloid 59.0
CD11b-Ly6G- 31.8
CD4+ T cells 25.00
Negative selection 75.0
gd T cells 5.00
Negative selection 95.0
CD8+ T cells 35.8
CD103-CD69+ T cells 63.2
CD103+CD69+ T cells 12.2
c
SPLEEN
Lymphocytes 20.7
Single cells 94.9
Live 98.6
CD45+ Leukocytes 99.6
Neutrophils 4.89
Myeloid 4.90
CD11b-Ly6G- 88.4
CD4+ T cells 25.4
Negative selection 74.5
gd T cells 1.44
Negative selection 98.4
CD8+ T cells
d
BLOOD
Lymphocytes 77.4
Single cells 99.2
Live 99.0
CD45+ Leukocytes 99.8
CD11b-Ly6G- 90.7
CD4+ T cells 44.2
Negative selection 55.3
gd T cells 1.60
Negative selection 98.1
CD8+ T cells 35.9
CD44+KLRG1+ 7.83
LFA-1 81.0
e
LIVER
Lymphocytes 84.8
Single cells 99.9
Live 99.4
Lymphocytes CD8+ 74.6
CD103+ 15.2
CD103- 84.9
SSC-A
FSC-H
FSC-A
PerCP-Cy5-5-A::7AAD
BV605-A::CD45
BV510-A::Ly6G
APC-Alexa700-A::CD11b
PE-Cy7-A::CD4
APC-A::gd T cells
APC-Cy7-A::CD8
BV650-A::CD69
BV421-A::CD103
PE-Texas Red-A::gd T cells
BV711-A::CD44
PE-A::KLRG1
FITC-A::LFA-1

Fig. 8 | Gating strategy. a, b, Gating strategies for the detection of CD103+ CD69+ and CD103- CD69+ Trm CD8+ T cells in brain (a) and meninges (b). **c,** Gating strategies for the detection of splenic CD8+ T cells. **d,** Gating strategy for the detection of circulating CD44+ KLRG1+ Effector ($Teff^{circ}$) and CD44+/- KLRG1- Tcm (Tcm^{circ}) CD8+ T lymphocytes, and the analysis of LFA-1 integrin surface expression on them. **e**, Dot plots showing the gating strategy used for the sorting of CD103+ and CD103- Trm CD8+ T cells from the liver of 3xTg-AD mice.

Single-cell RNA sequencing

Sample preparation

Meninges and brain were collected and homogenized as described above. Pools of eight female mice (3xTg-AD or WT Control) were used. The isolated leukocytes were washed with PBS 1X and labeled with an anti-CD45 BV480 antibody (1:20, BD Biosciences). After cell resuspension in PBS 1X with FBS10%, CD45+ and $CD45^{high}$ cells were sorted from meninges and brain, respectively. We used FACSAria Fusion device (BD) with BD FACSDiva software (8.0.1 BD). Both the 3xTg-AD and wild-type samples consisted of > 98% viable cells. Similarly, circulating leukocytes, isolated as previously described, after staining with anti-CD45 BV480 antibody (1:20, BD Biosciences) were sorted on FACSAria Fusion device (BD) with BD FACSDiva software (8.0.1 BD).

Sequencing

Sorted cells were resuspended to a final concentration of 700 cells/µl and cDNA sequencing libraries were prepared using the 10× Genomics Chromium Controller and the Chromium Single Cell 3′ GEM, Library and Gel Bead kit v3 (Pleasanton) following the manufacturer's instructions. Briefly, 10,000 live cells were loaded onto the Chromium Controller to recover 4000 single-cell gel-bead emulsions (GEMs) per inlet, uniquely barcoded. After cDNA synthesis, sequencing libraries were generated and final 10× library quality was assessed using the Fragment Analyzer High Sensitivity NGS kit (Agilent Technologies) before sequencing on the Illumina NextSeq500 platform, generating 75-bp paired-end reads (28 bp read 1, 91 bp read 2) at a depth of 50,000 reads per cell, yielding a median per-library depth of 72,783 reads per cell.

Single-cell RNA-seq data cleaning

Raw base call (BCL) files were processed using Cell Ranger v 6.0.1 (10× Genomics) to obtain a unique molecular identifier (UMI) count table for each sample. Briefly, two pipelines were used: *cellranger mkfastq*, which converts BCL files into FASTQ files, and *cellranger counts*, which takes FASTQ files from *cellranger mkfastq* and performs alignment, filtering, barcode counting, and UMI counting. To perform these steps, *Mus musculus* reference data (version mm10 2020-A) were downloaded from the 10× official website.

Normalization and analysis of Single cell RNAseq data

The SingleCellExperiment object was uploaded and analyzed using Partek Flow analysis software. As first, we filtered out low quality cells, such as doublets, damaged cells, or those with too few reads, evaluating the number of read counts per cell, the number of detected genes per cell and the percentage of mitochondrial reads per cell. After the recommended normalization, through which counts were normalized and presented in logarithmic scale in CPM (count per million) approach, features were filtered excluding genes that are not expressed by any cells in the dataset. Batch correction was provided using Harmony task, available in the Partek Flow. PCA and UMAP dimensional reduction were performed before cell clustering based on AUCell task, which is a tool that permits to identify cells that are actively expressing genes within a gene list. We used published and available gene lists to identify cells by AUCell function. CD8+ T cells were then extracted and subclustered. The identified cell subsets were characterized using the AUCell task basing on gene lists recently published in literature[100]. Clusters biomarkers were automatically computed by the software performing a Student' t-test on the selected attribute, comparing one subgroup at a time with all the others combined. Next, gene specific analysis (GSA), pathway analysis, and gene set enrichment analysis (GSEA) were performed on the cell population of interest using Partek Flow plugins. Similarly, we used Partek software to run, after the scaling expression, the trajectory analysis, based on monocle 3 R package. We thus identified states and branch points, also calculating pseudotime values. Partek was also used to generate Fig.s for violin plots representing gene expressions.

Analysis of other Single cell RNAseq dataset

We analyzed two available dataset of Single cell RNAseq data in human patients. One of CSF, by Gate et al.[156] (accessible under the accession code GSE134578), and the other of circulating leukocytes by Xu et al.[157] (accessible under the accession code GSE181279). We analyzed each of these datasets with PartekFlow software as previously described for our datasets but using human references.

Neurons isolation and culture

Hippocampal and cortical brain regions were dissected from the brains of new-born 3xTg-AD 3 to 9 days old and dissociated using the Adult Brain Dissociation kit (Miltenyi Biotec) and the gentleMACS Dissociator (Miltenyi Biotec) according to manufacturer's instructions. After removing debris and red blood cells, sample was labeled with a non-neuronal biotin antibody cocktail (Miltenyi Biotec), and neurons were enriched by negative selection. Neurons were resuspended in Neurobasal medium (Gibco) with 2% B-27 supplement (Gibco), 1% L-glutamine (Corning) and 1%

penicillin/streptomycin (Sigma-Aldrich). We seeded 200.000 neurons/well in 48-well plates pre-coated with poly-D-lysine and laminin (Sigma-Aldrich). Neurons were cultured for two weeks, and half of the culture medium was replaced with fresh medium every other day. Purity of neurons was over 95%, as previously checked.

Measurement of intracellular calcium release by neurons

In vitro co-cultures of CD8+ T cells on neurons

Neurons were labeled with Biotracker 609 Red Ca^{2+} AM Dye (Merck Millipore) according to the manufacturer's instructions. In parallel, CD103+ CD8+ and CD103- CD8+ T cells were washed and labelled with CellTracker™ Blue CMAC Dye (ThermoFisher Scientific). Thereafter, CD103+ CD8+ and CD103- CD8+ T cells were seeded separately on neurons in a 1:4 ratio. Neurons in absence of CD8+ T cells were used as negative control, whereas neurons treated with 10 μm ionomycin (Sigma-Aldrich) were used as positive controls. All cells were resuspended in phenol red-free medium to avoid potential phototoxic phenomena during acquisition. Ca^{2+}-dependent changes of intracellular fluorescence were acquired with a LD Plan-Neofluar 20×/0.4 Korr M27 objective mounted on AxioObserver 7 microscope (Zeiss), equipped with a thermostatic chamber and a Hamamatsu camera. Exposure time was manually set and eft unmodified through time-lapse experiments. Images were acquired every 10 minutes for 5 hours under controlled conditions. Multi-field acquisition was attained using the tiles tool with smart autofocus. For each scene, time lapse videos were split into individual frames and analyzed using ZEN v2.6 software (Zeiss). Data were expressed as the positive area for intracellular Ca^{2+} staining overtime.

In vitro co-cultures of neurons with purified GrK active enzyme and SCH79797 PAR-1 inhibitor

Neurons isolated as previously described were labeled with Biotracker 609 Red Ca^{2+} AM Dye (Merck Millipore) according to the manufacturer's instructions. Then they were resuspended in phenol red-free medium before adding mouse recombinant purified GrK active enzyme (Cusabio CSB-EP010084MO) at different final concentrations: 75 nM and 150 nM. Ca^{2+}-dependent changes were recorded and analyzed as previously described. Moreover, neurons were also co-cultured with GrK active enzyme (150 nM) in presence of SCH79797 PAR-1 inhibitor at different final concentrations: 50 nM and 100 nM

***In vitro* tracking of cell motility**

Sequences of image acquisition were transformed into two-dimensional time lapses, and CD103- CD8+ and CD103+ CD8+ T cell movement was analyzed frame by frame using Imaris software

version 9.6 (Bitplane, Inc). Two-dimensional spatial position of each cell was detected based on centroid fluorescent intensity. Tracks for each cell consisted of serial sets of x and y coordinates of single cell centroid. Cells were tracked over the time automatically and tracks greater than 50 min (≥ 5 time points) were manually corrected and then included in the analysis. We considered the following parameters to evaluate the behavior of the two subsets of CD8+ T cells along with time lapse experiment: Track displacement length, Track length, Track speed max, Track speed mean, Track spread min, Track speed variation, Track straightness. Thus, we performed a R-based t-distributed Stochastic Neighbor Embedding (tSNE) dimensional reduction to observe behavioral changes between CD103- and CD103+ CD8+ T lymphocytes.

Ablation of circulating CD8+ T cells

Female and male 3xTg-AD and WT control mice of 6 months of age were treated using an anti-CD8a depleting antibody (0.22 mg, BioXCell) for a total of four weeks. Treatment was performed every other day through an intraperitoneal injection. Control mice were treated with an isotype antibody. For this *in vivo* experiment we treated mice of the same cage half with the depleting antibody and half with the isotype control. Starting from 4 weeks before the experiment and throughout the experiment mice were housed in the same rack in order to minimize biological variability induced by external environment. Blood was drawn as previously described to confirm ablation of circulating CD8+ T cells.

Behavioral tests

We performed behavioral tests in a special animal experiment room at the animal facility of the University of Verona, under constant light and environmental conditions. Learning and spatial reference memory of treated mice and controls was determined using the Morris water maze (MWM) test, as previously described[74]. Differently, to assess the associative memory of treated and isotype control mice we performed contextual fear conditioning (CFC) task, as previously described[49,74]. Before MWM and CFC, we evaluate the basic abilities and anxiety of the mice through ledge, hindlimb clasping and open field tests. Ledge is a direct measure of coordination and consists in placing mice on cage's ledge, where they typically walk along, attempting to descend back to the cage. A scoring system is adopted to detect and evaluate coordination deficits, and the test was conducted in triplicate[158]. Differently, during hindlimb clasping test mice lifted, and hindlimb position was observed for 10 seconds. Depending by hindlimb retraction a score is given[158]. Open field is a more complex test that evaluates locomotion, exploration, and anxiety of mice. Mice were placed into the open field squared cage (50 x 50 x 30 cm) and were left free to explore the environment for

20 minutes: 10 of acclimatization and 10 of test. Videos were analyzed by AnyMaze software to determine the time spent in the central part of the arena, and in the peripheral zones and corners.

Neuropathological analyses of mouse brain tissues

After behavioral tests mice were anesthetized and perfused, as previously described, with 25 ml of cold PBS 1X with calcium and magnesium and 25 ml of 4% paraformaldehyde (PFA) (in PBS 1X pH = 7.4). Brains were collected and placed in 4% PFA overnight. Next, brains were transferred in 30% sucrose for cryoprotection. When fully soaked with sucrose, brains were frozen protected by tissue-tek optimal cutting temperature (OCT) embedded compound. Then, they were cut in 30 μm slice using a cryostat (CM1520 Leica). Coronal sections, after incubation with blocking buffer (2 % Normal Goat Serum, plus 0.4 % Triton X-100 in PBS 1X) for 1 hour, were stained with anti-Aβ (6e10, 1:1000 BioLegend) antibody, and with anti-pTau (AT180, 1:200 ThermoFisher Scientific), and anti-total tau (HT7, 1:200 ThermoFisher Scientific) antibodies. Particularly, for Tau staining, the sections were treated with citrate buffer pH = 6 (BioOptica) at 85°C for 30 minutes for antigen retrieval. After washing with PBS 1X plus 0.05% Tween, sections were added in 3 % H_2O_2 for 10 minutes at RT, followed by the incubation with the biotinylated goat anti-mouse secondary antibodies for 2 hours at RT. The immunoreactivity was visualized as previously described[49]. Images were acquired with Plan-Apochromat 20×/0.8 M27 objective on Axio Imager.Z2 microscope equipped with Axiocam 506 Color (Zeiss). Images were analyzed with ZEN blue software. Brightness, contrast, and color balance were adjusted over the whole image without eliminating any information present in the original. Investigators were blinded with respect to the genotype of the mice and the treatment. We analyzed a minimum of three regions of interest (ROIs) in each brain slice, from a minimum of five sections per mouse. All experiments were done with one male and one female mouse per group.

Immunofluorescence staining on mouse tissues and image analysis

Free-floating PFA-fixed coronal mouse brains sections were incubated in blocking buffer (2 % Normal Goat Serum, plus 0.4 % Triton X-100 in PBS 1X) for 2 h at room temperature and then treated with rabbit anti-mouse ZO-1 antibody (1:500, 40-2200, Invitrogen) in blocking solution, overnight at 4 °C. After washing with PBS 1X plus 0.05% Tween-20, we added a goat anti-rabbit Alexa Fluor 488 fluor secondary antibody (1:500, A11034, Invitrogen) Nuclei were stained with DAPI (1:1000, D9542, Sigma-Aldrich) for 8 min in the dark. In the end, the sections were washed with PBS 1X, transferred to glass slides and mounted with Dako medium. Images were acquired with Plan-Apochromat 20×/0.8 M27 objective on Axio Imager.Z2 microscope equipped with a Hamamatsu camera using Zen Module Tiles and Positions (Zeiss), allowing to collect multiple

images of the entire specimen and then stitch together into single image. Brightness and contrast were adjusted over the whole image without eliminating any information present in the original.

Cell suspension immunofluorescence staining

Hepatic CD103- CD8+ (200.000 cells) and CD103+ CD8+ (200.000 cells) T lymphocytes, isolated as previously described, were fixed with 4% PFA for 20 minutes at RT. Fixed cells were washed and resuspended in blocking solution (2% NGS, 2% BSA, 0.2% Triton X-100) for 1hour at 4°C. Cells were stained firstly with anti-mouse GrK (1:250, Invitrogen) primary antibody for 1 hour at RT, and then with goat anti-rabbit AlexaFluor 647 secondary antibody (1:1000, Invitrogen) for 1 hour at 4°C in the dark. Nuclei were counterstained with DAPI (1:2000, Sigma-Aldrich). Cells were transferred on a poly-lysinated glass slide and left adhering for 20 minutes. Slides were mounted and acquired under the microscope Axio Imager.Z2 microscope (Zeiss) with a Plan Apochromat 100×/1.46 oil DIC (UV) M27 objective equipped with Hamamatsu camera.

Human brain samples

Formalin-fixed paraffin-embedded (FFPE) hippocampal sections of controls and Alzheimer's disease (AD) cases were obtained from the Medical Research Council (MRC) London Neurodegenerative Disease Brain Bank. All material was collected from donors from whom written informed consent for brain autopsy and the use of the material and clinical information for research purposes had been obtained by MRC London Neurodegenerative Disease Brain Bank. The neuropathology studies on human brain samples were approved by the Ethical Committee from the University of Verona and "Azienda Ospedaliera Universitaria Integrata" di Verona (protocol nr. 20794).

Immunofluorescence staining of human brain tissues

FFPE sections were deparaffinized and incubated with antigen retrevial solution. Sections will be treated with primary antibodies: anti-CD8 alpha antibody (1:100, ab4055, abcam), anti-CD103 antibody (1:100, ab129202, abcam), anti-GrK antibody (1:100, PA550980, ThermoFisher Scientific). The sections were incubated sequentially overnight at 4°C in blocking solution (5% BSA, 2% Normal Goat Serum and 0.5% Triton x-100) and then add appropriate fluorophore-conjugated secondary antibodies. Nuclei were stained with DAPI (Sigma) for 7 min in the dark. Finally, the sections were mounted with Dako medium. Images were acquired blindly using a Zeiss Axio Imager.Z2 microscope (Zeiss).

Statistical analysis

For statistical analysis, the GraphPad Prism 9.0 (v 9.0.0) was used. Data are depicted as mean with standard deviation (SD) or standard error of the mean (SEM) as indicated in the respective Fig. legends. P -values of $p < 0.0001$ or $p < 0001$ were considered extremely significant, $p < 0.01$ very significant, and $p < 0.05$ significant. Data were tested with Student' t-test to compare unmatched groups with non-Gaussian distribution, or with two-way analysis of variance (ANOVA) followed by Turkey's multiple comparison to determine differences among multiple dataset (threshold for significance: $P \leq 0.05$). We used G*Power 3.1 software to calculate the effect size of each dataset starting from the mean and standard deviation of the two groups (n1 = n2) followed by the calculation of Cohen's d coefficient. Statistical analyses are all available in the supplementary section. The exact number of animals/samples used in each experiment is specified in Fig. legends.

Data and code availability

Our datasets of scRNA-seq data are deposited online in the GEO, and are publicly available under accession numbers GSE155214 for brain and meninges, and GSE216485 for blood analyses as of the date of publication. Similarly, human scRNA-seq datasets obtained from Xu et al. (Xu 2021, Frontiers), and Gate et al. (Gate, Nature 2020), are available under GSE181279 and GSE134578 accession codes, respectively. All data associated with this study can be found in the paper of in supplementary materials. Source data are provided with this paper. Microscopy data showed in this paper will be shared by the lead contact upon request.

RESULTS

Dysregulation of CD8 T cell compartment in the CNS of 3xTg-AD mice during early disease

It has been recently suggested that CD8+ T cells play a detrimental role during AD progression[50–53]. However, how CD8+ T lymphocytes contribute to AD pathology is still unknown. To uncover phenotypical and functional alterations of CD8+ T cells in the context of early AD development, we performed single-cell RNA sequencing (scRNAseq) of $CD45^{high}$ cells isolated from the meninges and brains of 6-month-old 3xTg-AD mice and sex- and age-matched WT controls (Fig. 9 a). Notably, the analysis of CD8+ T cells at single-cell level was never previously performed in mice with AD-like disease during early disease stages.

To relate changes in the CD8+ T cell population across tissues and conditions, we merged data from all anatomic sites (brain and meninges) from 3xTg-AD and WT control mice. The analyses performed with the PartekFlow software revealed the presence of 5 subsets of CD8+ T cells populating the brain and its borders: (i) CD103- Trm cells exhibiting high expression of *Cxcr6*, *Cxcr3*, and *Gzmk* genes; (ii) effector lymphocytes, which best biomarker genes were *Gzma*, *S1pr5*, and *Cx3cr1* ; (iii) Tcm cells characterized by the expression of *Sell* and *Ccr7*; (iv) Proliferating Trm (Trm^{PROL}) lymphocytes that upregulated *Chek1* and *Stmn1* genes; and (v) CD103+ Trm cells showing a high expression of *Gstp3* and *Foxo1* genes (Fig. 9 b-g). In addition, CD103+ Trm as well as Trm^{PROL} lymphocytes were characterized by the expression of *Itgae* gene, codifying for CD103 integrin, which binds E-cadherin cellular adhesion molecule (CAM), normally found on epithelial cells, permitting tissue retention and "residency" phenotype[99,108] (Fig. 9 h). Interestingly, effector and Tcm cell populations also highly expressed *Klf2* gene in agreement with their migratory phenotype, whereas in contrast, Trm lymphocytes downregulated this gene (data not shown) [99,159–161]. Moreover, the increased expression of Chekpoint Kinase 1 (CHK1) serine/threonine protein kinase and Stathmin 1 cytoplasmic phosphoprotein regulating cell cycle progression exhibited by Trm^{PROL} cells was associated with the upregulation of *Mki67* gene160, 161 (Fig. 9 i). This gene encodes for Ki67 proliferation marker, which expression was drastically impaired in 3xTg-AD mice compared to WT controls, suggesting a dysfunction of this T cell subset during early disease stages (Fig. 9 j). Interestingly, also the global expression of *Itgae* gene was dramatically reduced in 3xTg-AD mice compared to WT controls, highlighting that CD8+ T cells in the brains of AD mice lose the "residency" phenotype (Fig. 9 k). In line with this, pie charts showed a dramatic reduction of CD103+ Trm CD8+ T cells (blue), paralleled by a great increase in the fraction of *Cxcr6* expressing CD103- Trm CD8+ T compartment (red) in the brain of AD mice (Fig. 9 l). Flow cytometry analyses confirmed the presence of immune unbalances in the CD69+ Trm compartment of CD8+ T cells in the brains of 3xTg-AD mice, showing a significant increase of pro-inflammatory CD103- Trm cells paralleled by a significant decrease of

CD103+ Trm lymphocytes in the brain of 3xTg-AD mice compared to sex- and age-matched WT control animals (Fig. 9 m, n). In contrast, only slight differences were observed in the meninges of 3xTg-AD mice compared to WT controls, indicating that early CD8 T cells dysregulation mainly occur in the brain parenchyma (data not shown). Therefore, **we focused our work on CD8 T cell alterations occurring in the brains of AD mice** during the early stages of disease.

The great reduction of CD103+ Trm CD8+ T lymphocytes in the AD context was consistent with the strong downregulation of several genes related to this cell phenotype (*Fabp5*, *Stat1*, *Stat3*, *Stat4*, *Stat5a*, *Stat5b*, *Smad4*, *Smad6*, *Smad7*, *Smad9*) in CD8+ T cells of 3xTg-AD mice compared to control mice[109] (Fig. 9 o). Conversely, *Eomes* and *S1pr1* genes, whose expression inhibits the phenotype of CD103+ Trm cells, were highly upregulated by CD8+ T cells from 3xTg-AD mice compared to WT animals, as shown by both heatmap and violin plots[109] (Fig. 9 o, q). Besides, the loss of CD103+ Trm CD8+ T cells in 3xTg-AD mice was supported by the alteration of the cytokine squad secreted in the extracellular milieu of AD mice. Notably, our data show a global downregulation of all the genes codifying for key cytokines involved in the differentiation and maintenance of CD103+ Trm cells (*Il15*, *Il7*, *Tgfb3*, *Tgfb2*, *Tgfb1*, *Il21*, *Tnf*, *Il33*) in 3xTg-AD mice in respect to controls[109,163] (Fig. 9 p). Among them, we observed a drastic reduction of *Il21*, *and Il33*, as shown in the violin plots (Fig. 9 q). These data are in line with recent results showing that the anti-inflammatory role of IL- 33 is lost in AD[164], and with previous results demonstrating that IL-21 has a role in the induction of CD103+ Trm phenotype [165,166]. Globally, our data suggest a profound and early dysregulation of the Trm CD8+ T cell subsets, characterized by the loss of immune protection exerted by memory-like CD103+ Trm CD8+ T cells and the increase of pro-inflammatory CD103- Trm CD8+ T lymphocytes, potentially promoting disease development[111].

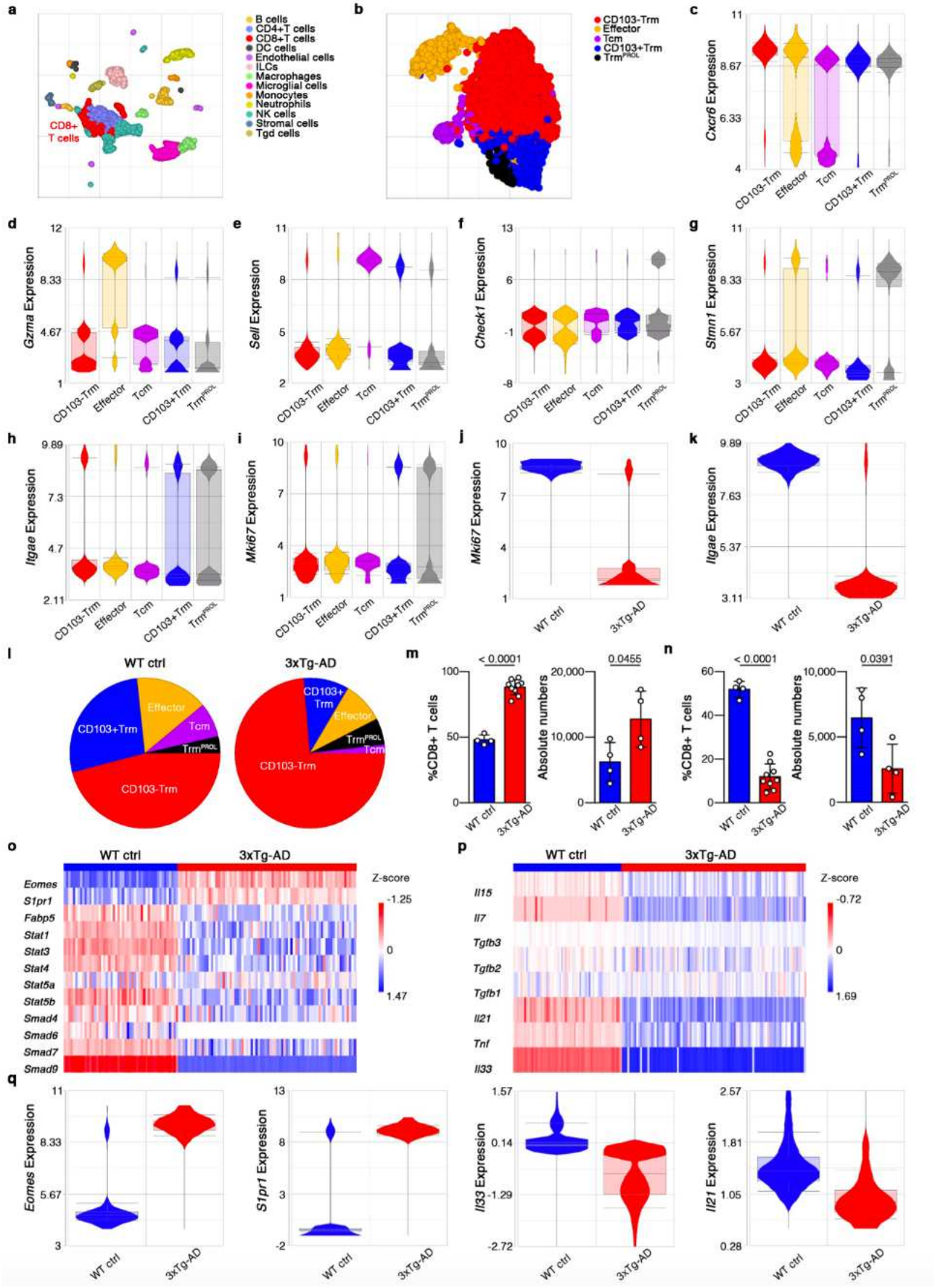

Fig. 9 | Pathological changes in Trm CD8+ T cell compartment in 3xTg-AD mice. a, UMAP plot of single cell transcriptome profiles showing immune cell subsets populating the brain and meninges of 6-month-old WT control (Control) and 3xTg-AD mice. **b**, UMAP plots showing CD8+ T cell sub-populations detected in the brain and meninges of 6-month-old WT Control and 3xTg-AD

mice. **c-k**, Violin plots showing *Cxcr6*, *Gzma*, *Sell*, *Check1*, *Stmn1*, *Itgae, Mki67* gene expressions in the different CD8+ T cells subsets in 3xTg-AD and WT Control mice. Box and whisker represent the mean and the SD of the plotted data. **l**, Pie plots representing the composition of the CD8+ T cell compartment in the brain of WT Control (left) and 3xTg-AD (right) mice. **m, n**, Percentages (left) and absolute numbers (right) of CD103- (o) and CD103+ (p) Trm CD8+ T cells in the brain of WT Control (n = 4) and 3xTg-AD (n = 4-9) mice at 6 months of age. *p*-values show Student' t-test for unpaired data. No bars indicate no significant difference. SD is plotted. **o-q**, Heatmaps and violin plots showing the expression of genes associated to the CD103- or CD103+ Trm CD8+ T cell phenotypes (q) or encoding for cytokines fundamental for the differentiation of CD103+ Trm CD8+ T lymphocytes (r) in 6-month-old WT Control and 3xTg-AD mice. Box and whisker represent the mean and the SD of the plotted data.

CD103- Trm CD8+ T lymphocytes are increased in the brains of 3xTg-AD mice

To further understand the alterations of CD8 T cell compartment in AD, we next performed a cell fate trajectory analysis of CD8+ T cells merging the data obtained from 3xTg-AD and WT mice. The results revealed two groups of CD8+ T lymphocytes: (i) the smallest one, organized as a continuum; and (ii) the largest one, in which the cells followed two differentiation paths, starting from a common root (Fig. 10 a). Arm "A" was more populated by *Itgae* expressing CD8+ T cells, whereas *Eomes* expressing CD8+ T lymphocytes, giving rise to the pro-inflammatory CD103- Trm population, were more abundant in the arm "B" of the trajectory plot (Fig. 10 b-c). Interestingly, trajectory plots clearly showed that only a small fraction of CD8+ T cells are present in the brain parenchyma of WT control mice, mainly differentiating into CD103+ Trm cells of the arm "A" (blue cells) (Fig. 10 d). On the contrary, CD8+ T lymphocytes accumulated in the brain of 3xTg-AD mice as CD103- Trm lymphocytes (red cells) of the arm "B" of the trajectory plot (Fig. 10 d). Of note, and in accordance with data shown above, few CD8+ T cells differentiate into the CD103+ Trm subset (blue cells) in the brain of 3xTg-AD mice. Together, these data further highlight a role for CD103-Trm cells in the pathogenesis of AD.

Our data also showed that CD103- Trm CD8+ T lymphocytes accumulating in the AD brains exhibit an increased expression of *Ifnar1* gene, which codifies for one of the two chains of interferons (IFN) type I receptors (Fig. 10 e)[12]. This suggests an activated effector phenotype for CD103- Trm CD8+ T cells populating the AD-brains during the early stages of the disease course[167]. Moreover, it was previously shown that activation of type I IFN signaling promotes the release of CXCR3+-effector T cells chemoattracts, such as CXCL10, whose expression was increased in the brain of $CD45^{high}$ leukocytes from 3xTg-AD mice compared to WT controls[168](Fig. 10 f). Notably, our single cell RNA sequencing analyses reported *Cxcr3* as the second biomarker gene of the CD103- Trm subset of CD8+ T lymphocytes, and, as expected, its expression was increased in the brain of 3xTg-AD mice compared to control animals, suggesting that these cells could be increasingly recalled into the AD brain by an augmented CXCL10 local production (Fig. 10 g). *Cxcr3* gene was also upregulated by effector CD8+ T cells in our dataset, highlighting common phenotypical traits between these two cell

populations, and suggesting a circulating origin for CD103- Trm CD8+ T lymphocytes. Altogether, these data suggest that *Cxcr3* expressing CD103- Trm CD8+ T lymphocytes with circulating origins accumulate in the brains of AD mice at the early stages of disease progression, probably following the CXCL10-CXCR3 axis.

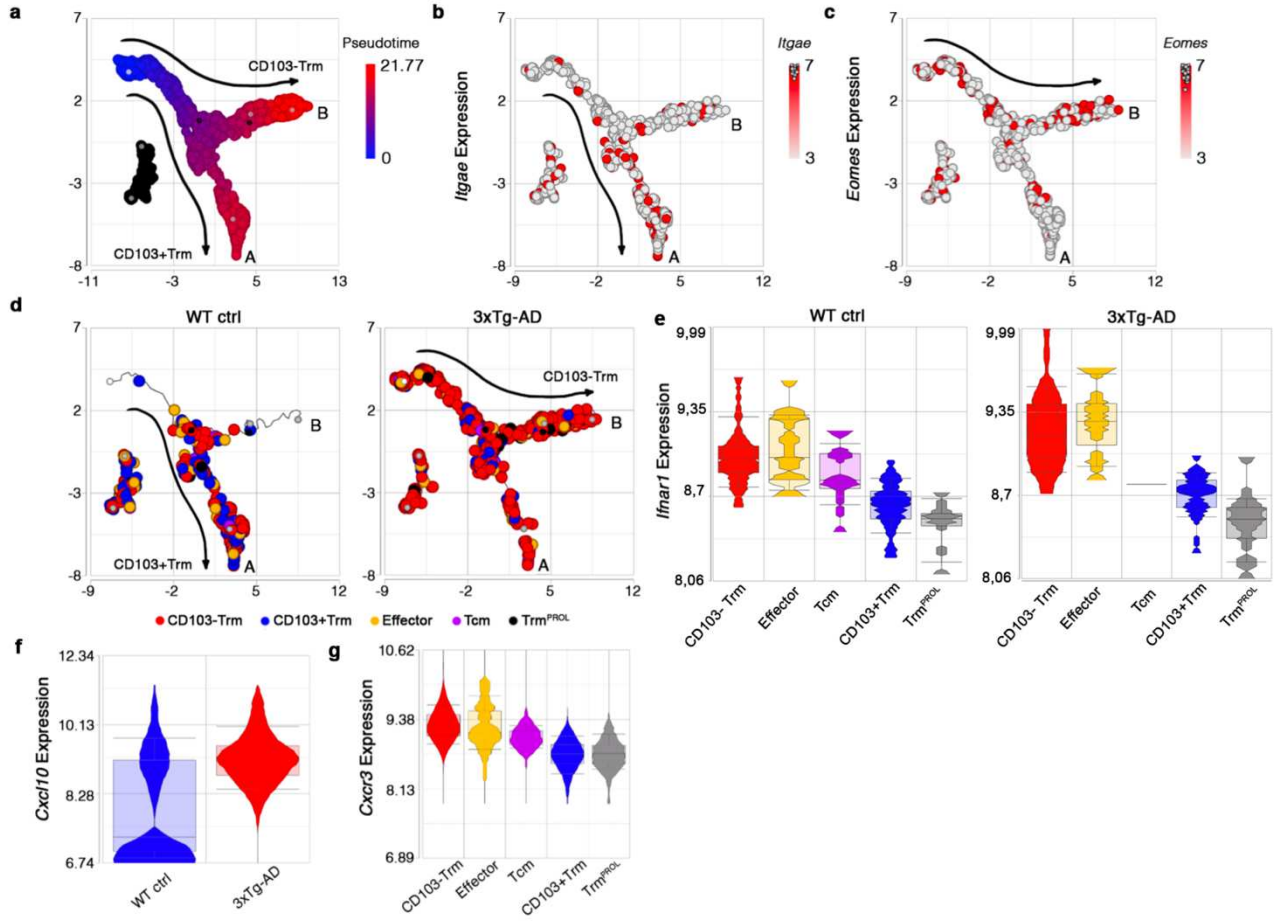

Fig. 10 | Trajectory analysis of CD8+ T lymphocytes in 3xTg-AD mice and WT controls. a, Trajectory analysis showing the pseudotime progression of CD8+ T cells in brain and meninges of WT controls and 3xTg-AD mice at 6 months of age. **b, c**, Same data from **a,** showing *Itgae* (b) and *Eomes* (c) gene expressions (red dots) along with the pseudotime progression. **d**, Same trajectory analysis showing CD8+ T lymphocytes distribution in the brain of WT Control (left) and 3xTg-AD (right) mice. **e**, Violin plots showing *Ifnar1,* gene expression in different subpopulations of brain CD8+ T cells of WT Control and 3xTg-AD mice at 6 months of age. Box and whisker represent the mean and the SD of the plotted data. **f,** Violin plot reporting the differential expression of *Cxcl10* gene in all CD45^{high} leukocytes detected in the brain of 6-month-old WT Control and 3xTg-AD mice. Box and whisker represent the mean and the SD of the plotted data. **g**, Violin plots showing *Cxcr3* gene expression in the different sub-populations of CD8+ T lymphocytes detected in the brain and meninges of WT Control and 3xTg-AD mice at 6 months of age. Box and whisker represent the mean and the SD of the plotted data.

CD103- Trm CD8+ T lymphocytes accumulated in the brain of 3xTg-AD mice expressed GrK

We next sought to determine which subset of CD8+ T cells detected in the brain of 3xTg-AD mice could promote the disease development. Thus, we tested each subset of CD8+ T cells for their expression of genes encoding for cytotoxic and pro-inflammatory molecules, classically produced by cytotoxic T lymphocytes. Bubble and violin plots showed that all subsets of CD8+ T cells upregulated *Tnf*, *Ifng,* and *Il2* genes in the brains of 3xTg-AD mice compared to WT animals, suggesting a broad activation process at the level of CD8 T cell compartment (Fig. 11 a, b). However, only the CD103- Trm population upregulated *Gzmk* gene in the brains of 3xTg-AD mice compared to controls, suggesting a potential key role for this molecule in AD (Fig. 11 a, b). Of note, our results excluded a role for GrB molecule in the AD course, and this was consistent with previous findings in the literature, further pointing to a selective role for *Gzmk* in CD8 T cell function inside the brain parenchyma[12].

The results described above suggest a global activation and cytotoxic potential of CD8+ T cells in the AD brains, also potentially supporting CD8 T cell-mediated immune responses. Indeed, IL-2 signals play a crucial role not only in driving clonal expansion of CD8+ T cells, but also in promoting the activation of Blimp-1 transcriptional factor, which mediates the cytotoxic differentiation program of Trm cells[159,166,169]. This was consistent with the upregulation of *Prdm1* gene, codifying for Blimp-1 TF, in the brain of 3xTg-AD mice (Fig. 11 c, d). Therefore, among the subsets of brain CD8+ T lymphocytes, *Prdm1* gene was highly expressed by both CD103- Trm and effector CD8+ T cells, confirming their phenotypic similarity and pro-inflammatory role in the AD context (Fig. 11 d). On the other hand, our results revealed that the CD103- Trm subset of CD8+ T cells, which was significantly increased in 3xTg-AD mice, could specifically trigger brain alterations in the AD context by releasing GrK lytic molecule. Despite the fact that the role of GrK in health and disease is not well understood, the function of this serine protease was previously associated to cytotoxicity, endothelial activation, and modulation of pro-inflammatory cytokine responses[170]. Flow cytometry analyses confirmed the findings from the single-cell RNAseq experiments, showing a significant increase of GrK-producing CD103- Trm CD8+ T cells in the brain of 6 months old 3xTg-AD mice compared to WT controls (Fig. 11 e). In particular, we observed no differences in the population of brain CD103- GrK- CD8+ T cells between AD and WT control mice, whereas the percentages of both GrK^{MED} and GrK^{HIGH} brain CD103- Trm CD8+ T cells were significantly increased in 3xTg-AD animals compared to control mice (Fig. 11 e, f). In addition, we further confirmed the increased GrK expression in CD103- Trm CD8+ T cells compared to the CD103+ counterpart (Fig. 11 g). Finally, bubble chart clearly showed that CD8+ T cells isolated from the brain of 3xTg-AD mice highly express GrK lytic molecule but lose CD103 expression compared to WT controls (Fig. 11 h).

Altogether, our data demonstrated that GrK+ CD103- Trm CD8+ T cells preferentially populate the brain of 3xTg-AD mice during early disease stages in 3xTg-AD mice, suggesting a potential role for these cells in disease development.

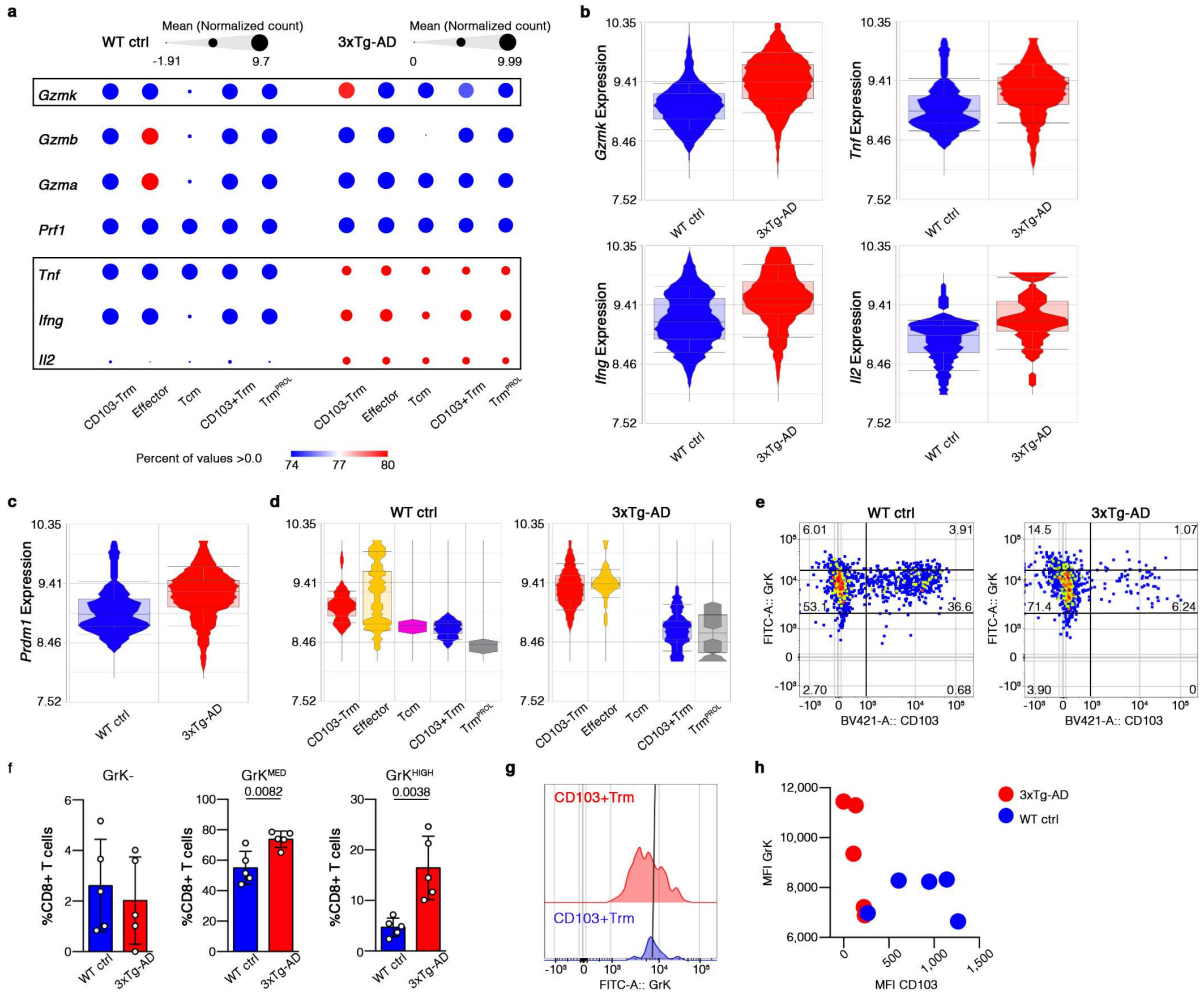

Fig. 11 | GrK expression by CD103- Trm CD8+ T cells in 3xTg-AD mice. a, Bubble and violin plots showing gene expressions for each subset of CD8+ T lymphocytes in the brain of WT control and 3xTg-AD mice at 6 months of age. Dots color represents the percentage of cells expressing each gene. Dots size represents the mean expression of each gene. **b**, Data showing *Gzmk, Tnf, Ifng,* and *Il2* gene expressions in CD103- Trm CD8+ T cells detected in the brain of WT Control and 3xTg-AD animals. Box and whisker represent the mean and the SD of the plotted data **c, d**, *Prdm1* gene expression in the brain of 6-month-old WT Control and 3xTg-AD mice divided for disease condition (c) or for CD8+ T cell subset (d). **e**, Representative dot plots showing CD103+ and CD103- Trm CD8+ T cells expressing GrK lytic molecule in the brain of WT Control (left) and 3xTg-AD (right) mice. **f,** Bar plots reporting the percentage of GrK producing CD103- Trm CD8+ T lymphocytes in the brain of 6-month old WT Control (n = 5) and 3xTg-AD (n = 5) mice. *P*-values show Student' t-test for unpaired data. SD is plotted. **g**, Representative histograms reporting the different expression (MFI) of GrK inside CD103- (red) and CD103+ (blue) Trm CD8+ T lymphocytes in the brain of 6-month-old 3xTg-AD mice. **h**, Scatter plot showing the average MFI expression of CD103 integrin (x axis) and GrK lytic molecule (y axis) for CD8+ T cells detected in the brains of WT Control (blue dots) and 3xTg-AD (red dots) mice.

Enrichment analyses point to a role for brain GrK+ CD103- Trm CD8+ T cells in AD

Next, we performed a pathway enrichment analysis on all subsets of brain CD8+ T cells detected in WT control and 3xTg-AD mice. The results confirmed that GrK+ CD103- Trm CD8+ T cells (red dots) were specifically involved in AD, more than other cell subsets and more than in other neurodegenerative disorders, such as PD, amyotrophic lateral sclerosis (ALS), and Huntington disease (HD) (Fig. 12 a). Indeed, the analysis showed a larger number of genes related to the *"Alzheimer Disease"* pathway for GrK+ CD103- Trm CD8+ T lymphocytes in AD mice. Contrarily, beneficial CD103+ Trm lymphocytes, as well as effector, Tcm, and proliferating Trm CD8+ T cells, were consistently less associated to this path, sustaining the data shown above (Fig. 12 a). As expected, no specific associations between CD8+ T cells subsets and disease pathways were obtained in WT control mice (Fig. 12 a).

Furthermore, gene set enrichment analysis (GSEA) on KEGG database revealed that GrK+ CD103- Trm CD8+ T lymphocytes in 3xTg-AD mice were linked to the AD development more than the same subset of cells in WT controls. Indeed, enrichment score (ES) of *"Alzheimer Disease"* pathway was significantly higher in 3xTg-AD animals compared to control mice, as reported by the enrichment profile plot (Fig. 12 b). In line with this, GSEA on gene ontology (GO) database showed an activated phenotype for GrK+ CD103- Trm CD8+ T cells in 3xTg-AD mice compared to WT controls (Fig. 12 c). Accordingly, among the best five biological processes enriched in this cell subset, were the "*Immune system process*" and the "*Regulation of immune system process*" pathways (GO:0002376 and GO:0002682), which indicate any process involved in the development of immune responses, and the "*Nitrogen compound transport*" pathway (GO:0071705) related to T cell activation (Fig. 12 d-f). Indeed, it was previously demonstrated that activated T cells consume glutamine as a source of nitrogen, enabling nucleotide synthesis and sustaining T cell activation[171]. The *"Hydrolase activity"* pathway (GO:0016787) was also enriched and it was previously shown to be involved in mediating secretion of IFN-γ and cytotoxic granules by CD8+ T cells[172–174] (Fig. 12 g). Therefore, the enrichment profiles plots clearly indicated the strong association between the above-mentioned pathways and the AD condition. Altogether, the upregulation of these biological processes and pathways strongly supports the activated and pro-inflammatory phenotype of GrK+ CD103- Trm CD8+ T cells populating the brain of 3xTg-AD mice, suggesting these cells are key players during early AD.

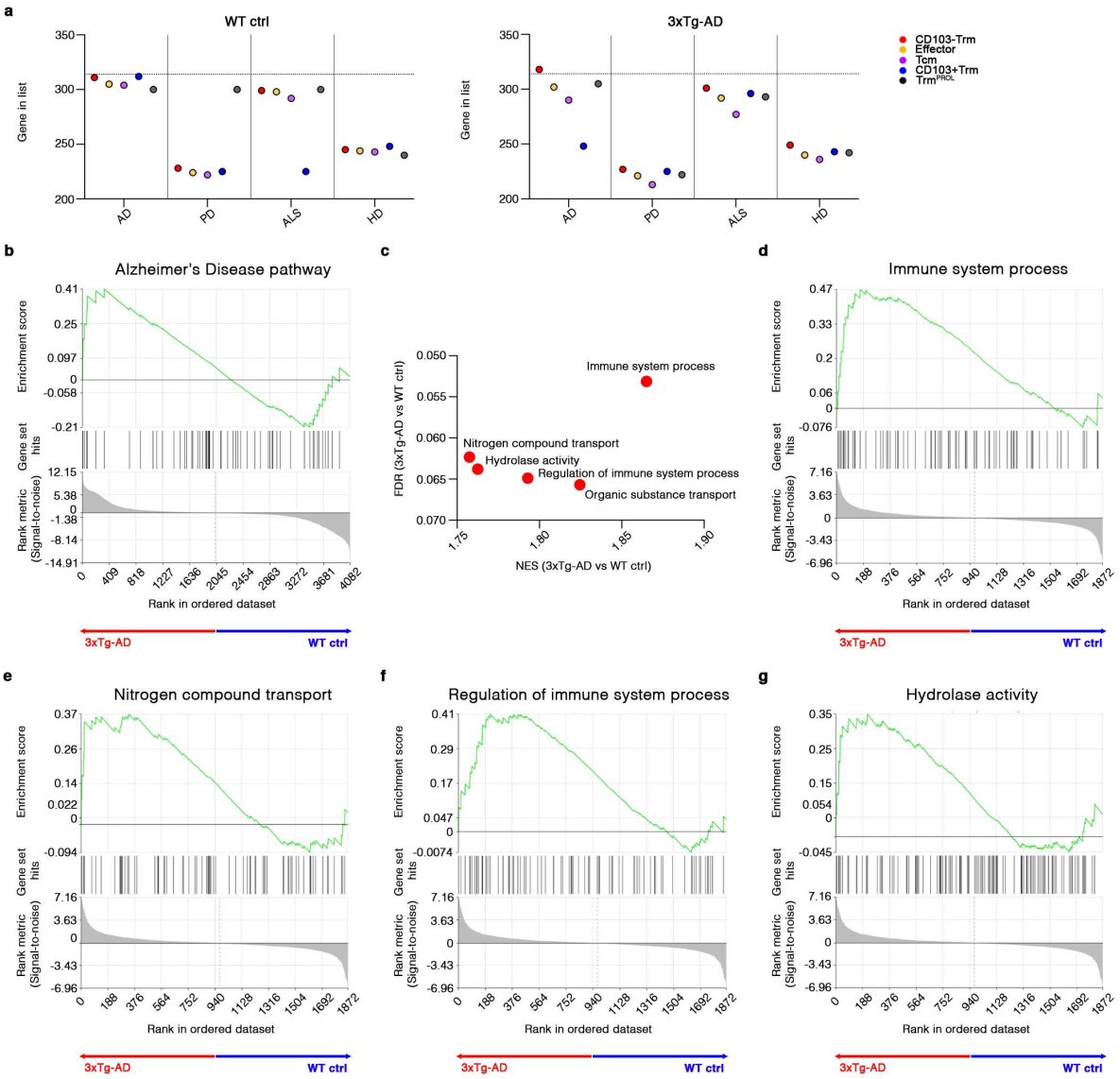

Fig. 12 | Enrichment analysis of single-cell RNA sequencing data. a, Pathway enrichment analysis showing the number of genes associated to "*Alzheimer's disease*" (AD), "*Parkinson disease*" (PD), "*Amyotrophic lateral sclerosis*" (ALS), and "*Huntington disease*" (HD) disease pathways for each subset of CD8+ T lymphocytes detected by single cell analyses in the brain of WT control (left) and 3xTg-AD (right) mice at 6 months of age. **b**, Enrichment profile plot showing the results of KEGG gene set enrichment analysis (GSEA) for the "*Alzheimer's disease*" pathway comparing 3xTg-AD and WT Control mice. **c**, Bubble plot reporting the best 5 enriched terms by GO GSEA comparing 3xTg-AD and WT Control mice. NES = Normalized enrichment score. FDR = False discovery rate. **d-g**, Profile plots of the previous best enriched GO pathways.

GrK+ CD103- Trm CD8+ T cells induce neuronal dysfunction through a PAR-1-dependent mechanism

Based on the promising data described above, we next sought to determine if GrK+ CD103- Trm CD8+ T lymphocytes can induce neuronal dysfunctions in 3xTg-AD mice. Thus, we co-cultured *in vitro* hippocampal neurons isolated from new-born 3xTg-AD mice with CD103- or CD103+ Trm CD8+ T cells isolated from 6-months old 3xTg-AD mice. These experimental conditions were

compared to negative (absence of CD8+ T cells) and positive (ionomycin stimulated neurons) controls. Time-lapse wide-field microscopy imaging from four independent experiments revealed that neurons in contact with pro-inflammatory CD103- Trm CD8+ T cells showed significantly higher cytoplasmic Ca^{2+} levels compared to neurons co-cultured with beneficial CD103+ Trm CD8+ T cells and the negative control, with the activation state reaching the levels of positive control (Fig. 13 a). Globally, these data clearly indicate that CD103- Trm CD8+ T cells invading the brain of 3xTg-AD mice induce intracellular Ca^{2+} dysregulation, which was previously associated with neuronal functional alterations[175,176].

Next, to better understand the interactions between CD8 T cells and neurons, we analyzed the motility behavior of CD103+ and CD103- Trm CD8+ T lymphocytes using live imaging and collecting quantitative variables of individual cell tracks. As first, we noticed that the two subsets of CD8+ T cells differently adapted their behavior over the time while interacting with neurons. Indeed, t-distributed stochastic neighbor embedding (tSNE) clearly showed a "stacking" behavior for CD103+ and CD103- Trm CD8+ T cells during the 1h (0-60 minutes) of co-culture, when neuronal intracellular Ca^{2+} release was still comparable between the two conditions (Fig. 13 b). Differently, during the 3h (120-180 minutes) and 5h (240-300 minutes) of live imaging, when Ca^{2+} levels exponentially increased in neurons co-cultured with CD103-Trm lymphocytes reaching the statistical significance, the behavior of the two subpopulations of CD8+ T cells become gradually different, as reflected by their increasingly separation on the tSNE plot (Fig. 13 b). In line with these observations, the analysis of individual quantitative features showed an increasingly longer and straighter displacement for CD103- Trm CD8+ T cells compared to the CD103+ counterpart during the time-lapse imaging, especially in the last hour of the experiment (Fig. 13 c). Besides, representative tracking (0-300 minutes) clearly confirmed the different behavior of pro-inflammatory CD103- Trm CD8+ T cells in comparison to the beneficial CD103+ lymphocytes when co-cultured with neurons (Fig. 13 d). These characteristics suggested that CD103- Trm CD8+ T cells are more motile and have a higher capacity to explore the environment comparing to the CD103+ counterpart, potentially establishing more neuronal interactions and leading to neuronal dysfunctions throughout a progressive detrimental process[177].

To demonstrate that CD103- Trm CD8+ T lymphocytes triggered neuronal alterations mainly through the release of GrK lytic molecule, as suggested by our data shown above, we performed IF staining on isolated CD103- and CD103+ Trm CD8+ T cells. As expected, data confirmed the high density of GrK granules inside pro-inflammatory CD103- Trm CD8+ T lymphocytes, compared to beneficial CD103+ CD8+ T cells (Fig. 13 e). Next, we evaluated the intracellular Ca^{2+} release by neurons cultured during the time lapse imaging without (Ctrl-) or with purified GrK active enzyme at different

concentrations (75 nM and 150 nM). Importantly, GrK induced a significant increase of intracellular Ca^{2+} release in the last hour (240-300 minutes) of the live imaging experiment, suggesting that this molecule is responsible for neuronal dysfunction induced by CD103- cells and indicating a secretory, extracellular mechanism of action for GrK cytolytic molecule (Fig. 13 f). Moreover, we observed that GrK triggered neuronal dysfunctions in a dose-dependent manner, further supporting the specificity of the activity exerted by this molecule in our AD-related context.

One of the extracellular receptors of GrK lytic molecule is the protease activated receptor family 1 (PAR-1), a thrombin receptor negatively implicated in synaptic plasticity and memory formation, but positively associated to the AD course[178]. Our data clearly showed a significant decrease of intracellular Ca^{2+} release in neurons cultured with purified GrK active enzyme (150 nM) in the presence of SCH79797 PAR-1 inhibitor in a dose-dependent manner, compared to the positive control (GrK 150 nM), reaching the levels of the negative control (normal condition in the absence of GrK) (Fig. 13 g). Representative images confirmed the significant reduction of intracellular Ca^{2+} released by neurons when co-cultured with SCH79797 PAR-1 inhibitor, especially in the last hour of the time-lapse imaging (Fig. 13 h). Altogether, these data propose GrK+ CD103- Trm CD8+ T cells as mediators of neuronal dysfunctions in AD progression. Moreover, we demonstrated, for the first time, that GrK lytic molecule sustain neuronal alterations in AD throughout an extracellular mechanism of action by binding to the PAR-1 receptor expressed by neurons.

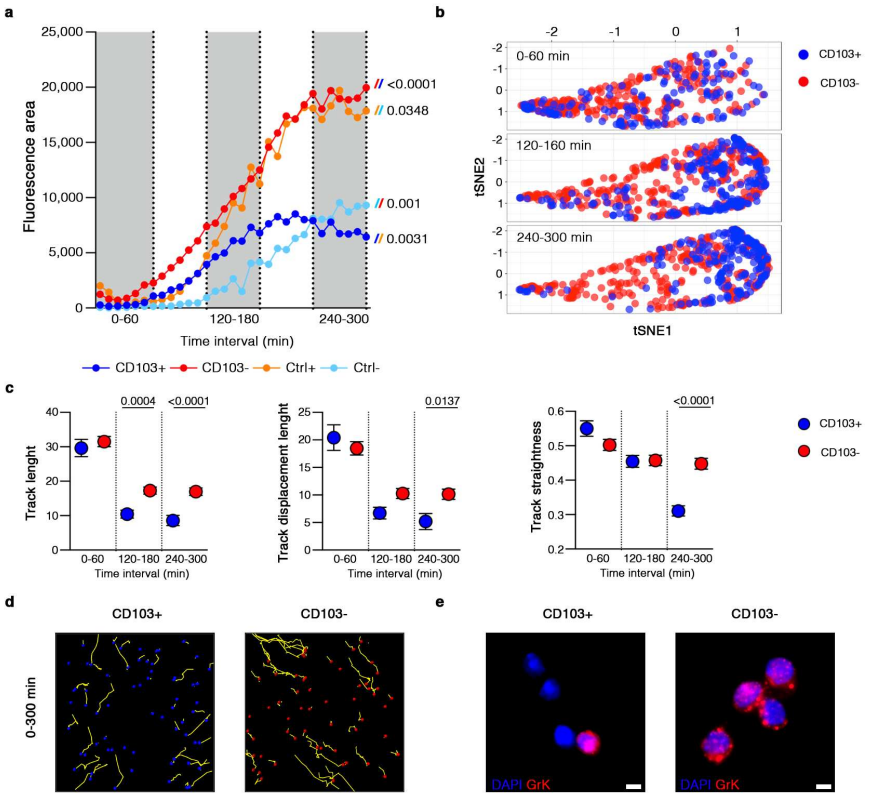

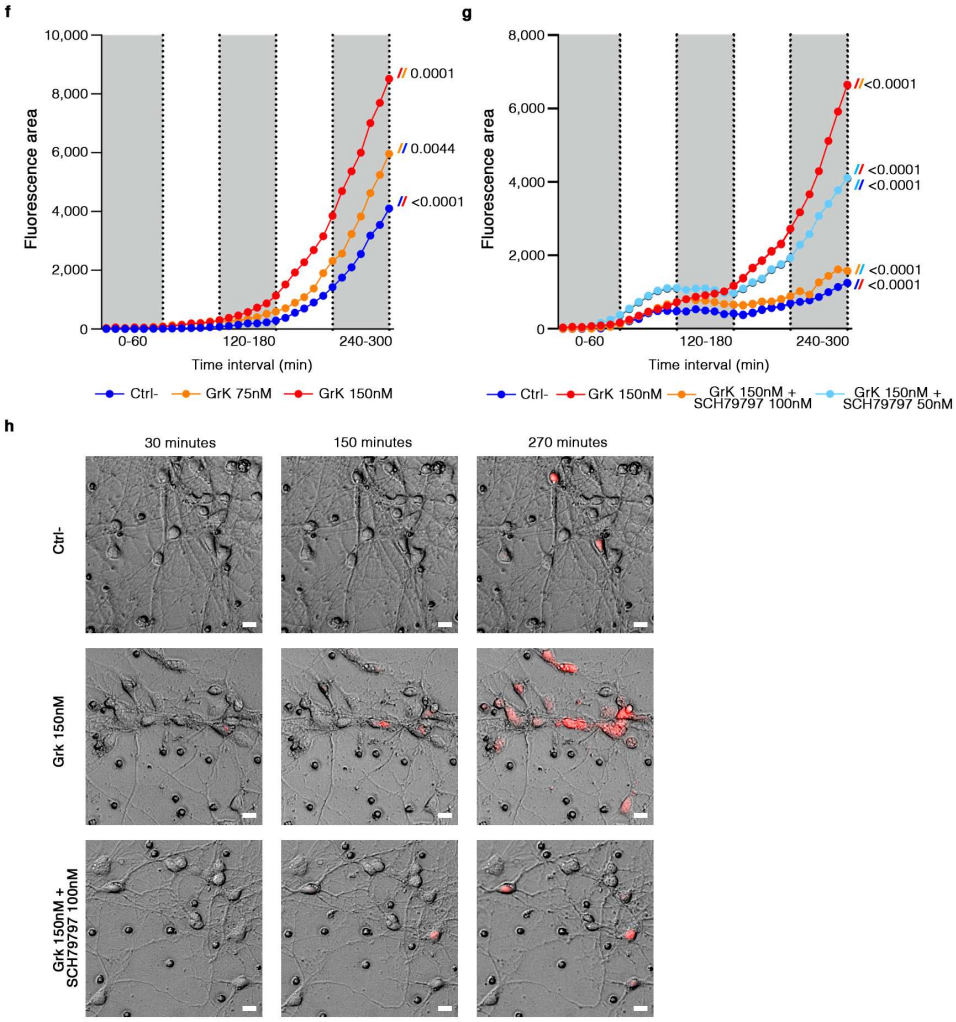

Fig. 13 | Trm CD8+ T cells induce neuronal dysfunction *in vitro*. a, Intracellular calcium release of neurons co-cultured for 5 hours (0-300 time interval) with CD103+ (blue) or CD103- (red) Trm CD8+ T cells was measured using BioTracker kit. Negative control (light blue) = neurons alone. Positive control (orange) = ionomycin stimulated neurons. *P*-values show 2way ANOVA multiple comparisons. Data are from 4 independent experiments. **b**, t-distributed stochastic neighbor embedding (t-SNE) showing the behavior of CD103- (red dots) and CD103+ (blue dots) Trm CD8+ T lymphocytes during the first (0-60 minutes), third (120-180 minutes) and fifth (240-300 minutes) hours of co-culture with neurons form 3xTg-AD mice. **c**, Scatter plot representing track length (left), track displacement length (middle), and track straightness (right) of CD103- (red) and CD103+ (blue) Trm CD8+ T lymphocytes at the first (0-60 minutes), third (120-180 minutes) and fifth (240-300 minutes) hours of co-culture. *P*-values show 2way ANOVA multiple comparisons. SEM is plotted. **d**, Representative tracking of CD103+ (left) and CD103- (right) Trm CD8+ T cells co-cultured with neurons during the live imaging (0-300 minutes). **e**, Immunofluorescent staining showing GrK granules (red) inside CD103+ (right) and CD103- (left) Trm CD8+ T cells. Nuclear staining with DAPI (blue). Scale bar = 3 μm. **f**, Intracellular calcium release of neurons cultured for 5 hours (0-300 time interval) in presence (75 nM orange; 150 nM red) or absence (blue) of purified GrK active enzyme was measured. *p*-values show 2way ANOVA multiple comparisons. Data are from 3 independent experiments. **g**, Intracellular calcium release of neurons cultured for 5 hours (0-300 time interval) with purified GrK active enzyme (150 nM) in red, or purified GrK active enzyme (150 nM) and SCH79797 PAR-1 inhibitor (orange 50 nM; light blue 100 nM). Negative control (blue) corresponds to the absence of GrK. *P*-values show 2way ANOVA multiple comparisons. Data from 3 independent experiments. **h**. Representative images of neurons at different time points (30, 150, 270 minutes) cultured in absence of GrK active enzyme (Ctrl-) on the top; in presence of GrK active enzyme (150 nM) in the middle; in presence of both GrK active enzyme (150 nM) and SCH79797 PAR-1 inhibitor (100 nM) at the bottom. Red signal represents intracellular calcium release. Scale bar = 20 μm.

GrK+ CD103- Trm CD8+ T lymphocytes have a circulating origin

In the light of our data suggesting a role for GrK+ CD103- Trm CD8+ T cells during early disease, our next aim was to understand how this cell population is produced, and why it is increased in 3xTg-AD mice at disease onset. Evidence in the literature recently reported that cytotoxic CD103- Trm CD8+ T lymphocytes originate from peripheral CX3CR1+ KLRG1+ effector CD8+ T cells, which progressively lose the expression of these markers during the differentiation steps[82,111]. Interestingly, our single-cell analyses revealed that CNS effector CD8+ T lymphocytes highly expressed *Cx3cr1* and *Klrg1* genes compared to all the other subsets of CD8+ T cells, including the CD103- Trm compartment (Fig. 14 a). Moreover, our data showed an increase expression of *S1pr5*, *Zeb2* and *Klf2* genes on effector cells, which are also among the most representative biomarker genes of the population (Fig. 14 a). Thus, our data suggest that effector CD8+ T cells may represent a source of GrK+ CD103- Trm CD8+ T lymphocytes detected in the CNS of AD mice and suggest a peripheral origin for brain neurotoxic CD103- Trm lymphocytes. Indeed, *S1pr5* and *Zeb2* genes, which codify for sphingosine 1-phosphate receptor 5 (S1PR5) and zinc finger E-box binding homeobox 2 (ZEB2), respectively, are known to mediate the infiltration of circulating T cells into peripheral organs, and their downregulation is mandatory for tissue retention (Ervard 2021). Similarly, *Klf2* gene, codifying for Kruppel-like factor 2 (KLF2) transcriptional factor, is classically associated to T cells tissue egression and recirculation, pointing to a circulating origin for effector CD8+ T cells detected in the brain of AD mice[159–161].

In a next approach, in order to assess a potential functional alteration of the circulating CD8 T cell compartment that may explain a peripheral origin of CNS effector CD8+ T lymphocytes, we performed scRNAseq on CD45+ leukocytes isolated from the blood of 6-month-old 3xTg-AD and WT control mice. The results showed the presence of two subsets of CD8+ T cells: (i) *Cd44* expressing circulating effector ($Teff^{Circ}$) lymphocytes, and (ii) *Ccr7* expressing circulating Tcm (Tcm^{Circ}) cells (Fig. 14 b). As expected, $Teff^{Circ}$ CD8+ T cells were marked by the upregulation of *Cx3cr1*, *Klrg1* and *Cxcr3* genes, suggesting that this cell population could be the precursor of CNS effector CD8+ T lymphocytes. Besides, our analysis clearly showed that CNS effector, but also CD103- Trm CD8+ T cells, shared a very similar gene signature with $Teff^{Circ}$ cells, further suggesting a peripheral origin of neurotoxic GrK+ CD103- Trm CD8+ T lymphocytes populating the brains of 3xTg-AD mice (Fig. 14 c). In support of this, GSEA KEGG enrichment analysis reported a strong association between $Teff^{Circ}$ CD8+ lymphocytes and the AD pathway in 3xTg-AD compared to WT control mice, as confirmed by the high normalized enrichment score (NES) and gene set size, combined with the low -value and false discovery rate (FDR) (Fig. 14 d). Differently, PD, HD and ALS disease pathways obtained lower NES and gene set size scores, highlighting that $Teff^{Circ}$ CD8+

cells were specifically involved in AD progression (Fig. 14 d). Finally, flow cytometry analyses on circulating leukocytes showed a significant increase of CD44+ KLRG1+ Teff^{Circ} CD8+ lymphocytes in the blood of 6-month-old AD mice compared to sex- and age-matched WT controls (Fig. 14 e), suggesting a role for Teff^{Circ} CD8+ lymphocytes in disease development in 3xTg-AD mice.

Teff^{Circ} CD8+ T cells invade the AD brains through an LFA-1-mediated molecular mechanism

On these bases, we investigated the molecular mechanisms guiding Teff^{Circ} CD8+ cells extravasation and brain invasion in 3xTg-AD mice. Our previous data reported an upregulation of intracellular adhesion molecule-1 (ICAM-1) and vascular cell adhesion molecule-1 (VCAM-1) CNS endothelial cells during early disease in AD mice. The counterligands of these adhesion molecules are LFA-1 and very late antigen-4 (VLA-4) integrins, respectively[49]. We have recently demonstrated that α4-integrins are not involved in CD8+ T cells extravasation in 3xTg-AD mice[74]. However, no study in literature investigated if LFA-1 integrin could drive CD8+ T lymphocytes trafficking in AD.

As first, we noticed an increased expression of both *Itgal* and *Itgb2* genes (Fig. 14 f), encoding for CD11a and CD18 subunits of LFA-1 integrin, respectively, in Teff^{Circ} compared to Tcm^{Circ} CD8+ T lymphocytes. This highlighted that Teff^{Circ} are more prone to migrate from the blood stream into the peripheral tissues. In accordance with this, flow cytometry analyses on circulating CD8+ T cells confirmed the dramatic increase of LFA-1 integrin expression on CD44+ KLRG1+ Teff^{Circ} lymphocytes when compared to the CD44+/- KLRG1- Tcm^{Circ} cell subset (Fig. 14 g). Our data also showed a significant increase of LFA-1 MFI expression on the surface of CD44+ KLRG1+ Teff^{Circ} in 3xTg-AD mice compared to WT controls (Fig. 14 h). This was associated to a significant increase in the percentage of LFA-1+ CD44+ KLRG1+ Teff^{Circ} CD8+ cells in AD animals (Fig. 14 i). Single cell analyses not only confirmed this evidence, but also highlighted the increased fraction of LFA-1+ CD8+ T cells in the Teff^{Circ} subset compared to Tcm^{Circ} CD8+ lymphocytes (Fig. 14 j). Altogether, these findings suggest a potential role for LFA-1 integrin in mediating the peripheral trafficking of Teff^{Circ} CD8+ cells in the brain of AD mice.

Next, to definitively assess the involvement of LFA-1 integrin in CD8+ T cells trafficking in the AD context, we evaluated the accumulation of CD8+ T lymphocytes in the brains of 3xTg-AD/*Itgal*$^{-/-}$ animals lacking LFA-1 integrin. As expected, the results reported a significant decrease in the percentage of CD8+ T lymphocytes in 3xTg-AD/*Itgal*$^{-/-}$ animals compared to control 3xTg-AD mice (Fig. 14 k). Notably, we observed a significant decrease in the percentage of detrimental CD103- Trm CD8+ T lymphocytes, paralleled by an increase of CD103+ Trm CD8+ T cells in the brain of AD mice lacking LFA-1 integrin compared to control 3xTg-AD animals (Fig. 14 l). This clearly indicates

a role for LFA-1 integrin in the migration of CD103- Trm CD8+ T cells into the CNS during AD-like disease.

We can thus hypothesize that peripheral Teff^{Circ} CD8+ cells invade the brain of 3xTg-AD mice during early disease through an LFA-1-dependent mechanism. Once arrived into the brain, we speculate that these cells give rise to GrK-producing CD103- Trm CD8+ T cells, mediating neuronal dysfunction and disease progression. Indeed, the lack of LFA-1 integrin induced a significant decrease in the neurotoxic subset of CD103- Trm CD8+ lymphocytes, which may contribute to the reduction of cognitive deficit and neuropathological changes previosuly observed by our group in 3xTg-AD/*Itgal*$^{-/-}$ animals[49].

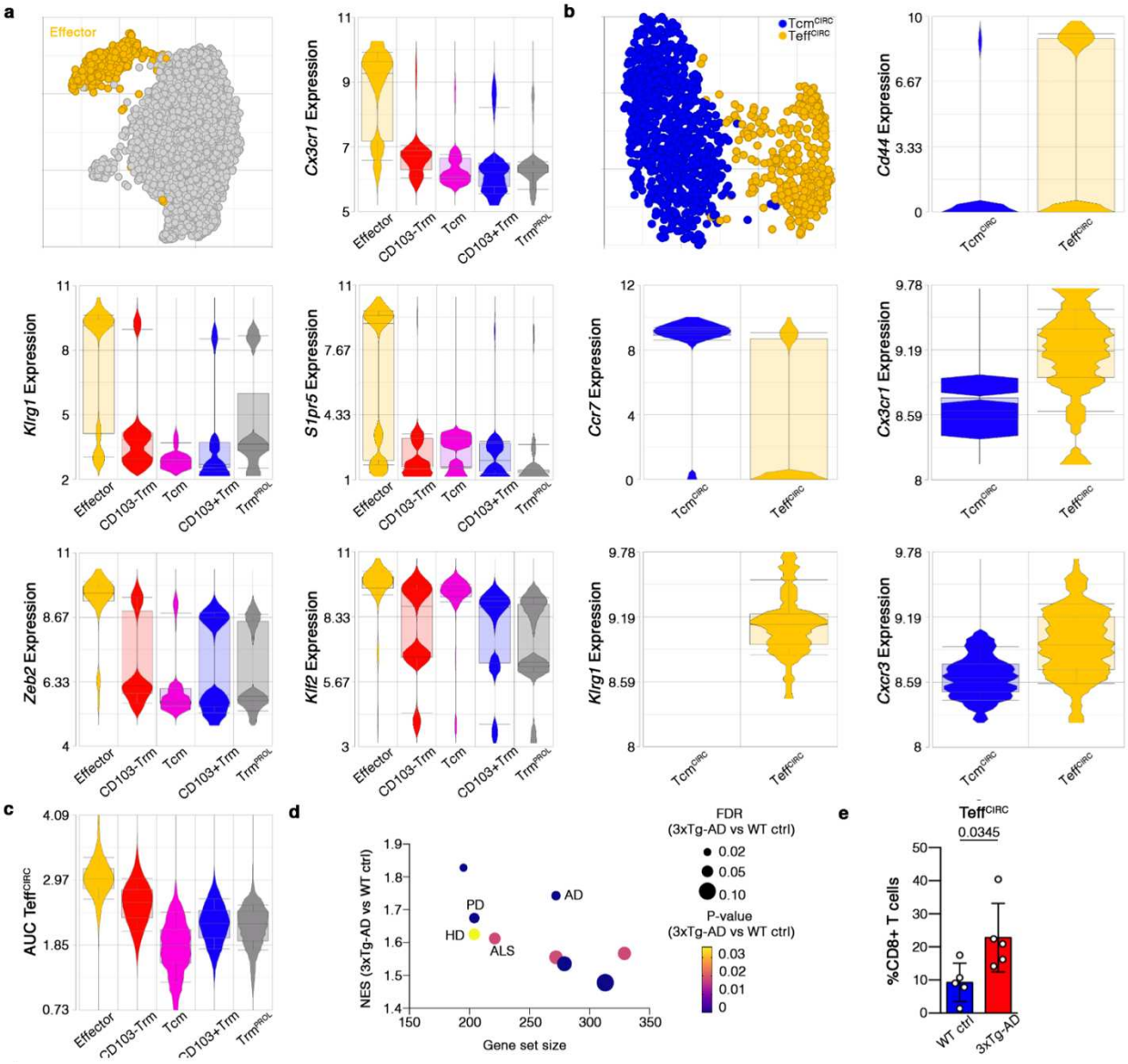

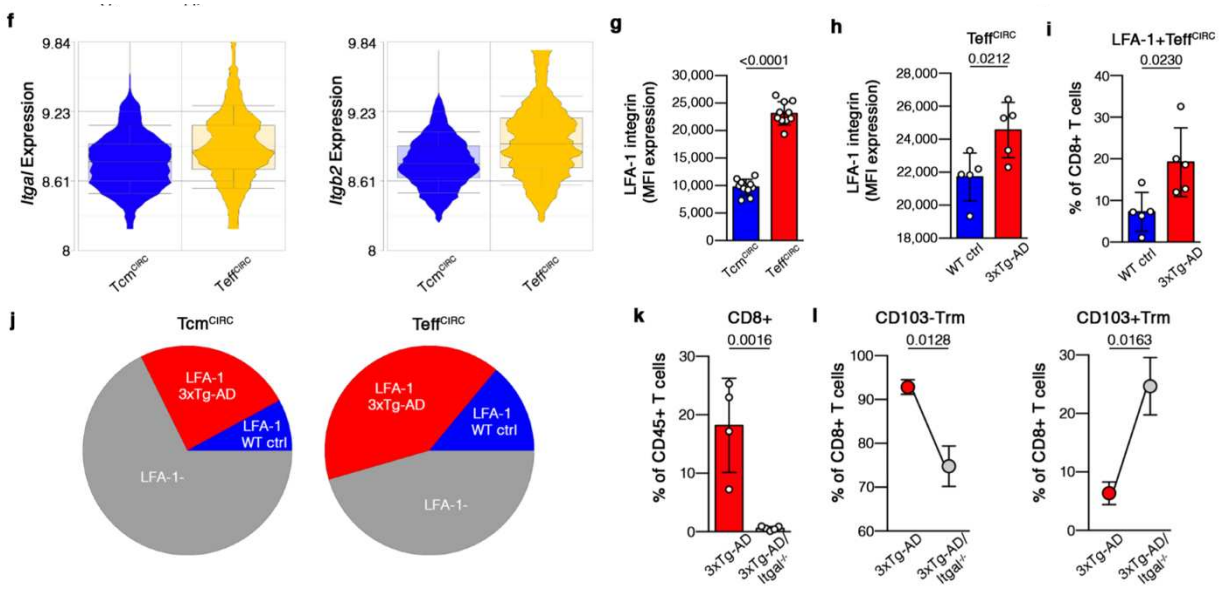

Fig. 14 | Analysis of CD8+ T cells in the CNS and blood of mice with AD-like disease. a, UMAP and violin plots showing CNS effector CD8+ T cells (yellow) and their marker genes in 6-month-old WT control and 3xTg-AD mice. Box and whisker represent the mean and the SD of the plotted data. **b**, UMAP and violin plots showing central memory (Tcm) (blue) and circulating effector ($Teff^{circ}$) (yellow) CD8+ T lymphocytes and their marker genes detected in the blood of 6-month-old WT Control and 3xTg-AD mice. Box and whisker represent the mean and the SD of the plotted data. **c**, AU cells (AUC) analysis showing the phenotypic similarity between the different subsets of CNS CD8+ T lymphocytes and circulating effector ($Teff^{circ}$) CD8+ T cells of the previous analyses. Box and whisker represent the mean and the SD of the plotted data **d**, KEGG gene set enrichment analysis (GSEA) on circulating effector ($Teff^{circ}$) CD8+ T cells detected by previous single cell analyses in the blood of 3xTg-AD mice compared to those of WT Control animals. AD = "Alzheimer's disease; PD = "Parkinson disease"; HD = "Huntington disease"; ALS = "Amyotrophic lateral sclerosis". NES = "Normalized enrichment score"; FDR = "False discovery rate" (dots size); Dots color depicts *P*-value. **e**, Bar plot depicting the percentage of CD44+ KLRG1+ circulating effector ($Teff^{circ}$) CD8+ T cells detected in the blood of in 6-month-old WT Control (n = 5) and 3xTg-AD (n = 5) mice. *P*-values show Student' t-test for unpaired data. SD is plotted. **f**, *Itgal* and *Itgb2* gene expressions of central memory (Tcm) and circulating effector ($Teff^{circ}$) CD8+ T cells detected in the single cell analyses. **g**, Bar plots showing the mean fluorescent intensity (MFI) expression of LFA-1 integrin on the surface of CD44+/- KLRG1- central memory (Tcm) and CD44+ KLRG1+ circulating effector ($Teff^{circ}$) CD8+ T lymphocytes in the blood of 6-month-old WT Control and 3xTg-AD mice (merged, n = 10). *P*-values show Student' t-test for unpaired data. SD is plotted. **h**, Bar plots showing the mean fluorescent intensity (MFI) expression of LFA-1 integrin on the surface of CD44+ KLRG1+ circulating effector ($Teff^{circ}$) CD8+ T cells detected in the blood of in 6-month-old WT Control (n = 5) and 3xTg-AD (n = 5) mice. *P*-values show Student' t-test for unpaired data. SD is plotted. **i**, Flow cytometry analyses reporting the percentage of LFA-1+ CD44+ KLRG1+ circulating effector ($Teff^{circ}$) CD8+ T cells in in the blood of in 6-month-old WT Control (n = 5) and 3xTg-AD (n = 5) mice. *P*-values show Student' t-test for unpaired data. SD is plotted. **j**, Pie plots depicting the fractions of central memory (Tcm) (left) and circulating effector ($Teff^{circ}$) (right) LFA-1+ CD8+ T cells in 3xTg-AD (red) and WT Control (blue) mice, and LFA-1- (grey) CD8+ T lymphocytes detected by single-cell analyses. **k**, Percentage of total CD8+ T cells in the brain of 3xTg-AD (n = 4) and 3xTg-AD/*Itgal*$^{-/-}$ (n = 5) mice at 6 months of age. *p*-values show Student' t-test for unpaired data. SD and SEM are plotted. **l**, Scatter plot highlighting the different percentage of CD103+ (left) and CD103- (right) CD8+ T lymphocytes detected in the brain of 3xTg-AD (n = 4) and 3xTg-AD/*Itgal*$^{-/-}$ (n = 5) mice at 6 months of age. *P*-values show Student' t-test for unpaired data.

Depletion of circulating CD8+ T lymphocytes prevents accumulation of CD103- Trm cells and ameliorates disease in 3xTg-AD mice

To assess the peripheral origin of brain CD103- Trm CD8 T cells and their detrimental role in disease pathogenesis and progression, we therefore depleted circulating CD8+ T cells in 6-month-old 3xTg-AD mice and sex-matched WT controls. We injected the animals *i.p.* every other day with a commercially available anti-CD8α depleting antibody unable to affect the Trm population[114]. With this treatment, CD8+ T cells were successfully ablated from the blood and spleen of mice, and the treatment was well tolerated by the animals. Notably, the treatment induced a significant reduction of brain CD103- Trm CD8+ T cells in CD8-depleted AD-like mice compared to isotype controls, reaching the levels of the control groups, supporting the circulating origin for this cell subset (Fig. 15 a). Conversely, as expected, we detected no differences in the percentage of CD103+ Trm CD8+ T lymphocytes after the treatment in 3xTg-AD as well as in WT control mice, confirming that the depleting antibody was unable to affect the stable brain Trm population (Fig. 15 a).

Thus, to demonstrate that CD103- Trm CD8+ T lymphocytes exert a detrimental role in AD, we analyzed hippocampal-dependent learning and spatial long-term memory of animals with Morris's water maze (MWM) behavioral test, in which the mice had to find a water submerged-hidden platform. The results from two independent experiments showed no significant differences between the four experimental groups in the cued stage, ensuring the absence of deficits in motor abilities. Remarkably, we reported a significant improvement in the hippocampal-dependent learning in 3xTg-AD mice depleted of CD8+ T cells, specifically at the second day of training (Fig. 15 b). Indeed, learning curve recorded during the training days of the test reported a significant decrease in test duration of 3xTg-AD mice ablated of CD8+ T cells compared to isotype controls (Fig. 15 b). Surprisingly, during the probe stage of the test, CD8-depleted 3xTg-AD mice didn't spend more time in the B zone (the region where the platform was located) compared to isotype control treated mice, suggesting no ameliorations in the long-term memory of 3xTg-AD mice after the depletion of circulating CD8+ T cells (data not shown). Despite this, representative tracking of three animals per group clearly showed that 3xTg-AD mice treated with the isotype control mAb swam in a random way, while 3xTg-AD mice depleted of CD8+ T cells swam in a "chaining" way, keeping away from the pool wall (Fig. 15 c). This indicated an active search of the platform and the maintenance of the memory of the original platform position, improving the escape performance[179]. In line with the cognitive improvements reported by MWM test, the contextual fear conditioning (CFC) associative learning task revealed an amelioration of contextual memory after CD8+ T cells depletion in 3xTg-AD mice. Data from two independent experiments reported a significant increase of the percentage of freezing in 3xTg-AD mice depleted of CD8+ T cells compared to isotype controls (Fig. 15 d). This

suggested that circulating CD8+ T cell ablation in the AD context can significantly improve the capability of mice to better associate the neutral context to the aversive stimulus.

To verify if amelioration of cognitive deficits after the anti-CD8α antibody treatment correlated with reduction of classical neuropathological hallmarks of AD, we stained coronal murine brain sections with anti-Aβ (6E10), anti-p-tau (AT180), and anti-total-tau (HT7) antibodies. Our data showed a significant decrease in both Aβ-load and levels of tau hyperphosphorylation in the hippocampus of 3xTg-AD mice depleted of circulating CD8+ T cells compared to animals treated with an isotype control mAb (Fig. 15 e). The levels of total tau were unchanged between conditions. Collectively, these results demonstrate the detrimental role of CD103-CD8+ T cells in 3xTg-AD mice during the early stages of the disease.

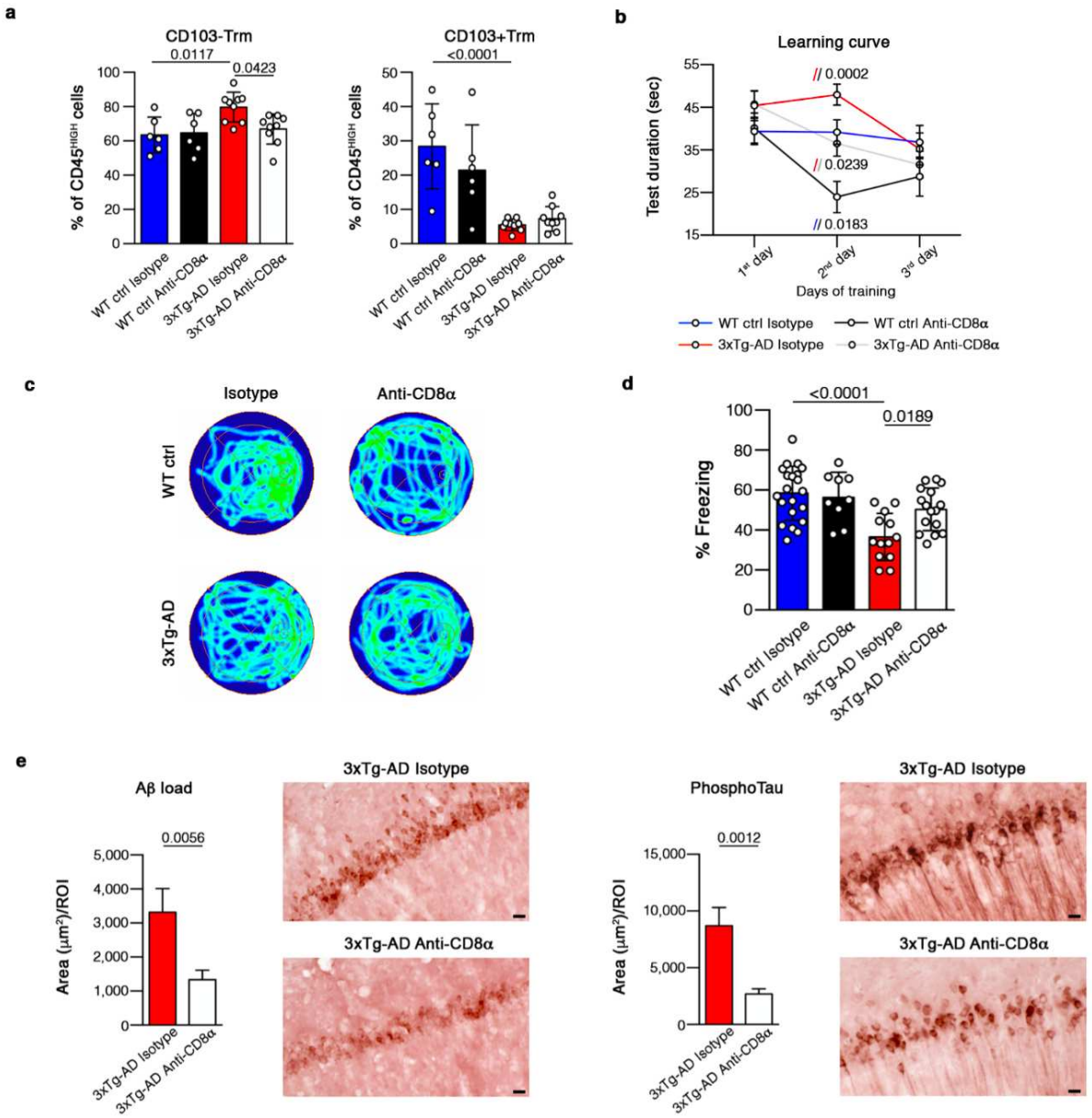

Fig. 15 | Depletion of circulating CD8+ T cells in mice with AD-like. a, Flow cytometry analyses reporting the percentage of CD103+ (left) and CD103- (right) CD8+ T cells in the brains of non-treated and treated WT Control (blue (n = 6) and black (n = 6), respectively), and 3xTg-AD (red (n = 9) and grey (n = 9), respectively) mice. *p*-values show 1way ANOVA multiple comparisons. SD is plotted. **b**, Time spent (seconds) by non-treated and treated WT control mice (blue (n = 22) and black (n = 10), respectively), and 3xTg-AD (red (n = 18) and grey (n = 21), respectively) during the different days (1 to 3) of the training stage of Morris water maze (MWM) behavioral test. *p*-values show 2way ANOVA multiple comparisons. SEM is plotted. Data from two independent experiments. **c**, Representative tracking of the behavior of 3 animals per group during the probe stage of Morris water maze (MWM) behavioral test. **d**, Bar plot showing the percentage of freezing during contextual fear conditioning (CFC) behavioral test for non-treated and treated WT Control (blue (n = 21) and black (n = 9), respectively), and 3xTg-AD (red (n = 13) and grey (n = 16), respectively) mice. *p*-values show 1way ANOVA multiple comparisons. SEM is plotted. Data from two independent experiments. **e**, Immunohistochemical analyses (IHC) on the hippocampus of non-treated (n = 2, slices per sample = 6) and treated (n = 2, slices per sample = 6) 3xTg-AD mice evaluating the Aβ load (left) and the levels of hyperphosphorylated tau-protein (right), with their representative images. Scale bar 20 μm. *p*-values show Student' t-test. SEM is plotted. ROI = 624.7 μm x 501.22 μm.

GrK-producing CD8+ T cells are increased in the brain, CSF and blood of AD patients

To understand the translational potential of our data, we performed IF staining on human brain tissues. Importantly, our data showed the presence of both intraparenchymal and intravascular GrK+ CD103- CD8+ T lymphocytes near hippocampal neurons of AD patients (Fig. 16 a). Conversely, only GrK- CD103+ CD8+ T cells were detected in the hippocampus of control subjects, suggesting a role for GrK producing cells in AD (Fig. 16 a). These results are in agreement with our data obtained in 3xTg-AD mice, suggesting that peripheral CD8+ T cells mediate neuronal dysfunctions via GrK lytic molecule also in AD patients. In order to strengthen these observations, we analyzed a freely accessible scRNAseq dataset of CSF immune cells deposited online in the Gene Expression Omnibus (GEO) (accession code GSE134578)[50]. Firstly, we noticed the presence of two subsets of CD8+ T cells: (i) Trm cells, which expressed *CD69* gene, fundamental for tissue retention[180]; and (ii) CD8+ T cells with migratory phenotype characterized by the expression of *KLF2* gene (Fig. 16 b). Notably, and in agreement with our mouse data, the majority of *CD69* expressing CSF Trm CD8+ T lymphocytes were characterized by the expression of *GZMK,* the first biomarker of this population, and *S1PR1* genes, suggesting a detrimental GrK+ CD103- phenotype for these CD8+ T cells (Fig. 16 c). Of note, also *KLRG1* and *CX3CR1* genes were detected among the biomarkers of this cell sub-population, sustaining its peripheral origin also in AD patients. Differently, the rest of CSF Trm CD8+ T cells upregulated *XCL1* and *KLRC1* genes, which expression was previously associated to the CD103+ Trm profile[12,95] (Fig. 16 c). Besides, in accordance with our findings in 3xTg-AD mice, we observed an increase in the GrK+ CD103- subset along with disease progression, paralleled by a gradual decrease in the percentage of CD103+ Trm lymphocytes (Fig. 16 d). Next, our analyses showed a significant increase of *GZMK* expression in CD103-, but not in CD103+, cells in AD patients compared to control subjects and MCI patients suggesting this gene may have a role during early disease, as suggested by our mouse data (Fig. 16). Together, these data strongly suggest a

disease-dependent detrimental role of GrK-producing CD103- Trm CD8+ T lymphocytes also during human disease.

Of note, GrK+ CD103-, and CD103+ Trm CD8+ T cells equally expressed *NKG7*, *GZMA* and *GZMH* genes, which characterize T_{EMRA} cells[50], expanding previous knowledge of CD8+ T cells subsets in AD (Gate 2020). Therefore, our data show that among CSF T_{EMRA} CD8+ T lymphocytes it is possible to detect a cell population with CD103- Trm phenotypic traits characterized by a disease-dependent increased production of GrK cytotoxic molecule, which has never been previously identified in the context of AD.

Finally, to verify that circulating CD8+ T cells also infiltrate the CNS of AD patients through an LFA-1-mediated pathway, we analyzed a published scRNAseq dataset (accession code GSE181279) of CD45+ cells isolated from the blood of negative control (NC) and AD patients[157]. After the detection of CD8+ T lymphocytes, we used published gene signatures to characterize the subsets of CD8+ T cells in the dataset, identifying Naïve, Tcm^{Circ} and $Teff^{Circ}$ populations[90] (Fig. 16 f). In line with our results in mice, we detected an increased percentage of all the subsets of LFA-1+ CD8+ T cells in AD patients compared to NCs (Fig. 16 g). Moreover, the $Teff^{Circ}$ sub-population was composed by a higher fraction of LFA-1+ CD8+ T cells compared to both Naïve and Tcm^{Circ} subsets (Fig. 16 g). This confirmed that in AD human patients, as well as in mouse models, $Teff^{Circ}$ CD8+ T cells were more prone to evade the blood streaming through an LFA-1 integrin-mediated molecular mechanism.

Globally, these evidences from human subjects clearly support our results from animal models of AD, strengthening the impact of our findings, and suggesting that blocking GrK cytolytic activity could be a promising therapeutic approach for the treatment of AD.

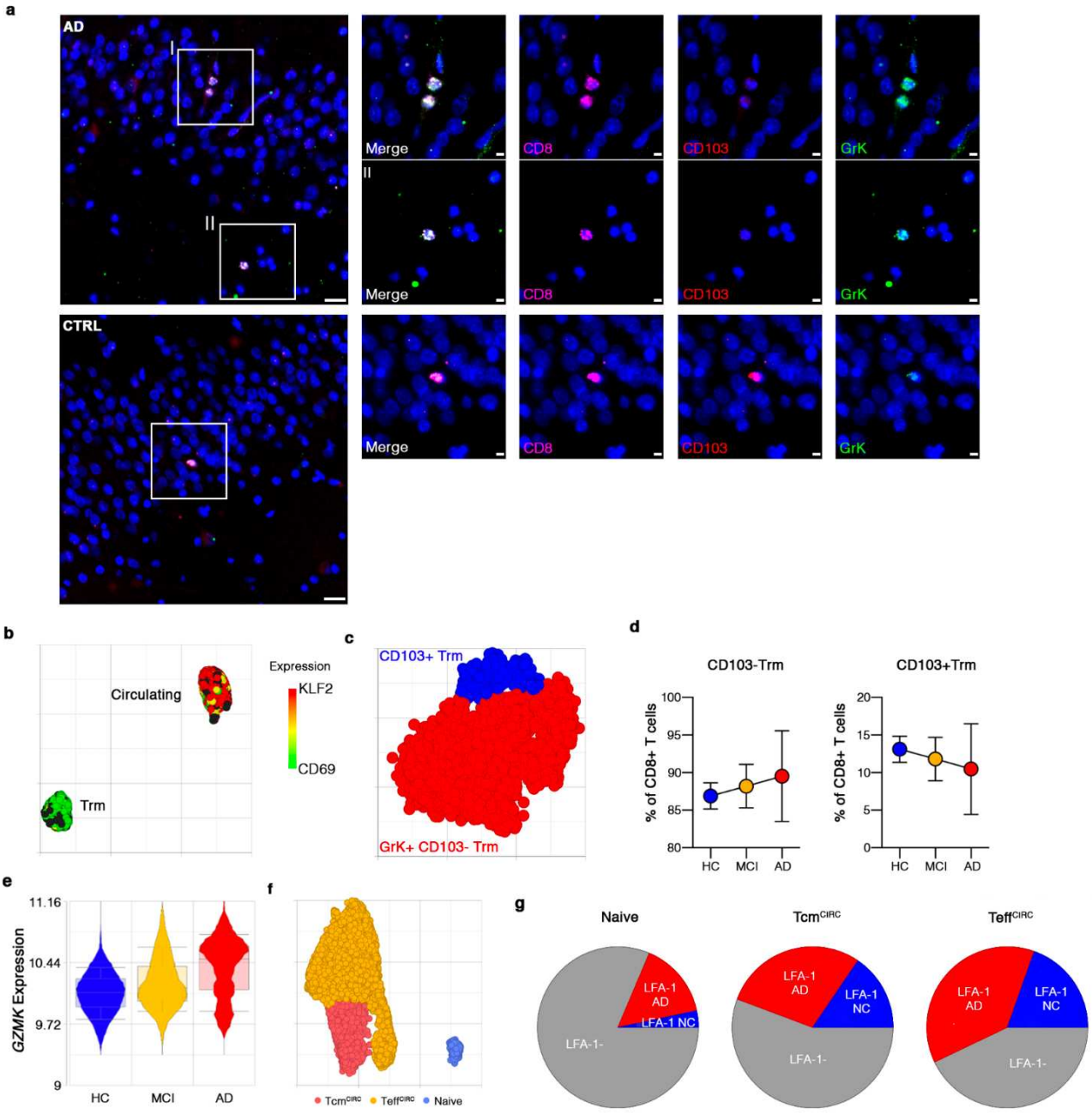

Fig. 16 | CD8+ T cells in brain, CSF and blood of human patients. **a**, Immunofluorescence (IF) analyses of control (upper) and AD (bottom) human brain tissues. CD8 = Purple, CD103 = Red, GrK = Green; Scale bar = 40 µm. Magnifications on the right; Scale bar = 15 µm. **b**, UMAP plot showing tissue resident memory (Trm) and circulating CD8+ T cells expressing *CD69* (green) and *KLF2* (red) genes in the cerebrospinal fluid (CSF) of healthy controls (HC), mild cognitive impairment (MCI), and Alzheimer's disease (AD) patients. **c**, UMAP plot showing GrK+ CD103- (red) and CD103+ (blue) cell subsets inside the previously detected Trm population of CD8+ T lymphocytes in CSF of HC, MCI, and AD patients. **d**, Percentage of GrK+ CD103- (left) and CD103+ (right) Trm CD8+ T cells detected in CSF of HC, MCI, and AD patients. SD is plotted. **e**, Violin plots reporting *GZMK* gene expression in CSF GrK+ CD103- Trm CD8+ T cells of HC, MCI, and AD patients. Box and whisker represent the mean and the SD of the plotted data. **f**, UMAP plot showing central memory (Tcm^{circ}), effector ($Teff^{circ}$) and naïve CD8+ T cells in the blood of AD patients and negative controls (NCs). **g**, Pie charts depicting the fraction of LFA-1+ CD8+ T cells in AD patients (red) and NCs (blue), and LFA-1- CD8+ T lymphocytes (grey) in circulating naïve (left), Tcm^{circ} (middle), and $Teff^{circ}$ (right) cell sub-populations.

DISCUSSION

A growing number of studies reported the involvement of CD8+ T cells in different neurodegenerative disorders, including AD[12,50–54,73,103]. However, so far no study identified CD8 T cell-dependent molecular mechanisms contributing to the induction of pathological changes and sustaining disease progression in the context of AD. Identifying the pathogenic mechanisms responsible for CD8 T cell-mediated cytotoxicity may lead to the discovery of novel therapeutic strategies in AD, a disease which has no cure and affects dozens of millions of people around the world.

In this study, we suggest that $Teff^{Circ}$ CD8+ T cells invade the AD brains in the early stages of the disease through an LFA-1 integrin-dependent pathway. We speculate that these cells give rise to GrK-producing CD103- Trm CD8+ T cells, which in turn exert detrimental functions via GrK lytic molecule, amplifying neuronal alterations and contributing to memory deficit during early AD. The peripheral origin of GrK+ CD103- Trm CD8+ T cells was demonstrated by the pharmacological ablation of circulating CD8+ T lymphocytes by an anti-CD8 antibody, which induced a consistent decrease of detrimental Trm cells in the brain of 3xTg-AD mice, paralleled by the cognitive and neuropathological amelioration in treated animals.

We also reported the loss of memory-like CD103+ Trm CD8+ T lymphocytes in AD-like mice, which can in turn sustain disease progression due to a decreased immune surveillance activity[111]. Accordingly, enrichment of CD103+ Trm CD8+ T cells is yet associated in literature to a favorable prognosis in various human cancers, and in Inflammatory Bowel Disease (IBD)[181,182]. Of note, the reduction of beneficial CD103+ Trm CD8+ T cells in the AD condition was directly connected with a drastic change of the extracellular brain milieu. Depending on specific environmental conditions, such as during chronic inflammation, environmental signals can be altered, unbalancing the number and function of Trm lymphocytes detected in peripheral tissues[166]. Indeed, we recorded the downregulation, in 3xTg-AD mice, of all the genes encoding for the most important cytokines involved in the differentiation and maintenance of CD103+ Trm lymphocytes[109]. In line with this, recent studies clarified that cytokines within the tissue-microenvironment are crucial to shape the phenotype and the function of Trm cells. Among the studied cytokines, IL-33, whose expression was dramatically impaired in 3xTg-AD mice, is one of the most important factors for brain CD103+ Trm CD8+ T cells production and survival[166]. In accordance with our data, a recent work showed that the homeostatic anti-inflammatory role of IL-33 is lost in AD, whereas IL-33 administration ameliorates neuropathological and cognitive impairments in AD-like mice[164,183]. Our data demonstrated that this impaired differentiation of beneficial CD103+ Trm CD8+ T lymphocytes is paralleled by an increased fraction of detrimental CD103- Trm CD8+ T cells, which may contribute to early AD

development. Interestingly, similar unbalances in the Trm compartment of CD8+ T cells were reported also in patients with IBD. Particularly, it was previously shown an increase of CD103- Trm CD8+ T lymphocytes paralleled by a decrease of CD103+ Trm CD8+ T cells in the gut of both Chron's disease (CD) and ulcerative colitis (UC) patients at the outcome of the disease. Notably, restoration of the balance between CD103- and CD103+ Trm CD8+ T lymphocytes was associated to IBD remission, suggesting this may be the case also during AD[182]. Notably, gut and brain CD103+ and CD103- Trm CD8+ T cells share a similar gene signature, including GrK expression[106]. This suggests that common pathogenic mechanisms may underlie AD and autoimmune processes during IBD progression, proposing the rebalance of the Trm compartment of CD8+ T cells as a therapeutic approach also in AD. Indeed, we have previous suggested that common immune mechanisms between AD and another autoimmune disease, multiple sclerosis, may also open new avenues for shared therapies targeting immune dysfunction and chronic inflammation in these diseases[80].

Despite the fact that more studies are required to define a way to boost beneficial CD103+ Trm cell differentiation in the AD brains, our data suggest that modulating GrK cytolytic activity exerted by CD103- Trm CD8+ T cells, and directed toward neurons, could be an interesting therapeutic target to slow down disease progression. Several studies have shown that GrK has both intracellular and extracellular effects. These include cytotoxicity (activation of extrinsic apoptosis pathway) and inhibition of viral replication for intracellular activities and induction of production of IL-1β, MCP-1, IL-6, IL-8 and expression of adhesion molecules (e.g. ICAM-1, VCAM-1, E-selectin). Although we cannot exclude a rapid effect of GrK on neurons, our *in vitro* measurements suggest a long-lasting mechanism of action for detrimental CD103- Trm CD8+ T cells on AD neurons and an extracellular role for GrK in determining neuronal alterations[170]. In this context, we speculate that GrK may not activate the apoptotic cascade, but it could modulate cell activation and dysfunction through the cleavage and activation of some transmembrane receptors[170]. Among them, GrK activates a member of the protease activated receptor (PAR) family, PAR-1, which is a thrombin receptor and it is considered an important activator of endothelial cells. Apparently, GrK has no toxic effects on endothelial cells, but activates these cells leading to a PAR-1-dependent increased expression of adhesion molecules (ICAM-1, E-selectin and VCAM-1) through activation of mitogen-activated protein kinase (MAPK) p38 phosphorylation[170,184], which, in turn, may promote the adhesion of blood immune cells. In addition to expression of adhesion molecules, GrK-mediated PAR-1 activation leads to production and secretion of pro-inflammatory cytokines[184]. Importantly, PAR-1, was shown to be negatively implicated in synaptic plasticity and memory formation, and was found increased in the AD brains[170,185]. Also, PAR-1 inhibition was associated in recent studies to an ameliorated of

cognitive performance and synaptic plasticity in AD, supporting our data and further pointing to GrK as a new therapeutic target in AD[178].

Our data also suggest that an interesting therapeutic approach in AD could be the selective inhibition of detrimental CD8+ T cells brain infiltration from the periphery. Indeed, our study suggested the importance of the CXCR3/CXCL10 axis in promoting the infiltration of pro-inflammatory circulating CD8+ T cells into the AD brains. To note, the increased CXCL10 expression detected in the CNS of mice with AD-like disease was consistent with the augmented fraction of CXCR3+ effector CD8+ T cells shown in the AD brains, which subsequently may potentially differentiate into neurotoxic GrK-producing CXCR3+ CD103- Trm CD8+ T lymphocytes. Furthermore, an established vicious cycle could strengthen the impact of the CXCR3/CXCL10 axis in worsening AD progression. Indeed, the increased concentration of CXCL10 chemokine in the brains of mice with AD-like disease is sustained, on one hand, by the upregulation of the type I IFN signaling by CD8+ T cells, while, on the other hand, by the presence of dysfunctional neurons[168]. Accordingly, it was shown that, under inflammatory conditions, neuronal cells secrete CXCL10 chemokine, which in turn recruiting peripheral cytotoxic CXCR3+ CD8+ T cells into the inflamed brains[186,187]. In support of this, it has been reported a reduced concentration of pro-inflammatory cytokines in the brains of CXCR3-deficient AD-like mice, with a consequent attenuation of behavioral deficits, and reduction of Aβ load and plaque burden[188]. Altogether, these data confirmed that interfering with the CXCR3-dependent brain infiltration of peripheral CD8+ T cells may be an efficient therapeutic target in AD. However, it is crucial to avoid affecting key molecular mechanisms involved in the homeostatic control of immune responses. This goal is difficult to achieve, because the CXCR3/CXCL10 axis, as well as the LFA-1 migration pathway, which we show to be involved in the recruitment of activated CD8 T cells into the brain of 3xTg-AD mice, are extensively used by several immune cell populations in a wide variety of diseased and non-diseased conditions[189]. In the light of this consideration, therapeutic targeting of LFA-1 integrin or CXCR3/CXCL10 axis in AD may have some collateral effects as may interfere with beneficial immune responses. Despite this, herein we firstly demonstrated a role for LFA-1 integrin in driving the trafficking of circulating CD8+ T lymphocytes to the AD brains, which, to date, was only suggested by the augmented expression of *Itgb2* gene, encoding for the CD18 subunit of LFA-1 integrin, in the hippocampus of a mouse model of tauopathy compared to control animals[54,55]. This result is further supported by the increased expression of ICAM-1 adhesion receptor on brain endothelial cells of AD-like mice, previously reported by our group[49].

Evidence in the literature reported a crucial role of CXCR3 chemokine receptor also in mediating Ag-independent immune responses[190]. This suggests that the entry of peripheral CD8+ T cells into

the AD brains could be the consequence of a bystander activation during immune responses. Accordingly, GrK+ CD103- Trm and Effector CD8+ T cells in our dataset upregulated *Klrk1* gene, which encodes for NKG2D molecule, classically expressed by bystander activated CD8+ T lymphocytes[191] (data not shown). This may represent an important difference between AD and other neurodegenerative disorders, such as MS, in which clonally expanded effector-like CD8+ T cells are specifically recruited into the CNS[192–194]. Despite this difference, AD and MS seem to share several common pathogenic mechanisms involving both innate and adaptive[80]. Indeed, not only CD8+ T cells infiltrate the CNS via an LFA-1-mediated molecular pathway in both disorders, but they also favor disease progression by releasing GrK lytic molecule in MS as well as in AD[103,192]. Moreover, in both cases, GrK release was induced shortly after the entry into the CNS parenchyma, and a high expression of PAR-1 receptor was detected on neurons near subcortical lesions in MS patients[103,195]. This confirms that GrK-producing CD8+ T cells could sustain the MS course similarly to what we have shown for AD in this PhD thesis. Interestingly, GrK-producing Trm CD8+ T cells were not only augmented in MS lesions, but they also expressed CXCR6 receptor, highlighting another common point with AD[104]. Finally, the loss of the Trm CD103+ phenotype for CD8+ T lymphocytes was reported also in early MS brain lesions, strengthening the commonalities between AD and MS, two chronic inflammatory neurological disorders in which there is no cure yet[104,194].

In conclusion, we have found a novel CD8+ T cell-mediated GrK-dependent cytotoxic mechanism underlying AD, highlighting the role of CD8+ T lymphocytes in neuronal dysfunction, accumulation of abnormal Aβ and tau, and cognitive impairment. Currently, therapies for AD only provide temporary improvements. Therefore, we propose that targeting the cytotoxic mechanisms exerted by neurotoxic GrK+ CD103- Trm CD8+ T cells could interfere with early pathogenesis of AD, protecting patients suffering from this neurodegenerative disorder from neuronal dysfunctions and memory impairment. However, there are no available drugs to specifically inhibit GrK activity, and further investigations are needed to identify innovative synthetic or natural compounds able to specifically block the neurotoxic and pro-inflammatory potential of this molecule in AD and in other neurodegenerative disorders.

BIBLIOGRAPHY

1. Breijyeh, Z. & Karaman, R. Comprehensive Review on Alzheimer's Disease: Causes and Treatment. *Molecules* vol. 25 Preprint at https://doi.org/10.3390/MOLECULES25245789 (2020).
2. Tonkonogy, J. & Moak, G. S. *Alois Alzheimer on Presenile Dementia at a meeting of the*. *J Geriatr Psychiatry Neurol* vol. 1 (1988).
3. Knopman, D. S. *et al.* Alzheimer disease. *Nat Rev Dis Primers* **7**, (2021).
4. Deture, M. A. & Dickson, D. W. The neuropathological diagnosis of Alzheimer's disease. *Molecular Neurodegeneration* vol. 14 Preprint at https://doi.org/10.1186/s13024-019-0333-5 (2019).
5. Maji, S. K., Anoop, A., Singh, P. K. & Jacob, R. S. CSF biomarkers for Alzheimer's disease diagnosis. *International Journal of Alzheimer's Disease* Preprint at https://doi.org/10.4061/2010/606802 (2010).
6. Dubois, B. *et al.* Clinical diagnosis of Alzheimer's disease: recommendations of the International Working Group. *The Lancet Neurology* vol. 20 484–496 Preprint at https://doi.org/10.1016/S1474-4422(21)00066-1 (2021).
7. Niemantsverdriet, E., Valckx, S., Bjerke, M. & Engelborghs, S. Alzheimer's disease CSF biomarkers: clinical indications and rational use. *Acta Neurologica Belgica* vol. 117 591–602 Preprint at https://doi.org/10.1007/s13760-017-0816-5 (2017).
8. Weller, J. & Budson, A. Current understanding of Alzheimer's disease diagnosis and treatment. *F1000Research* vol. 7 Preprint at https://doi.org/10.12688/f1000research.14506.1 (2018).
9. Zhang, X. Y., Yang, Z. L., Lu, G. M., Yang, G. F. & Zhang, L. J. PET/MR imaging: New frontier in Alzheimer's disease and other dementias. *Frontiers in Molecular Neuroscience* vol. 10 Preprint at https://doi.org/10.3389/fnmol.2017.00343 (2017).
10. Johnson, K. A., Fox, N. C., Sperling, R. A. & Klunk, W. E. Brain imaging in Alzheimer disease. *Cold Spring Harb Perspect Med* **2**, (2012).
11. König, T. & Stögmann, E. Genetics of Alzheimer's disease. *Wiener Medizinische Wochenschrift* **171**, 249–256 (2021).
12. Altendorfer, B. *et al.* Transcriptomic Profiling Identifies CD8 + T Cells in the Brain of Aged and Alzheimer's Disease Transgenic Mice as Tissue-Resident Memory T Cells . *The Journal of Immunology* **209**, 1272–1285 (2022).
13. Feringa, F. M. & van der Kant, R. Cholesterol and Alzheimer's Disease; From Risk Genes to Pathological Effects. *Frontiers in Aging Neuroscience* vol. 13 Preprint at https://doi.org/10.3389/fnagi.2021.690372 (2021).
14. Xie, B., Shi, X., Xing, Y. & Tang, Y. Association between atherosclerosis and Alzheimer's disease: A systematic review and meta-analysis. *Brain and Behavior* vol. 10 Preprint at https://doi.org/10.1002/brb3.1601 (2020).
15. Nguyen, T. T., Ta, Q. T. H., Nguyen, T. K. O., Nguyen, T. T. D. & Giau, V. Van. Type 3 diabetes and its role implications in alzheimer's disease. *International Journal of Molecular Sciences* vol. 21 Preprint at https://doi.org/10.3390/ijms21093165 (2020).
16. Zhang, T. *et al.* Dietary Fatty Acid Factors in Alzheimer's Disease: A Review. *Journal of Alzheimer's Disease* vol. 78 887–904 Preprint at https://doi.org/10.3233/JAD-200558 (2020).
17. Samieri, C. *et al.* Fish Intake, Genetic Predisposition to Alzheimer Disease, and Decline in Global Cognition and Memory in 5 Cohorts of Older Persons. *Am J Epidemiol* **187**, 933–940 (2018).
18. Montagne, A. *et al.* APOE4 leads to blood–brain barrier dysfunction predicting cognitive decline. *Nature* **581**, 71–76 (2020).

19. van Olst, L. *et al.* Crossing borders in Alzheimer's disease: A T cell's perspective. *Advanced Drug Delivery Reviews* vol. 188 Preprint at https://doi.org/10.1016/j.addr.2022.114398 (2022).
20. Santos-Lima, B., Pietronigro, E. C., Terrabuio, E., Zenaro, E. & Constantin, G. The role of neutrophils in the dysfunction of central nervous system barriers. *Front Aging Neurosci* **14**, 904 (2022).
21. Li, R., Wang, X. & He, P. The most prevalent rare coding variants of TREM2 conferring risk of Alzheimer's disease: A systematic review and meta-analysis. *Exp Ther Med* **21**, (2021).
22. Qin, Q. *et al.* Gene mutations associated with early onset familial Alzheimer's disease in China: An overview and current status. *Molecular Genetics and Genomic Medicine* vol. 8 Preprint at https://doi.org/10.1002/mgg3.1443 (2020).
23. Nardini, E., Hogan, R., Flamier, A. & Bernier, G. Alzheimer's disease: A tale of two diseases? *Neural Regeneration Research* vol. 16 1958–1964 Preprint at https://doi.org/10.4103/1673-5374.308070 (2021).
24. Yegambaram, M., Manivannan, B., Beach, T. G. & Halden, R. U. *Send Orders for Reprints to reprints@benthamscience.ae Role of Environmental Contaminants in the Etiology of Alzheimer's Disease: A Review*. *Current Alzheimer Research* vol. 12 http://www.worldlifeexpectancy.com/cause-of-death/alzheimers-dementia/by-country/. (2015).
25. Ristori, E., Donnini, S. & Ziche, M. New Insights Into Blood-Brain Barrier Maintenance: The Homeostatic Role of β-Amyloid Precursor Protein in Cerebral Vasculature. *Frontiers in Physiology* vol. 11 Preprint at https://doi.org/10.3389/fphys.2020.01056 (2020).
26. Hampel, H. *et al.* The β-Secretase BACE1 in Alzheimer's Disease. *Biological Psychiatry* vol. 89 745–756 Preprint at https://doi.org/10.1016/j.biopsych.2020.02.001 (2021).
27. Yang, Y. H., Huang, L. C., Hsieh, S. W. & Huang, L. J. Dynamic Blood Concentrations of Aβ1–40 and Aβ1–42 in Alzheimer's Disease. *Front Cell Dev Biol* **8**, (2020).
28. Gu, L. & Guo, Z. Alzheimer's Aβ42 and Aβ40 peptides form interlaced amyloid fibrils. *J Neurochem* **126**, 305–311 (2013).
29. Liu, J., Chang, L., Song, Y., Li, H. & Wu, Y. The role of NMDA receptors in Alzheimer's disease. *Frontiers in Neuroscience* vol. 13 Preprint at https://doi.org/10.3389/fnins.2019.00043 (2019).
30. Babaei, P. NMDA and AMPA receptors dysregulation in Alzheimer's disease. *European Journal of Pharmacology* vol. 908 Preprint at https://doi.org/10.1016/j.ejphar.2021.174310 (2021).
31. Serrano-Pozo, A., Frosch, M. P., Masliah, E. & Hyman, B. T. Neuropathological alterations in Alzheimer disease. *Cold Spring Harb Perspect Med* **1**, (2011).
32. Querfurth, H. W. & LaFerla, F. M. Alzheimer's Disease. *New England Journal of Medicine* **362**, 329–344 (2010).
33. Drubin, D. G. & Kirschner, M. W. *Tau Protein Function in Living Cells*. (1986).
34. Poorkaj, P. *et al.* Tau is a candidate gene for chromosome 17 frontotemporal dementia. *Ann Neurol* **43**, 815–825 (1998).
35. Muralidar, S., Ambi, S. V., Sekaran, S., Thirumalai, D. & Palaniappan, B. Role of tau protein in Alzheimer's disease: The prime pathological player. *International Journal of Biological Macromolecules* vol. 163 1599–1617 Preprint at https://doi.org/10.1016/j.ijbiomac.2020.07.327 (2020).
36. Li, D. & Cho, Y. K. High specificity of widely used phospho-tau antibodies validated using a quantitative whole-cell based assay. *J Neurochem* **152**, 122–135 (2020).
37. Cuello, A. C. *et al.* Early-stage inflammation and experimental therapy in transgenic models of the Alzheimer-like amyloid pathology. in *Neurodegenerative Diseases* vol. 7 96–98 (2010).

38. Domínguez-Álvaro, M., Montero-Crespo, M., Blazquez-Llorca, L., DeFelipe, J. & Alonso-Nanclares, L. 3D electron microscopy study of synaptic organization of the normal human transentorhinal cortex and its possible alterations in alzheimer's disease. *eNeuro* **6**, 1–17 (2019).
39. Ozelik, T. *et al. Synaptophysin: Structure of the Human Gene and Assignment to the X Chromosome in Man and Mouse*. *Am. J. Hum. Genet* vol. 47 (1990).
40. Subramanian, J., Savage, J. C. & Tremblay, M. È. Synaptic Loss in Alzheimer's Disease: Mechanistic Insights Provided by Two-Photon in vivo Imaging of Transgenic Mouse Models. *Frontiers in Cellular Neuroscience* vol. 14 Preprint at https://doi.org/10.3389/fncel.2020.592607 (2020).
41. Montero-Crespo, M., Dominguez-Alvaro, M., Alonso-Nanclares, L., Defelipe, J. & Blazquez-Llorca, L. Three-dimensional analysis of synaptic organization in the hippocampal CA1 field in Alzheimer's disease. *Brain* **144**, 553–573 (2021).
42. Mukhin, V. N., Pavlov, K. I. & Klimenko, V. M. Mechanisms of Neuron Loss in Alzheimer's Disease. *Neurosci Behav Physiol* **47**, 508–516 (2017).
43. Karisetty, B. C. *et al.* Amyloid-β Peptide Impact on Synaptic Function and Neuroepigenetic Gene Control Reveal New Therapeutic Strategies for Alzheimer's Disease. *Frontiers in Molecular Neuroscience* vol. 13 Preprint at https://doi.org/10.3389/fnmol.2020.577622 (2020).
44. Fang, F. *et al.* RAGE mediates Aβ accumulation in a mouse model of Alzheimers disease via modulation of β- and γ-secretase activity. *Hum Mol Genet* **27**, 1002–1014 (2018).
45. Cheignon, C. *et al.* Oxidative stress and the amyloid beta peptide in Alzheimer's disease. *Redox Biology* vol. 14 450–464 Preprint at https://doi.org/10.1016/j.redox.2017.10.014 (2018).
46. Donev, R., Kolev, M., Millet, B. & Thome, J. Neuronal death in Alzheimer's disease and therapeutic opportunities. *J Cell Mol Med* **13**, 4329–4348 (2009).
47. Whitson, H. E. *et al.* Infection and inflammation: New perspectives on Alzheimer's disease. *Brain, Behavior, and Immunity - Health* vol. 22 Preprint at https://doi.org/10.1016/j.bbih.2022.100462 (2022).
48. Heneka, M. T. *et al.* Neuroinflammation in Alzheimer's disease. *The Lancet Neurology* vol. 14 388–405 Preprint at https://doi.org/10.1016/S1474-4422(15)70016-5 (2015).
49. Zenaro, E. *et al.* Neutrophils promote Alzheimer's disease-like pathology and cognitive decline via LFA-1 integrin. *Nat Med* **21**, 880–886 (2015).
50. Gate, D. *et al.* Clonally expanded CD8 T cells patrol the cerebrospinal fluid in Alzheimer's disease. *Nature* **577**, 399–404 (2020).
51. Unger, M. S. *et al.* CD8+ T-cells infiltrate Alzheimer's disease brains and regulate neuronal- and synapse-related gene expression in APP-PS1 transgenic mice. *Brain Behav Immun* **89**, 67–86 (2020).
52. Merlini, M., Kirabali, T., Kulic, L., Nitsch, R. M. & Ferretti, M. T. Extravascular CD3+ T Cells in Brains of Alzheimer Disease Patients Correlate with Tau but Not with Amyloid Pathology: An Immunohistochemical Study. *Neurodegener Dis* **18**, 49–56 (2018).
53. Ferretti, M. T. *et al.* T-cell brain infiltration and immature antigen-presenting cells in transgenic models of Alzheimer's disease-like cerebral amyloidosis. *Brain Behav Immun* **54**, 211–225 (2016).
54. Togo, T. *et al. Occurrence of T cells in the brain of Alzheimer's disease and other neurological diseases*. www.elsevier.com/locate/jneuroim (2002).
55. Laurent, C. *et al.* Hippocampal T cell infiltration promotes neuroinflammation and cognitive decline in a mouse model of tauopathy. *Brain* **140**, 184–200 (2017).
56. DiSabato, D. J., Quan, N. & Godbout, J. P. Neuroinflammation: the devil is in the details. *J Neurochem* **139**, 136–153 (2016).

57. Cabezas, R. *et al.* Astrocytic modulation of blood brain barrier: Perspectives on Parkinson's disease. *Frontiers in Cellular Neuroscience* vol. 8 Preprint at https://doi.org/10.3389/fncel.2014.00211 (2014).
58. Babić Leko, M. *et al.* IL-1β, IL-6, IL-10, and TNFα Single Nucleotide Polymorphisms in Human Influence the Susceptibility to Alzheimer's Disease Pathology. *Journal of Alzheimer's Disease* **75**, 1029–1047 (2020).
59. Onyango, I. G., Jauregui, G. V., Čarná, M., Bennett, J. P. & Stokin, G. B. Neuroinflammation in Alzheimer's disease. *Biomedicines* vol. 9 Preprint at https://doi.org/10.3390/biomedicines9050524 (2021).
60. Minter, M. R., Taylor, J. M. & Crack, P. J. The contribution of neuroinflammation to amyloid toxicity in Alzheimer's disease. *Journal of Neurochemistry* vol. 136 457–474 Preprint at https://doi.org/10.1111/jnc.13411 (2016).
61. Hansen, D. V., Hanson, J. E. & Sheng, M. Microglia in Alzheimer's disease. *Journal of Cell Biology* vol. 217 459–472 Preprint at https://doi.org/10.1083/jcb.201709069 (2018).
62. Cai, Z., Hussain, M. D. & Yan, L. J. Microglia, neuroinflammation, and beta-amyloid protein in Alzheimer's disease. *International Journal of Neuroscience* vol. 124 307–321 Preprint at https://doi.org/10.3109/00207454.2013.833510 (2014).
63. Franco-Bocanegra, D. K. *et al.* Microglial morphology in Alzheimer's disease and after Aβ immunotherapy. *Sci Rep* **11**, (2021).
64. Schitine, C., Nogaroli, L., Costa, M. R. & Hedin-Pereira, C. Astrocyte heterogeneity in the brain: From development to disease. *Frontiers in Cellular Neuroscience* vol. 9 Preprint at https://doi.org/10.3389/fncel.2015.00076 (2015).
65. Preman, P., Alfonso-Triguero, M., Alberdi, E., Verkhratsky, A. & Arranz, A. M. Astrocytes in alzheimer's disease: Pathological significance and molecular pathways. *Cells* vol. 10 1–19 Preprint at https://doi.org/10.3390/cells10030540 (2021).
66. Zhang, F. & Jiang, L. Neuroinflammation in Alzheimer訃s disease. *Neuropsychiatric Disease and Treatment* vol. 11 243–256 Preprint at https://doi.org/10.2147/NDT.S75546 (2014).
67. Frost, G. R. & Li, Y. M. The role of astrocytes in amyloid production and Alzheimer's disease. *Open Biology* vol. 7 Preprint at https://doi.org/10.1098/rsob.170228 (2017).
68. Zhang, Y. *et al.* Depletion of NK Cells Improves Cognitive Function in the Alzheimer Disease Mouse Model. *The Journal of Immunology* **205**, 502–510 (2020).
69. van Olst, L. *et al.* Crossing borders in Alzheimer's disease: A T cell's perspective. *Adv Drug Deliv Rev* **188**, (2022).
70. Tiberti, S. *et al.* GZMKhigh CD8+ T effector memory cells are associated with CD15high neutrophil abundance in non-metastatic colorectal tumors and predict poor clinical outcome. *Nat Commun* **13**, (2022).
71. Ley, K., Laudanna, C., Cybulsky, M. I. & Nourshargh, S. Getting to the site of inflammation: The leukocyte adhesion cascade updated. *Nature Reviews Immunology* vol. 7 678–689 Preprint at https://doi.org/10.1038/nri2156 (2007).
72. Walling, B. L. & Kim, M. LFA-1 in T cell migration and differentiation. *Frontiers in Immunology* vol. 9 Preprint at https://doi.org/10.3389/fimmu.2018.00952 (2018).
73. Capece, T. *et al.* A novel intracellular pool of LFA-1 is critical for asymmetric CD8+ T cell activation and differentiation. *Journal of Cell Biology* **216**, 3817–3829 (2017).
74. Pietronigro, E. *et al.* Blockade of α4 integrins reduces leukocyte–endothelial interactions in cerebral vessels and improves memory in a mouse model of Alzheimer's disease. *Sci Rep* **9**, (2019).
75. Germain, R. N. t-cell development and the CD4-CD8 lineage decision. *Nature Reviews Immunology* vol. 2 309–322 Preprint at https://doi.org/10.1038/nri798 (2002).
76. Spits, H. Development of αβ T cells in the human thymus. *Nature Reviews Immunology* vol. 2 760–772 Preprint at https://doi.org/10.1038/nri913 (2002).

77. Diao, H. & Pipkin, M. Stability and flexibility in chromatin structure and transcription underlies memory CD8 T-cell differentiation [version 1; peer review: 2 approved]. *F1000Research* vol. 8 Preprint at https://doi.org/10.12688/f1000research.18211.1 (2019).
78. Youngblood, B. *et al.* Effector CD8 T cells dedifferentiate into long-lived memory cells. *Nature* **552**, 404–409 (2017).
79. Martin, M. D. & Badovinac, V. P. Defining memory CD8 T cell. *Frontiers in Immunology* vol. 9 Preprint at https://doi.org/10.3389/fimmu.2018.02692 (2018).
80. Rossi, B., Santos-Lima, B., Terrabuio, E., Zenaro, E. & Constantin, G. Common Peripheral Immunity Mechanisms in Multiple Sclerosis and Alzheimer's Disease. *Front Immunol* **12**, (2021).
81. Gerlach, C. *et al.* The Chemokine Receptor CX3CR1 Defines Three Antigen-Experienced CD8 T Cell Subsets with Distinct Roles in Immune Surveillance and Homeostasis. *Immunity* **45**, 1270–1284 (2016).
82. Herndler-Brandstetter, D. *et al.* KLRG1+ Effector CD8+ T Cells Lose KLRG1, Differentiate into All Memory T Cell Lineages, and Convey Enhanced Protective Immunity. *Immunity* **48**, 716-729.e8 (2018).
83. Plumlee, C. R., Sheridan, B. S., Cicek, B. B. & Lefrançois, L. Environmental cues dictate the fate of individual CD8+ T cells responding to infection. *Immunity* **39**, 347–356 (2013).
84. Reading, J. L. *et al.* The function and dysfunction of memory CD8+ T cells in tumor immunity. *Immunological Reviews* vol. 283 194–212 Preprint at https://doi.org/10.1111/imr.12657 (2018).
85. Arsenio, J. *et al.* Early specification of CD8+T lymphocyte fates during adaptive immunity revealed by single-cell gene-expression analyses. *Nat Immunol* **15**, 365–372 (2014).
86. Brinkman, C. C., Rouhani, S. J., Srinivasan, N. & Engelhard, V. H. Peripheral Tissue Homing Receptors Enable T Cell Entry into Lymph Nodes and Affect the Anatomical Distribution of Memory Cells. *The Journal of Immunology* **191**, 2412–2425 (2013).
87. Van Stipdonk, M. J. B., Lemmens, E. E. & Schoenberger, S. P. *Naïve CTLs require a single brief period of antigenic stimulation for clonal expansion and differentiation*. http://immunol.nature.com (2001).
88. Kaech, S. M. & Ahmed, R. *Memory CD8 + T cell differentiation: initial antigen encounter triggers a developmental program in naïve cells*. http://immunol.nature.com (2001).
89. Buchholz, V. R. *et al.* Disparate individual fates compose robust CD8+ T cell immunity. *Science (1979)* **340**, 626–630 (2013).
90. Andreatta, M. *et al.* Interpretation of T cell states from single-cell transcriptomics data using reference atlases. *Nat Commun* **12**, (2021).
91. Soares, A. *et al.* Novel application of Ki67 to quantify antigen-specific in vitro lymphoproliferation. *J Immunol Methods* **362**, 43–50 (2010).
92. Kamphorst, A. O. *et al.* Proliferation of PD-1+ CD8 T cells in peripheral blood after PD-1-targeted therapy in lung cancer patients. *Proc Natl Acad Sci U S A* **114**, 4993–4998 (2017).
93. de Araújo-Souza, P. S. *et al.* Differential interferon-γ production by naive and memory-like CD8 T cells. *J Leukoc Biol* **108**, 1329–1337 (2020).
94. MacKay, L. K. *et al.* The developmental pathway for CD103+ CD8+ tissue-resident memory T cells of skin. *Nat Immunol* **14**, 1294–1301 (2013).
95. Bottois, H. *et al.* KLRG1 and CD103 Expressions Define Distinct Intestinal Tissue-Resident Memory CD8 T Cell Subsets Modulated in Crohn's Disease. *Front Immunol* **11**, (2020).
96. Sheridan, B. S. *et al.* Oral infection drives a distinct population of intestinal resident memory cd8+ t cells with enhanced protective function. *Immunity* **40**, 747–757 (2014).
97. Obar, J. J. & Lefrançois, L. Early Signals during CD8 + T Cell Priming Regulate the Generation of Central Memory Cells . *The Journal of Immunology* **185**, 263–272 (2010).

98. Van der Gracht, E. T. I. *et al.* Memory CD8+T cell heterogeneity is primarilydriven by pathogen-specific cues and additionallyshaped by the tissue environment. *iScience CellPress* (2021) doi:doi.org/10.1016/j.isci. 2020.101954.
99. Chen, Y., Shen, J., Kasmani, M. Y., Topchyan, P. & Cui, W. Single-cell transcriptomics reveals core regulatory programs that determine the heterogeneity of circulating and tissue-resident memory cd8+ t cells. *Cells* **10**, (2021).
100. Groh, J. *et al.* Accumulation of cytotoxic T cells in the aged CNS leads to axon degeneration and contributes to cognitive and motor decline. *Nat Aging* **1**, 357–367 (2021).
101. Smolders, J., van Luijn, M. M., Hsiao, C. C. & Hamann, J. T-cell surveillance of the human brain in health and multiple sclerosis. *Seminars in Immunopathology* Preprint at https://doi.org/10.1007/s00281-022-00926-8 (2022).
102. Smolders, J. *et al.* Tissue-resident memory T cells populate the human brain. *Nat Commun* **9**, (2018).
103. Koetzier, S. C. *et al.* Distinct Effector Programs of Brain-Homing CD8+ T Cells in Multiple Sclerosis. *Cells* **11**, (2022).
104. Fransen, N. L. *et al.* Tissue-resident memory T cells invade the brain parenchyma in multiple sclerosis white matter lesions. *Brain* **143**, 1714–1730 (2020).
105. Wakim, L. M. *et al.* The Molecular Signature of Tissue Resident Memory CD8 T Cells Isolated from the Brain. *The Journal of Immunology* **189**, 3462–3471 (2012).
106. FitzPatrick, M. E. B. *et al.* Human intestinal tissue-resident memory T cells comprise transcriptionally and functionally distinct subsets. *Cell Rep* **34**, (2021).
107. Campisi, L. *et al.* Clonally expanded CD8 T cells characterize amyotrophic lateral sclerosis-4. *Nature* **606**, 945–952 (2022).
108. Takamura, S. Niches for the long-term maintenance of tissue-resident memory T cells. *Frontiers in Immunology* vol. 9 Preprint at https://doi.org/10.3389/fimmu.2018.01214 (2018).
109. Milner, J. J. & Goldrath, A. W. Transcriptional programming of tissue-resident memory CD8 + T cells. *Current Opinion in Immunology* vol. 51 162–169 Preprint at https://doi.org/10.1016/j.coi.2018.03.017 (2018).
110. Crowl, J. T. *et al.* Tissue-resident memory CD8+ T cells possess unique transcriptional, epigenetic and functional adaptations to different tissue environments. *Nat Immunol* **23**, 1121–1131 (2022).
111. Milner, J. J. *et al.* Heterogenous Populations of Tissue-Resident CD8+ T Cells Are Generated in Response to Infection and Malignancy. *Immunity* **52**, 808-824.e7 (2020).
112. Walsh, D. A. *et al.* The Functional Requirement for CD69 in Establishment of Resident Memory CD8 + T Cells Varies with Tissue Location . *The Journal of Immunology* **203**, 946–955 (2019).
113. McNamara, H. A. *et al.* Up-regulation of LFA-1 allows liver-resident memory T cells to patrol and remain in the hepatic sinusoids. *Sci Immunol* **2**, (2017).
114. Steinbach, K. *et al.* Brain-resident memory T cells represent an autonomous cytotoxic barrier to viral infection. *Journal of Experimental Medicine* **213**, 1571–1587 (2016).
115. Milner, J. J. *et al.* Delineation of a molecularly distinct terminally differentiated memory CD8 T cell population. *PNAS* (2020) doi:10.1073/pnas.2008571117/-/DCSupplemental.
116. Verdon, D. J., Mulazzani, M. & Jenkins, M. R. Cellular and molecular mechanisms of CD8+ T cell differentiation, dysfunction and exhaustion. *International Journal of Molecular Sciences* vol. 21 1–28 Preprint at https://doi.org/10.3390/ijms21197357 (2020).
117. Wherry, E. J. T cell exhaustion. *Nature Immunology* vol. 12 492–499 Preprint at https://doi.org/10.1038/ni.2035 (2011).
118. Giles, J. R. *et al.* Shared and distinct biological circuits in effector, memory and exhausted CD8+ T cells revealed by temporal single-cell transcriptomics and epigenetics. *Nat Immunol* (2022) doi:10.1038/s41590-022-01338-4.

119. Dolina, J. S., Van Braeckel-Budimir, N., Thomas, G. D. & Salek-Ardakani, S. CD8+ T Cell Exhaustion in Cancer. *Frontiers in Immunology* vol. 12 Preprint at https://doi.org/10.3389/fimmu.2021.715234 (2021).
120. Mognol, G. P. *et al.* Exhaustion-associated regulatory regions in CD8+ tumor-infiltrating T cells. *Proc Natl Acad Sci U S A* **114**, E2776–E2785 (2017).
121. Ashouri, J. F. & Weiss, A. Endogenous Nur77 Is a Specific Indicator of Antigen Receptor Signaling in Human T and B Cells. *The Journal of Immunology* **198**, 657–668 (2017).
122. Khan, O. *et al.* TOX transcriptionally and epigenetically programs CD8+ T cell exhaustion. *Nature* **571**, 211–218 (2019).
123. Man, K. *et al.* Transcription Factor IRF4 Promotes CD8+ T Cell Exhaustion and Limits the Development of Memory-like T Cells during Chronic Infection. *Immunity* **47**, 1129-1141.e5 (2017).
124. Grebinoski, S. *et al.* Autoreactive CD8+ T cells are restrained by an exhaustion-like program that is maintained by LAG3. *Nat Immunol* **23**, 868–877 (2022).
125. Schietinger, A. *et al.* Tumor-Specific T Cell Dysfunction Is a Dynamic Antigen-Driven Differentiation Program Initiated Early during Tumorigenesis. *Immunity* **45**, 389–401 (2016).
126. Zhao, Y., Shao, Q. & Peng, G. Exhaustion and senescence: two crucial dysfunctional states of T cells in the tumor microenvironment. *Cellular and Molecular Immunology* vol. 17 27–35 Preprint at https://doi.org/10.1038/s41423-019-0344-8 (2020).
127. Jiang, Y., Li, Y. & Zhu, B. T-cell exhaustion in the tumor microenvironment. *Cell Death and Disease* vol. 6 Preprint at https://doi.org/10.1038/cddis.2015.162 (2015).
128. Saleh, R. *et al.* Expression of immune checkpoints and T cell exhaustion markers in early and advanced stages of colorectal cancer. *Cancer Immunology, Immunotherapy* **69**, 1989–1999 (2020).
129. Okagawa, T. *et al.* Cooperation of PD-1 and LAG-3 in the exhaustion of CD4+ and CD8+ T cells during bovine leukemia virus infection. *Vet Res* **49**, 50 (2018).
130. Jin, H. T. *et al.* Cooperation of Tim-3 and PD-1 in CD8 T-cell exhaustion during chronic viral infection. *Proc Natl Acad Sci U S A* **107**, 14733–14738 (2010).
131. Nakamoto, N. *et al.* Synergistic reversal of intrahepatic HCV-specific CD8 T cell exhaustion by combined PD-1/CTLA-4 blockade. *PLoS Pathog* **5**, (2009).
132. Ravi, V. M. *et al.* T-cell dysfunction in the glioblastoma microenvironment is mediated by myeloid cells releasing interleukin-10. *Nat Commun* **13**, (2022).
133. Zhang, Z. *et al.* Pan-cancer landscape of T-cell exhaustion heterogeneity within the tumor microenvironment revealed a progressive roadmap of hierarchical dysfunction associated with prognosis and therapeutic efficacy. *EBioMedicine* **83**, 104207 (2022).
134. Larbi, A. & Fulop, T. From 'truly naïve' to 'exhausted senescent' T cells: When markers predict functionality. *Cytometry Part A* vol. 85 25–35 Preprint at https://doi.org/10.1002/cyto.a.22351 (2014).
135. Pereira, B. I. *et al.* Sestrins induce natural killer function in senescent-like CD8+ T cells. *Nat Immunol* **21**, 684–694 (2020).
136. Tedeschi, V. *et al.* CD8+ T Cell Senescence: Lights and Shadows in Viral Infections, Autoimmune Disorders and Cancer. *International Journal of Molecular Sciences* vol. 23 Preprint at https://doi.org/10.3390/ijms23063374 (2022).
137. Callender, L. A. *et al.* Human CD8 + EMRA T cells display a senescence-associated secretory phenotype regulated by p38 MAPK. *Aging Cell* **17**, 1–9 (2018).
138. Shive, C. L. *et al.* Markers of T Cell Exhaustion and Senescence and Their Relationship to Plasma TGF-β Levels in Treated HIV+ Immune Non-responders. *Front Immunol* **12**, (2021).
139. Wang, T. W. *et al.* Blocking PD-L1–PD-1 improves senescence surveillance and ageing phenotypes. *Nature* **611**, 358–364 (2022).

140. Mogilenko, D. A., Shchukina, I. & Artyomov, M. N. Immune ageing at single-cell resolution. *Nature Reviews Immunology* vol. 22 484–498 Preprint at https://doi.org/10.1038/s41577-021-00646-4 (2022).
141. Brenchley, J. M. *et al.* Expression of CD57 defines replicative senescence and antigen-induced apoptotic death of CD8+ T cells. *Blood* **101**, 2711–2720 (2003).
142. Henson, S. M., Macaulay, R., Riddell, N. E., Nunn, C. J. & Akbar, A. N. Blockade of PD-1 or p38 MAP kinase signaling enhances senescent human CD8+ T-cell proliferation by distinct pathways. *Eur J Immunol* **45**, 1441–1451 (2015).
143. Lee, S. W. *et al.* CD8 + TILs in NSCLC differentiate into TEMRA via a bifurcated trajectory: Deciphering immunogenicity of tumor antigens. *J Immunother Cancer* **9**, (2021).
144. Covre, L. P., De Maeyer, R. P. H., Gomes, D. C. O. & Akbar, A. N. The role of senescent T cells in immunopathology. *Aging Cell* vol. 19 Preprint at https://doi.org/10.1111/acel.13272 (2020).
145. Kumar, B. V., Connors, T. J. & Farber, D. L. Human T Cell Development, Localization, and Function throughout Life. *Immunity* vol. 48 202–213 Preprint at https://doi.org/10.1016/j.immuni.2018.01.007 (2018).
146. Martínez-Zamudio, R. I. *et al.* Senescence-associated β-galactosidase reveals the abundance of senescent CD8+ T cells in aging humans. *Aging Cell* **20**, (2021).
147. Fessler, J. & Angiari, S. The Role of T Cell Senescence in Neurological Diseases and Its Regulation by Cellular Metabolism. *Frontiers in Immunology* vol. 12 Preprint at https://doi.org/10.3389/fimmu.2021.706434 (2021).
148. Dulken, B. W. *et al.* Single-cell analysis reveals T cell infiltration in old neurogenic niches. *Nature* (2019) doi:10.1038/s41586-019-1362-5.
149. Fulop, T. *et al.* Immunosenescence and inflamm-aging as two sides of the same coin: Friends or Foes? *Frontiers in Immunology* vol. 8 Preprint at https://doi.org/10.3389/fimmu.2017.01960 (2018).
150. Gate, D. *et al.* CD4+ T cells contribute to neurodegeneration in Lewy body dementia. *Science (1979)* **374**, 868–874 (2021).
151. Galiano-Landeira, J., Torra, A., Vila, M. & Bovè, J. CD8 T cell nigral infiltration precedessynucleinopathy in early stages ofParkinson's disease. *Brain* vol. 143 3717–3733 Preprint at https://doi.org/10.1093/brain/awaa269 (2020).
152. Veroni, C. & Aloisi, F. The CD8 T Cell-Epstein-Barr Virus-B Cell Trialogue: A Central Issue in Multiple Sclerosis Pathogenesis. *Frontiers in Immunology* vol. 12 Preprint at https://doi.org/10.3389/fimmu.2021.665718 (2021).
153. Jenkins, E. C. *et al.* Telomere shortening in T lymphocytes of older individuals with Down syndrome and dementia. *Neurobiol Aging* **27**, 941–945 (2006).
154. Jenkins, E. C. *et al.* Shorter telomeres may indicate dementia status in older individuals with Down syndrome. *Neurobiol Aging* **31**, 765–771 (2010).
155. Panossian, L. A. *et al. Telomere shortening in T cells correlates with Alzheimer's disease status*. *Neurobiology of Aging* vol. 24 (2003).
156. Gate, D. *et al.* Clonally expanded CD8 T cells patrol the cerebrospinal fluid in Alzheimer's disease. *Nature* **577**, 399–404 (2020).
157. Xu, H. & Jia, J. Single-Cell RNA Sequencing of Peripheral Blood Reveals Immune Cell Signatures in Alzheimer's Disease. *Front Immunol* **12**, (2021).
158. Guyenet, S. J. *et al.* A simple composite phenotype scoring system for evaluating mouse models of cerebellar ataxia. *Journal of Visualized Experiments* (2010) doi:10.3791/1787.
159. Kurd, N. S. *et al. Early precursors and molecular determinants of tissue-resident memory CD8 + T lymphocytes revealed by single-cell RNA sequencing*. *Sci. Immunol* vol. 5 http://immunology.sciencemag.org/ (2020).

160. Preston, G. C., Feijoo-Carnero, C., Schurch, N., Cowling, V. H. & Cantrell, D. A. The Impact of KLF2 Modulation on the Transcriptional Program and Function of CD8 T Cells. *PLoS One* **8**, (2013).
161. Merkler, D., Vincenti, I., Masson, F. & Liblau, R. S. Tissue-resident CD8 T cells in central nervous system inflammatory diseases: present at the crime scene and …guilty. *Current Opinion in Immunology* vol. 77 Preprint at https://doi.org/10.1016/j.coi.2022.102211 (2022).
162. Pabla, N., Bhatt, K. & Dong, Z. Checkpoint kinase 1 (Chk1)-short is a splice variant and endogenous inhibitor of Chk1 that regulates cell cycle and DNA damage checkpoints. *Proc Natl Acad Sci U S A* **109**, 197–202 (2012).
163. Wienke, J. *et al.* T cell interaction with activated endothelial cells primes for tissue-residency. *Front Immunol* **13**, (2022).
164. Saresella, M. *et al.* IL-33 and its decoy sST2 in patients with Alzheimer's disease and mild cognitive impairment. *J Neuroinflammation* **17**, (2020).
165. Ren, H. M. *et al. IL-21 from high-affinity CD4 T cells drives differentiation of brain-resident CD8 T cells during persistent viral infection*. *Sci. Immunol* vol. 5 https://www.science.org (2020).
166. Kok, L., Masopust, D. & Schumacher, T. N. The precursors of CD8+ tissue resident memory T cells: from lymphoid organs to infected tissues. *Nature Reviews Immunology* vol. 22 283–293 Preprint at https://doi.org/10.1038/s41577-021-00590-3 (2022).
167. Crouse, J., Kalinke, U. & Oxenius, A. Regulation of antiviral T cell responses by type i interferons. *Nature Reviews Immunology* vol. 15 231–242 Preprint at https://doi.org/10.1038/nri3806 (2015).
168. Labarta-Bajo, L. *et al.* Type I IFNs and CD8 T cells increase intestinal barrier permeability after chronic viral infection. *Journal of Experimental Medicine* **217**, (2020).
169. Kalia, V. & Sarkar, S. Regulation of Effector and Memory CD8 T Cell Differentiation by IL-2—A Balancing Act. *Frontiers in Immunology* vol. 9 Preprint at https://doi.org/10.3389/fimmu.2018.02987 (2018).
170. Bouwman, A. C., van Daalen, K. R., Crnko, S., ten Broeke, T. & Bovenschen, N. Intracellular and Extracellular Roles of Granzyme K. *Frontiers in Immunology* vol. 12 Preprint at https://doi.org/10.3389/fimmu.2021.677707 (2021).
171. Howie, D., Waldmann, H. & Cobbold, S. P. Nutrient sensing via mTOR in T cells maintains a tolerogenic microenvironment. *Front Immunol* **5**, (2014).
172. Smyth, M. J. *et al.* Unlocking the secrets of cytotoxic granule proteins. *J Leukoc Biol* **70**, 18–29 (2001).
173. Chang, H. F. *et al.* Identification of distinct cytotoxic granules as the origin of supramolecular attack particles in T lymphocytes. *Nat Commun* **13**, (2022).
174. Herz, J. *et al.* Acid sphingomyelinase is a key regulator of cytotoxic granule secretion by primary T lymphocytes. *Nat Immunol* **10**, 761–768 (2009).
175. Adeoye, T., Shah, S. I., Demuro, A., Rabson, D. A. & Ullah, G. Upregulated Ca2+ Release from the Endoplasmic Reticulum Leads to Impaired Presynaptic Function in Familial Alzheimer's Disease. *Cells* **11**, (2022).
176. Zündorf, G. & Reiser, G. *Calcium Dysregulation and Homeostasis of Neural Calcium in the Molecular Mechanisms of Neurodegenerative Diseases Provide Multiple Targets for Neuroprotection*. www.liebertonline.com=ars (2011).
177. Lemaître, F. *et al.* Capturing T Lymphocytes' Dynamic Interactions With Human Neural Cells Using Time-Lapse Microscopy. *Front Immunol* **12**, (2021).
178. Zare, D. *et al.* Inhibition of protease-activated receptor 1 (PAR1) ameliorates cognitive performance and synaptic plasticity impairments in animal model of Alzheimer's diseases. *Psychopharmacology (Berl)* (2021) doi:10.1007/s00213-021-05798-8/Published.

179. Wolfer, D. P. & Lipp, H.-P. Dissectingthebehaviouroftransgenicmice:isitthemutation,thegeneticbackground,ortheenvironment? *Exp Physiol* (2000).
180. Topham, D. J. & Reilly, E. C. Tissue-Resident Memory CD8+ T Cells: From Phenotype to Function. *Front Immunol* (2018) doi:doi: 10.3389/fimmu.2018.00515.
181. Jin, K. *et al.* CD103+ CD8+ tissue-resident memory T cell infiltration predicts clinical outcome and adjuvan therapeutic benefit in muscle-invasive bladder cancer. *Br J Cancer* (2022).
182. Roosenboom, B. *et al.* Intestinal CD103+CD4+ and CD103+CD8+ T-Cell Subsets in the Gut of Inflammatory Bowel Disease Patients at Diagnosis and during Follow-up. *Inflamm Bowel Dis* **25**, 1497–1509 (2019).
183. Fu, A. K. Y. *et al.* IL-33 ameliorates Alzheimer's disease-like pathology and cognitive decline. *Proc Natl Acad Sci U S A* **113**, E2705–E2713 (2016).
184. Sharma, M. *et al.* Extracellular granzyme K mediates endothelial activation through the cleavage of protease-activated receptor-1. (2016) doi:10.1111/febs.13699.
185. Iannucci, J., Renehan, W. & Grammas, P. Thrombin, a Mediator of Coagulation, Inflammation, and Neurotoxicity at the Neurovascular Interface: Implications for Alzheimer's Disease. *Frontiers in Neuroscience* vol. 14 Preprint at https://doi.org/10.3389/fnins.2020.00762 (2020).
186. Klein, R. S. *et al.* Neuronal CXCL10 Directs CD8 + T-Cell Recruitment and Control of West Nile Virus Encephalitis . *J Virol* **79**, 11457–11466 (2005).
187. Chai, Q., She, R., Huang, Y. & Fu, Z. F. Expression of Neuronal CXCL10 Induced by Rabies Virus Infection Initiates Infiltration of Inflammatory Cells, Production of Chemokines and Cytokines, and Enhancement of Blood-Brain Barrier Permeability. *J Virol* **89**, 870–876 (2015).
188. Krauthausen, M. *et al.* CXCR3 promotes plaque formation and behavioral deficits in an Alzheimer's disease model. *Journal of Clinical Investigation* **125**, 365–378 (2015).
189. Gérard, A., Cope, A. P., Kemper, C., Alon, R. & Köchl, R. LFA-1 in T cell priming, differentiation, and effector functions. *Trends in Immunology* vol. 42 706–722 Preprint at https://doi.org/10.1016/j.it.2021.06.004 (2021).
190. Maurice, N. J., McElrath, M. J., Andersen-Nissen, E., Frahm, N. & Prlic, M. CXCR3 enables recruitment and site-specific bystander activation of memory CD8+ T cells. *Nat Commun* **10**, (2019).
191. Bergamaschi, L. *et al.* Longitudinal analysis reveals that delayed bystander CD8+ T cell activation and early immune pathology distinguish severe COVID-19 from mild disease. *Immunity* **54**, 1257-1275.e8 (2021).
192. Salou, M. *et al.* Expanded CD 8 T-cell sharing between periphery and CNS in multiple sclerosis . *Ann Clin Transl Neurol* **2**, 609–622 (2015).
193. Salou, M., Nicol, B., Garcia, A. & Laplaud, D. A. Involvement of CD8+ T cells in multiple sclerosis. *Frontiers in Immunology* vol. 6 Preprint at https://doi.org/10.3389/fimmu.2015.00604 (2015).
194. van Nierop, G. P. *et al.* Phenotypic and functional characterization of T cells in white matter lesions of multiple sclerosis patients. *Acta Neuropathol* **134**, 383–401 (2017).
195. Lee, P. R. *et al.* Protease-activated receptor-1 activation by granzyme B causes neurotoxicity that is augmented by interleukin-1β. *J Neuroinflammation* **14**, (2017).